Joint Centre for Mesoscale Meteorology, Reading, UK

The Use of Water Vapour Imagery and PV Inversion to Adjust Initial Conditions in NWP

S. J. Swarbrick

Internal Report No. 108
NWP Technical Report No. 291

September 1999

Met Office Joint Centre for Mesoscale Meteorology Department of Meteorology
University of Reading PO Box 243 Reading RG6 6BB United Kingdom
Tel: +44 (0)118 931 8425 Fax: +44 (0)118 931 8791
www.metoffice.com

Designed and produced by the Met Office © Crown copyright 2001 01/0240 The Met Office logo is a registered trademark.

The Use of Water Vapour Imagery and PV Inversion to Adjust Initial Conditions in NWP

Final Project Report

Sean J Swarbrick

UK Met Office / Joint Centre for Mesoscale Meteorology

Sept 1999

Author's address:
Dr. S.J.Swarbrick, JCMM, Dept. of Meteorology, University of Reading, PO Box 43, Reading RG6 6BB, UK. Email: sjswarbrick@meto.gov.uk

SUMMARY

It is considered desirable to make greater use of satellite imagery in the generation of NWP analyses. This project has explored one possible method for doing this, using the Meteosat water vapour channel. The technique attempts to utilise a proposed relationship between water vapour imagery and upper-tropospheric PV fields. This relation, if properly understood, could facilitate the detection of errors in the initial state of a forecast.

The basis of the PV – water vapour methodology employed by this study is as follows. The objective is to reduce errors in forecasts of N Atlantic cyclonic weather systems. The PV field on an appropriate isentropic or isobaric surface, at the initial time of the forecast, is compared with the corresponding water vapour image in order to reveal mismatches between the image and the PV field. The PV field is then adjusted to correct these mismatches. The PV adjustments may involve scaling and/or displacement of PV elements, on a range of pressure levels. (Note that scaling factors are arrived at only by guesswork, since the PV/water vapour comparison provides no scaling information). PV inversion is used to derive wind and temperature increments from the PV adjustments. These wind and temperature increments are applied to the initial forecast fields in a way that preserves dynamical balance. The forecast is then rerun from the adjusted initial state.

A number of case studies have been carried out using this methodology. No unequivocal positive impacts have been achieved. In some cases the impact was positive in certain respects, but negative in others. The case studies have established that there is often a direct relationship between the strength of an upper-tropospheric PV anomaly and the depth of the corresponding surface low; scaling up the anomaly will deepen the low. In addition, positional adjustments applied to a PV anomaly will affect the trajectory of the surface low, but the way in which the trajectory is affected is unpredictable. The results overall have not demonstrated that the PV – water vapour methodology has the potential to be useful for operational forecast initialisation, but rather tend to suggest the opposite.

The most significant scientific difficulty with which the project has had to contend is the fact that the PV – water vapour image relation is not yet defined in a quantitative sense. It is reasonably well understood in a qualitative sense, and this understanding has been successfully applied by other investigators in the context of subjective verification, but this level of understanding appears to be insufficient for the purposes of forecast initialisation. No adequate quantitative relation between PV and water vapour images has yet been established, although this is being pursued by various workers.

The greatest difficulty of all which has impeded progress in this project is a technical one – the fact that the only means available to modify PV fields is by manual editing of pp files. This procedure is extremely crude and laborious, and has severely limited the scope of possible PV adjustments. Until adequate technical means for PV adjustment are available, it will not be possible to explore the PV-water vapour methodology fully. In order to establish such a technique for PV adjustment, it would first be necessary to establish a *quantitative* PV-water vapour image relation by one means or another.

1. SCIENTIFIC BACKGROUND

1.1 Scope of this report

An interim report for this project was produced as JCMM 102 (Swarbrick, 1999). In order to make the present report self-contained, a significant amount of the background material in JCMM 102, chapters 1,2 & 3, has been repeated, although in an updated form. Some of the background material in JCMM 102 is now obsolete (particularly sections 3.1 & 3.2). The account of the PV inversion program, given in chapter 4 of JCMM 102, has been also been appropriately updated and included in this report as an appendix. This report is therefore totally self-contained and does not assume any familiarity with JCMM 102.

JCMM 102 contains accounts of the twelve vn4.3 LAM case studies carried out up to the writing of that report. The present report contains only accounts of the six vn4.4 Global Operational case studies which have been carried out since JCMM 102 was produced. One of these is a "dry eye" case, carried out by N. Keeley. The results of these case studies may be considered, in a sense, as being more meaningful than the previous LAM case studies, due to improvements in the methodology which are explained in the report.

1.2 Project objective and motivation

This project has investigated the feasibility of one proposed method to incorporate information derived from satellite imagery into the initial state of an NWP model. The type of imagery employed is water vapour imagery, specifically the Meteosat 6.7 micron channel. The objective is to obtain wind and temperature increments which can be used to adjust the model's initial state in a balanced and consistent manner, in order to make it conform more closely with the actual state of the atmosphere as revealed by the imagery. It is hoped that such adjustments would, in particular, improve the forecasting of N Atlantic cyclones.

The process of obtaining wind and temperature increments from WV images has two main stages. The first stage exploits the relation between WV imagery and upper-tropospheric PV fields. This relationship, if properly understood, should enable errors in the NWP model's analysed upper-tropospheric PV fields to be detected, since such errors would appear as 'mismatches' between the PV distribution and the WV image. The PV could then (in principle) be adjusted so as to correct these errors. The second stage involves PV inversion, by means of which the PV adjustments are converted to wind and temperature increments. These increments are then used to adjust the model's initial state.

1.3 The relation between upper-tropospheric PV and water vapour images

The relation between PV and WV images has been explored by numerous authors, eg. Demirtas (1996,97), Georgiev (1996,99), Rosting (1996), and, in particular, Mansfield (1996,97). The Mansfield papers are the most useful for the purposes of this project and have been consulted closely.

The water vapour channel, wavelength around 6-7 microns, is not an atmospheric window. This radiation is absorbed and emitted by atmospheric water vapour. The WV radiance field which the satellite sees is produced by radiation integrated over the depth of the upper troposphere. This tropospheric layer is generally 400-600hPa, although this varies according to wavelength, atmospheric humidity distribution, and whether there is cloud present. A water vapour image thus represents the humidity distribution of the upper troposphere. Low humidity regions generally have the highest radiance, since the radiation from such regions has originated from lower (and therefore warmer) levels. However, the air temperature also strongly influences the radiance – this is a complicating factor. Of particular interest are intrusions of dry stratospheric air into the upper-troposphere, which occur in association with cyclogenesis – such regions usually have high radiance. They give rise to a localised lowering, and sometimes "folding", of the tropopause. The accurate modelling of such tropopause features is a major concern of this project.

Having noted that upper tropospheric intrusions of dry stratospheric air appear as high radiance features on WV images, we can also note that stratospheric air has high static stability (i.e. high vertical gradient of potential temperature), and therefore has high PV. We may therefore expect a high radiance feature in a water vapour image to correspond with a high PV feature on an upper-tropospheric PV distribution (generally referred to as a "positive PV anomaly", or simply "PV anomaly"). Such correspondences are most clearly revealed when the PV distribution is displayed on a surface which is close to, or a little below, the tropopause. This is generally the case, at polar front latitudes, for isentropic surfaces in the range 315-330K, or isobaric surfaces in the range 300-400hPa. Since PV is conserved on isentropic surfaces, it may appear that they are the most natural surfaces to use. However, in practice the isobaric surfaces have to be utilised, simply because the PV inversion algorithm is formulated on isobaric surfaces, and so its input and output PV fields are on these surfaces. Isentropic PV fields may also be examined to assist in the subjective assessment of the PV – WV relation however. Other types of PV display can also be useful for subjective assessment, eg. height of the PV=2 surface (particularly favoured for diagnostic purposes by Mansfield, see refs.)

It appears from the above considerations that we expect some sort of correspondence between an upper-tropospheric PV field and its contemporaneous WV image. To some extent, high radiance features should be matched with high PV features. We must now ask, over what region are such correspondences meaningful? How reliable is the PV/water vapour relation – are there any factors which can mislead or make interpretation difficult? Unfortunately, there are many restrictions on the PV – WV relation, and many misleading and complicating factors. The PV – WV relation is in fact extremely subtle, complex, and variable. It is certainly not a simple 1-1 correspondence between high PV and high radiance. Various factors which should be taken into account when interpreting the PV – WV relation are listed below. See Mansfield (1996, 97) for a detailed discussion of these issues, with numerous illustrative examples.

(1) As already noted, air temperature affects the radiance. Thus, a dry stratospheric intrusion which is very cold would have fairly low radiance. In such a case, high PV would correspond with relatively low radiance rather than high radiance.

(2) Stratospheric intrusions occur in the vicinity of the polar front, so the PV – WV relation is valid only in this vicinity, and also to some extent on the cold side (i.e. the polar side) of the polar front. There is essentially no PV – WV correspondence on the equatorward or warm side of the polar front. Regions of warm tropical air mass on the warm side of the polar front would have high radiance simply because they are warm. Also, anticyclonic regions give rise to high radiance because of adiabatic warming caused by descent. In such cases, high radiance would correspond with low PV.

(3) Stratospheric intrusions can be obscured from the satellite's view by overlying cloud or moist regions. This can be misleading when attempting to relate the PV distribution to the WV distribution in such regions. This often happens in regions where the tropopause is "folded", for example. In order to understand such configurations of moist and dry air, it is necessary to examine the PV distribution on a number of different vertical levels (eg., 300, 350 & 400 hPa). Vertical cross sections through the PV field can also help.

(4) There is a more general problem of how to interpret the 2-d satellite image in a 3-d sense, since we wish to make PV adjustments through a certain depth of the upper troposphere. Since the image is made up of radiation received from a range of vertical levels, it does to some extent contain implied information on the vertical distribution of water vapour, but it is difficult to interpret this because it has of course been projected onto a 2-d radiance field. In practice it is necessary to compare the PV distribution on various levels with the image; in general different levels relate to the image in different ways. By this means it is possible to arrive at subjectively estimated PV adjustments on a range of vertical levels, sometimes as far down as 600hPa.

(5) High PV can arise from high vorticity as well as high stability. Thus it can be helpful to plot the vorticity and stability fields (i.e the component factors of the PV) separately, which helps to identify air of stratospheric origin.

(6) The PV – WV relation is considered specifically in the context of developing cyclonic systems. It is not valid for decaying cyclones, since by that stage of development the dry intrusion air has become

mixed up with moist air. The application of PV - WV analysis is generally most appropriate during the early stages of cyclonic development; as the cyclone matures it becomes more difficult to apply.

(7) In applying the PV – WV relation to cyclonic development, it is also necessary to consider the interaction between upper and lower level forcing. In particular, the 850hPa θ_w distribution should be examined. Cyclogenesis may be enhanced if an upper level PV anomaly moves into an appropriate "phase relation" with a low level baroclinic zone, i.e, if the anomaly and the baroclinic zone are positioned in such a way relative to each other that their respective induced circulations can enhance each other by mutual interaction (Hoskins et al. 1985). A WV image does not provide any guidance on how to make PV adjustments at lower levels, and in fact lower level adjustment is beyond the scope of this project; but the point is that the relation between the upper and lower levels should be taken into account when making upper level adjustments.

1.4 Choice of forecasts for case studies

The initial aim of the case study work was to establish reasonably well-defined rules to enable decisions to be made as to whether there is a mismatch between the model's upper-tropospheric PV distribution and the satellite WV image in any particular case, and what adjustments should be made to correct the mismatch if it exists. The approach taken was to choose suitable cases of inaccurately forecast cyclonic development in the N Atlantic, and to apply the guidelines given by Mansfield (1996,97) in order to assess PV-WV mismatches and attempt to correct them. Conceptual models of cyclogenesis were also were also utilised to interpret satellite images in terms of PV distributions (see eg. Semple 1998). It was hoped that this approach would lead on to a further stage of "blind" test cases, although this has not yet been possible owing to the inconclusive nature of the case study results.

The forecast case studies presented in this report are all from the period Jan-July 1999, and were carried out with the UKMO UM, global operational configuration. (Global UM horizontal mesh dimensions are 325 rows by 425 columns). The cases were chosen on the basis of a daily forecast monitoring scheme devised by A.T. Semple of JCMM (to appear as a JCMM report). This scheme provides a simple assessment of analysis/forecast accuracy for N Atlantic cyclones. The forecast error at T+12 is assessed in terms of (a) the difference between the values of surface pressure at the forecast and analysed low centres; (b) the difference between the positions of the forecast and analysed low centres expressed as a percentage of the "system radius", the system radius being defined as the distance from the low centre to the outside of the cloud head.

The results of this program of daily monitoring for the period Jan-July 99 are presented in fig. 1.1. The forecasts included in the graph are all cyclonic cases; non-cyclonic cases are of no interest for this project. For convenience the graph is divided arbitrarily into "classes". All but one of the cases presented in this report have forecast error of at least "class III". One result to emerge from this scheme of monitoring is that cyclonic forecasts with very significant errors (classes V and VI) are rare. Significant test cases in these classes are shown on the graph. Thus, none of the cyclone cases available for study in this project has a location error greater than 45%. This is often quite a small error – it usually corresponds to an actual location error on the order of 2 or 3 degrees (depending on the actual radius of the system). Any PV-WV mismatches which occur in such cases are generally very subtle and not at all obvious. It is difficult to reliably detect such mismatches solely by subjective judgement. The apparent scarcity of major errors in cyclonic model forecasts has been something of a disadvantage for this project – the cases available for study seem to offer little scope for subjective detection of definite PV-WV mismatches.

1.5 The PV inverter

A detailed account of the PV inversion program is given in chapter 4 of Swarbrick (1999). In the interests of completeness, this account has been included in this report as an appendix.

The program in its original limited-area domain form was created by Zemianski (1994), and further developed by Griffiths (1999) for the mesoscale domain. The program was subsequently modified by

N. Keeley of JCMM (to appear) for a limited-area subset of the global domain. This form of the program has been used in the case studies reported here.

The program inverts Ertel PV specified on a range of pressure levels. The balance condition assumed by the algorithm is Charney non-linear balance (Holton, 1992). The boundary condition chosen for the lowest pressure level is to specify theta, i.e. the vertical derivative of geopotential height. The other boundary conditions are given in the appendix. The PV inversion domain is mainly oceanic; its precise extent is case dependent, but is generally from 60N (S tip of Greenland) to about 35N, and from 295 (taking in a small part of W Canada) to about 350 longitude. The horizontal mesh is the same as for the global UM. There are 38 vertical levels, from 850 to 100 hPa. The PV inverter outputs temperature and the non-divergent part of the wind on these 38 levels.

It should be noted that the PV inversion domain does not extend down to the surface, consequently the influence of any PV adjustments does not extend down to the surface. In principle it is possible to extend the domain below 850hPa, but in practice this is usually not possible because the lower pressure levels intersect the surface. In any case, even if the domain is extended down to lower levels, the surface pressure is not adjusted, which introduces an inconsistency. This limitation on the vertical influence of PV adjustments may be a significant handicap.

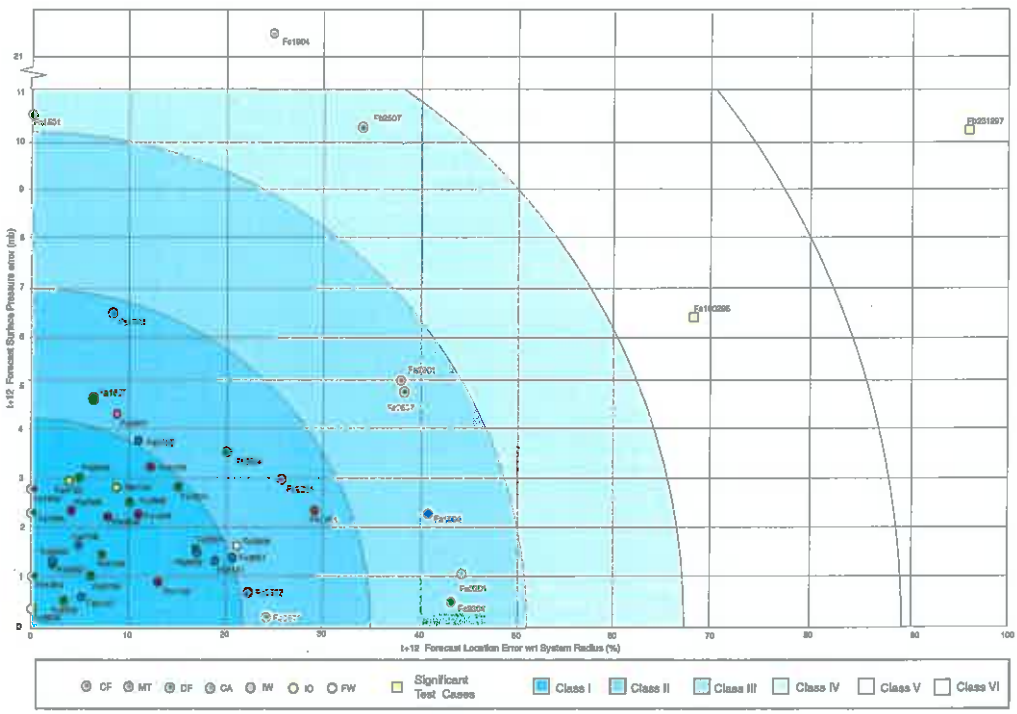

Fig. 1.1 Results of daily forecast assessment for N Atlantic cyclones, Jan-July 1999 (courtesy of A.T. Semple, JCMM).

Fx denotes initial time of forecast, where x=a for 0z, x=b for 6z, etc.

2. METHODOLOGY

2.1 Outline of the case study procedure

The steps involved in carrying out a case study are as follows.

(1) Compare the background PV field corresponding to the analysis time of the forecast with the contemporaneous water vapour image. Determine whether any mismatches are present, and decide on what adjustments to make.

(2) Adjust the background PV field to improve its fit to the water vapour image. This process is semi-automated but has an essential manual element.

(3) Carry out a PV inversion on the unmodified set of PV fields, and then carry out another PV inversion on the modified set of PV fields. Each PV inversion outputs a set of wind and temperature fields on the 38 pressure levels. Take the difference of the these two sets, to obtain a set of wind and temperature increment fields.

(4) Rerun the UM forecast from the adjusted initial state. The wind and temperature increments are incorporated into the model's initial state using the incremental analysis update facility (IAU). The forecast is rerun without data assimilation. The rerun forecast is compared to the original forecast run both with and without data assimilation to see if there is a positive impact against either.

In deciding on what PV adjustments to make in each case, the guidelines for the PV – WV image relation given in Mansfield (1996,97) were consulted and a serious attempt was made to apply them (although the author of that paper never intended that they should be used in this way, as the PV analysis presented there is essentially to do with post-forecast verification, not pre-forecast initialisation). Further guidance was also provided by A.T. Semple, using the conceptual model approach as described in Semple (1998).

2.2 The IAU input mechanism for wind and temperature increments

The differencing procedure used to obtain the wind and temperature increments is not strictly valid because the Ertel PV inversion is of course a highly non-linear problem. However, as long as the increments are not too large it is a reasonable thing to do. In any case, there is clearly no alternative if the model's initial state is to be adjusted directly rather than adjusted via the data assimilation mechanism (apart from the possibility of linearising the PV inversion problem).

The IAU inputs the wind and temperature increments as equal sub-increments over 24 timesteps, from T-3 to T+3. This ensures that the model's balance is maintained and also smooths out the discontinuities introduced by the semi-manual PV adjustment process. One could of course introduce the full increments into the initial dump; this is what was done in the case studies reported in Swarbrick (1999). However this causes imbalance in the initial state and leads to a great deal of gravity wave activity over the first 6-12 hours of the rerun.

2.3 Manual PV adjustment

The mechanism by which PV field adjustment has been carried out in this project is essentially manual. No adequate automated facility for PV adjustment has yet been developed, so there was no practical alternative to the manual approach. This method involved writing a fortran program which would (a) read the PV fields from a pp file into an array; (b) overwrite specified elements of this array with new values; (c) write the adjusted array to another pp file. This output pp file would then act as an input file for the PV inverter. The lines of code which carried out the overwriting of array elements would be constructed on the basis of the subjective PV / water vapour image comparison.

This approach has a number of serious disadvantages:

(a) It is based on the subjective PV/WV comparison, which is very poorly defined and obviously not standardised in any sense.
(b) It is very slow, tedious and laborious.
(c) It is very crude – the most that can be practically achieved by this technique, without requiring unreasonable expenditure of time and labour, is to bodily displace rectangular portions of a PV field, and/or to apply scaling factors to such rectangular portions, and/or to perform other simple operations such as levelling off the PV field within such a rectangular portion.

The unavoidable crudity of this manual PV adjustment technique has imposed a considerable limitation on the case study investigations.

2.4 Possibilities for automated PV adjustment

In order for the PV/water vapour image methodology to provide the basis for a practical operational initialisation system, it would be essential to establish a sufficiently precise quantitative relation between upper tropospheric PV fields and water vapour images. The statistical studies of Georgiev (1996,1999) have given some indication of the extent to which such a relation actually exists. If such a relation can be established by whatever means, then it could possibly lead to an automatic means of adjusting PV fields in conjunction with water vapour imagery, and so replace the undesirable subjective element of the methodology.

Two possible solutions to this problem have been proposed, and have been investigated to some extent by projects related to the present study, although neither has yet provided a satisfactory PV adjustment system.

One of these proposed solutions, due to Hoffman et al. (1995), involves the "Distortion Representation" approach, which attempts to align a "pseudo water vapour image" with the corresponding satellite water vapour image. The "displacement field" derived from this procedure would then be applied to the corresponding PV field on an appropriate upper-tropospheric surface, so rearranging that field in a way that should (it is hoped) improve its fit to the satellite WV image. The pseudo WV image is derived from model-generated temperature and humidity fields via a radiation-transfer algorithm (eg. Schmetz and van de Berg, 1994).

The Distortion Representation approach assumes that displacements derived from the comparison of satellite and pseudo WV images can be applied to an upper-tropospheric PV field to yield an improved fit with the satellite WV image. This sounds reasonable in theory, but in reality it appears to be a dubious assumption. In a number of the case studies undertaken in this project, a pseudo WV image was generated and compared (subjectively) to the satellite WV image, and in every case this comparison appeared not to yield any guidance as to how to adjust the PV field. As far as gross features are concerned, the pseudo WV image generally resembles the satellite WV image. Mismatches between the two can certainly be seen, but these tend to be localised and not obviously related to the disposition of the PV field. Another uncertain feature of this approach is that there is no clear way of deciding at which upper-tropospheric surface the PV displacements should be applied, even if it were possible to obtain a well-defined displacement field.

The other proposed solution has been investigated by G. Pankiewicz of the UK Met. Office (Pankiewicz, 1997). This involves trying to infer the PV field, on an upper-tropospheric isentropic surface, from the water vapour image, by means of neural net pattern recognition software. The neural net is "trained" by processing a large sample of water vapour images and their corresponding PV fields on the chosen isentropic surface. Like the Distortion Representation approach, the neural net approach attempts only to establish a quantitative PV – WV image relation on a 2-d surface, leaving unanswered the question of how to extend this relation into the vertical dimension. However, in the neural net case the vertical level of the 2-d surface in question is at least defined from the outset. In the Distortion Representation approach the vertical location of the 2-d surface is undefined, since the relation established is between an observed WV image and a model-generated WV image, rather than between the WV image and a PV field.

The neural net approach is clearly more direct in its attempt to establish a quantitative PV – WV image relation than the Distortion Representation approach, but neither approach has yet yielded a workable software tool.

2.5 Lower level PV adjustment

The project with which this report is concerned has involved only upper-tropospheric PV adjustment (i.e. levels which are seen by WV imaging). A related project being carried out by A.T.Semple of JCMM (not yet published) is attempting to utilise adjustment of PV fields (and/or other fields such as geopotential heights) throughout the depth of the troposphere, i.e. the adjustments are not restricted to upper levels. These adjustments are guided in general by satellite imagery (infra red and water vapour) together with conceptual models analysis. The conceptual models analysis is an essential element in this more general approach to initial field modification; lower level adjustment in particular cannot be related to water vapour imagery. The field modifications are carried out using the "Fieldmod" software developed by E.B. Carroll of the UK Met. Office (Carroll 1996). This software uses QGPV inversion to derive consistent field adjustments. Using this technique, some valuable results have been obtained for the "Christmas Eve Storm" case of Dec. 1997.

3. CASE STUDY RESULTS - Concise summary

Each summary indicates, in brackets, the cyclone location error and pstar error at T+12 as shown on Semple's graph (fig. 1.1). A brief indication of the PV adjustment made is also given.

Case 1 00z 3/1/99 (40%, 5hPa) Positive impact on pstar, negative impact on location
Little impact at 500hPa.
PV adjustments: involved simultaneous scaling and displacement of anomalies & contours, although the displacements seemed to be attenuated by T+6.

Case 2 06z 28/1/99 (40%,5hPa) Small negative impact at surface & 500hPa
PV adjustments: rearrangement of anomalies.

Case 3 06z 5/2/99 (25%, 3hPa) Positive impact at surface, negative impact at 500hPa
PV adjustments: scaling only. An adjustment involving rearrangement was attempted, but the UM rerun crashed with a floating point error.

Case 4 12z 23/4/99 (45%,0.5hPa) Small positive impact on position & pressure at surface
Negligible impact at 500hPa
PV adjustment involved scaling (factor of 1.2) only. Water vapour/PV comparison was not useful – cyclone was a mature system.

Case 5 00z 6/7/99 (40%,5hPa) Negligible impact at surface and 500hPa
PV adjustment: scaling factor of 1.5 applied to upper-level anomaly. Cyclone was insensitivite to this adjustment.

Cases are 1,2,4 & 5 "class III" in the Semple plot, fig. 1.1. Case 3 is class II. There are of course several other cases in these classes in fig.1.1 which have not been looked at – the only reason for this was lack of time – the case study procedure is very laborious and time-consuming.

4. CASE STUDY RESULTS – detailed accounts

CASE 1: 00z 3/1/99 (40%, 5hPa)

Pmsl fields (figs. 4.1.1,2,3): This case concerned a cyclone in W Atlantic, moving NE and deepening. The cyclone in question is the one at the same latitude as Newfoundland and Brittany. At T+12 the central pressure was ~5hPa too high and the location ~2 deg too far S in the forecast run from the original analysis. The forecast run from the original background was very similar to that from the analysis.

500hPa height fields (figs. 4.1.4,5,6) : The 500hPa trough which corresponded to the surface low was also under-developed and had about the same location error as the surface low in both the forecast from analysis and forecast from background.

WV image & PV at 400hPa (fig. 4.1.7): The WV image for 00z 3/1/99 shows a dry intrusion S of Newfoundland and cyclonically curving over the Atlantic, which evidently corresponds to the cyclone in question. The analysed PV contours appear to be well matched with this feature. A PV maximum lies a few degrees SW of the "head" of the dry intrusion and a sharp PV gradient region follows the curve of the intrusion across the Atlantic. The PV contours curve anticyclonically over the cloud head lying just N of the head of the dry intrusion. This is all generally in accordance with the "Mansfield guidelines" (Mansfield 1996, 97). It could be argued that the PV maximum should be closer to the head of the dry intrusion, and that the PV gradient should be tighter. (This cannot be tested, however, since the IAU-based methodology only enables adjustments to be made to the background, not to the analysed fields).

The 400hPa background PV field (fig. 4.1.8) shows the same kind of relation to the WV image as the analysed field, but the PV gradient and PV maximum are much weaker. The analysed fields appear to be much better matched to the WV image than the background fields (as one would expect), although, as noted above, the forecast from analysis and forecast from background show virtually the same (small) errors in the pmsl and 500hPa height fields.

850hPa theta-w field (fig. 4.1.9): The 850hPa theta-w field shows a baroclinic region apparently in close association with the 400hPa PV maximum. Coupling between them would be expected, so modification of the PV field should have a significant influence on the cyclone's development.

Rerun : The PV maximum referred to above was scaled up by 1.5 and displaced slightly eastwards to (possibly) improve the fit with the WV image (fig. 4.1.10). The adjustments were carried out from 380 to 500 hPa, every 20 hPa. The displacement of the PV element which can be seen in the manually adjusted field is barely noticeable in the T+6 PV fields, although the intensity adjustment is still apparent (fig. 4.1.11).

The impact on pmsl was mixed (fig. 4.1.12). The intensity error at T+18 was well corrected, but the location error was increased to about twice its original size. Impact at 500hPa was insignificant.

Convergence difficulties: Convergence of the PV inverter was very difficult for this case. For the unmodified PV fields, the first attempt failed to converge. The error parameters did not actually diverge, but maintained roughly constant large values over many iterations. Eventually, convergence was achieved after adjusting the W domain boundary (it was moved a few gridpoints westwards), but still took 150-200 iterations. After PV inversion convergence was even more difficult; in the second rerun it could only be achieved after reducing the relaxation parameters to 0.3, and took over 250 iterations.

This case illustrates that PV/WV mismatches associated with even relatively bad forecasts (in the period covered by Semple's graph, fig.1.1) are insufficiently clear to provide definite guidance in determining analysis errors.

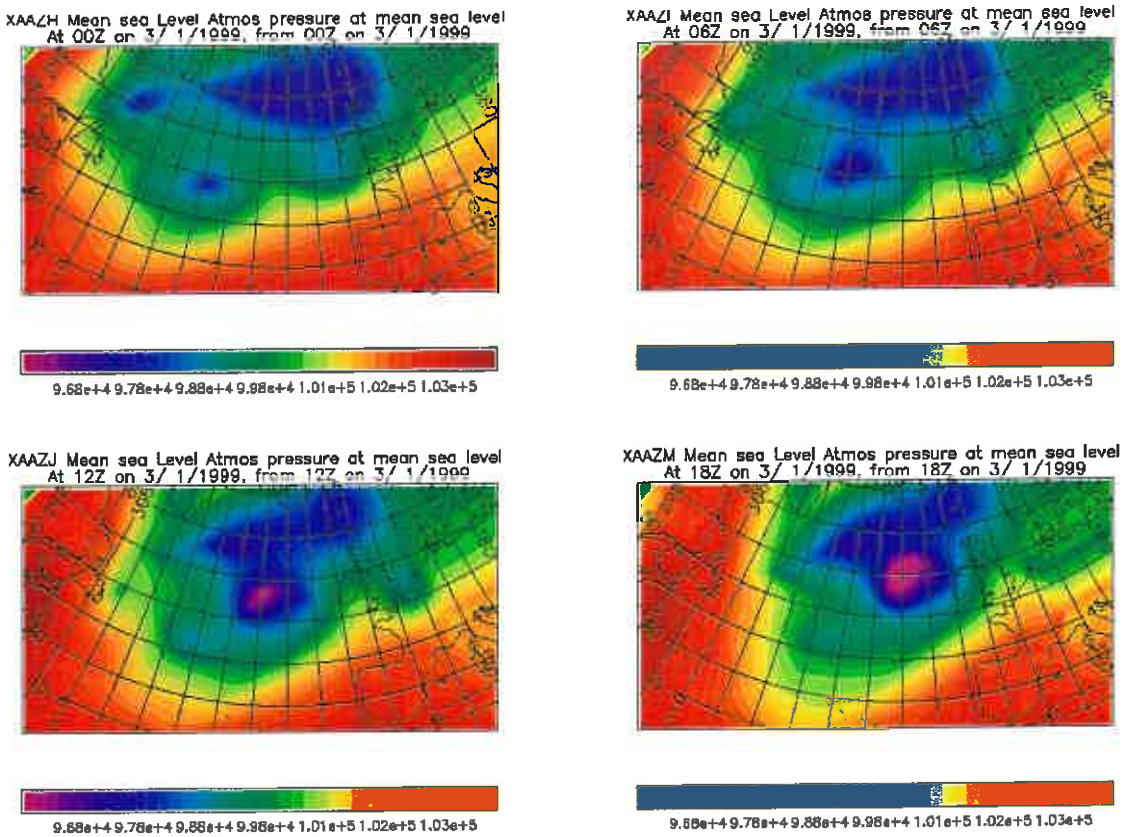

Fig. 4.1.1 Case 1 : PMSL analyses

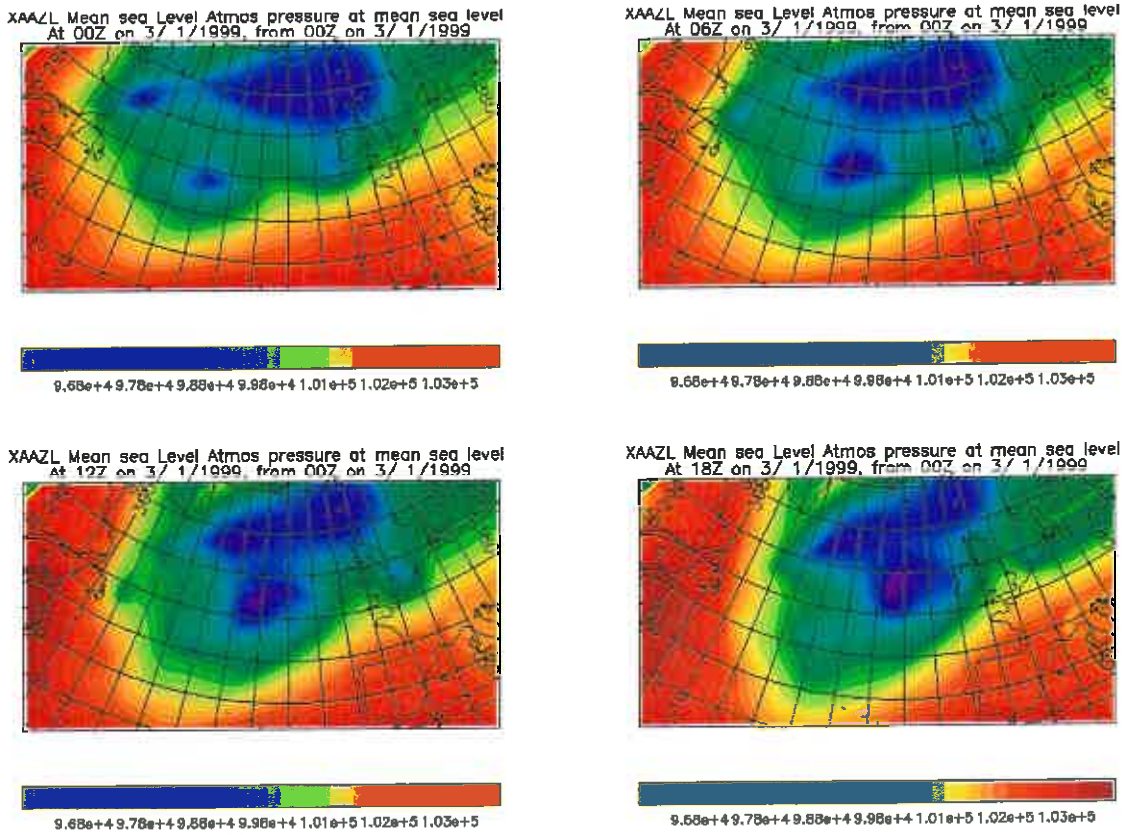

Fig. 4.1.2 Case 1: PMSL forecast from analysis

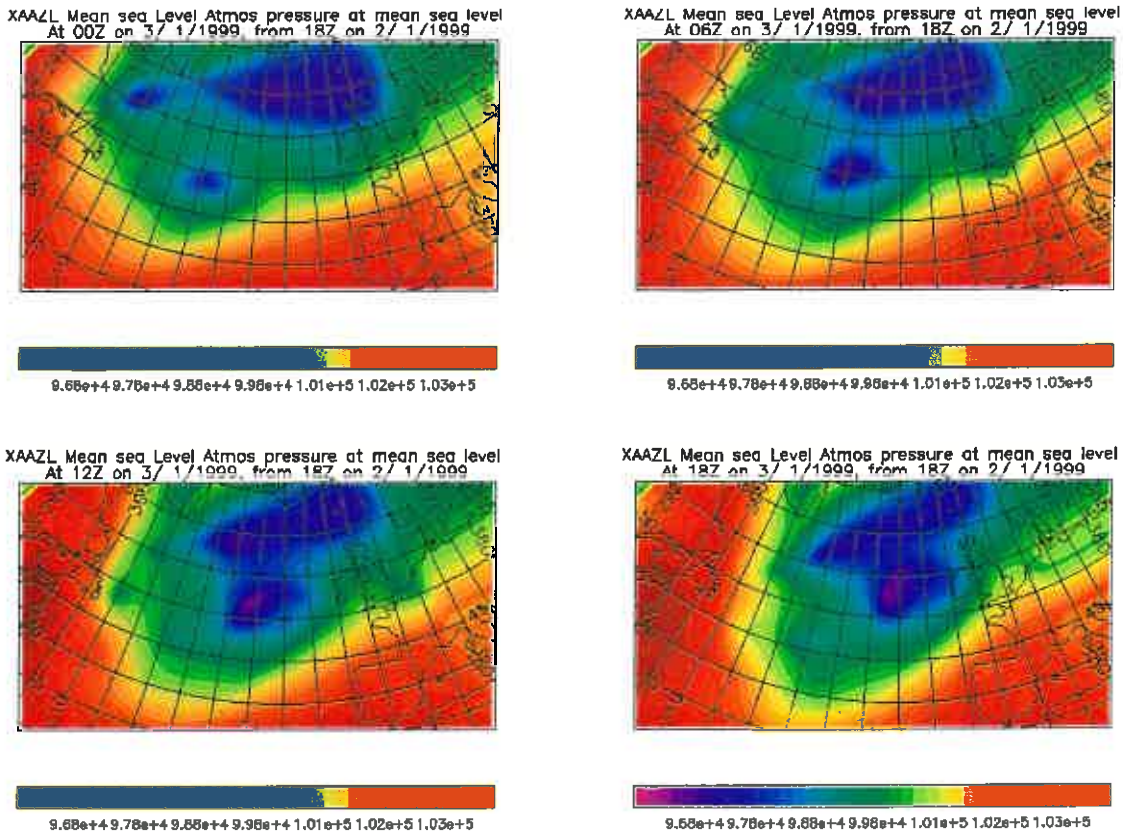

Fig. 4.1.3 Case 1: PMSL forecast from background

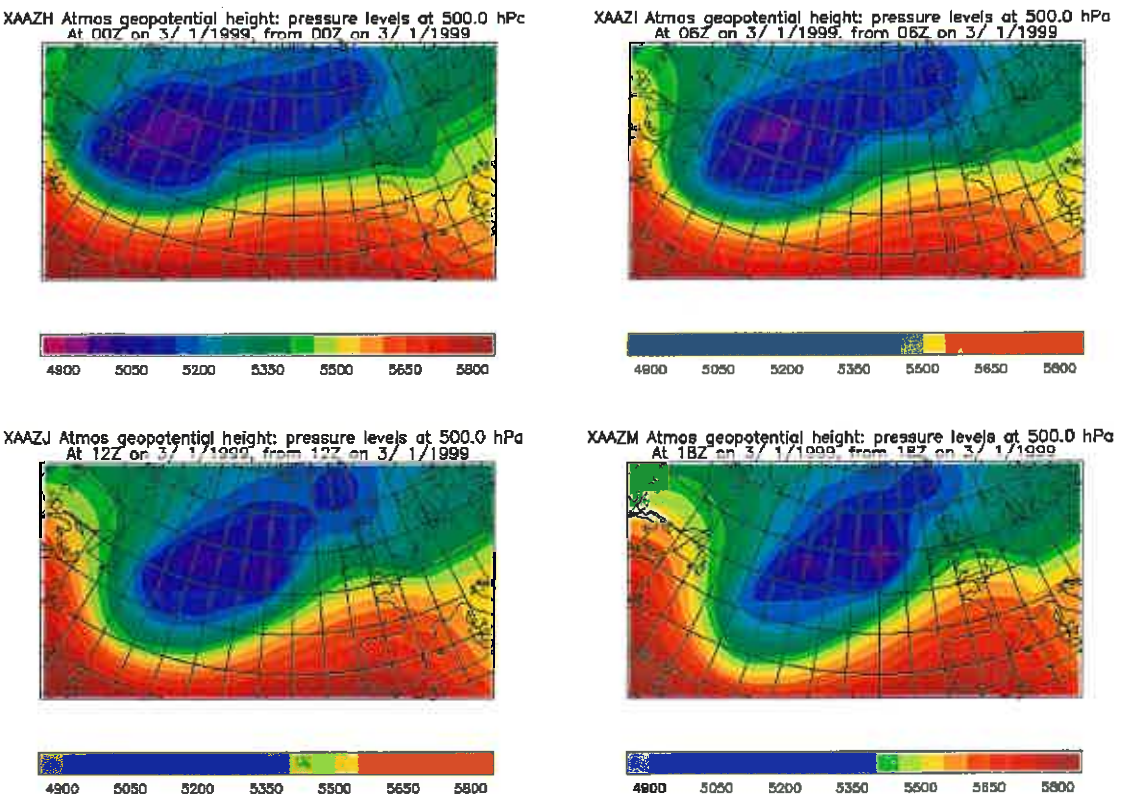

Fig. 4.1.4 Case 1: 500hPa height analyses

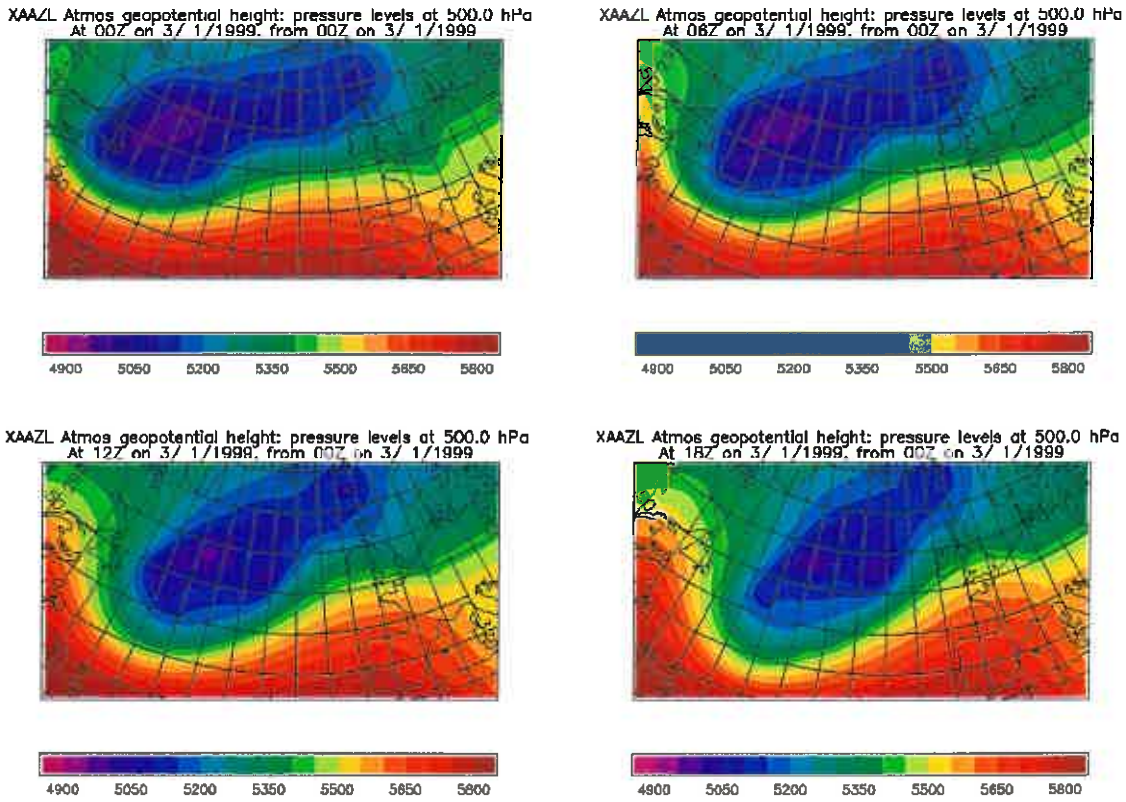

Fig. 4.1.5 Case 1: 500hPa height, forecast from analysis

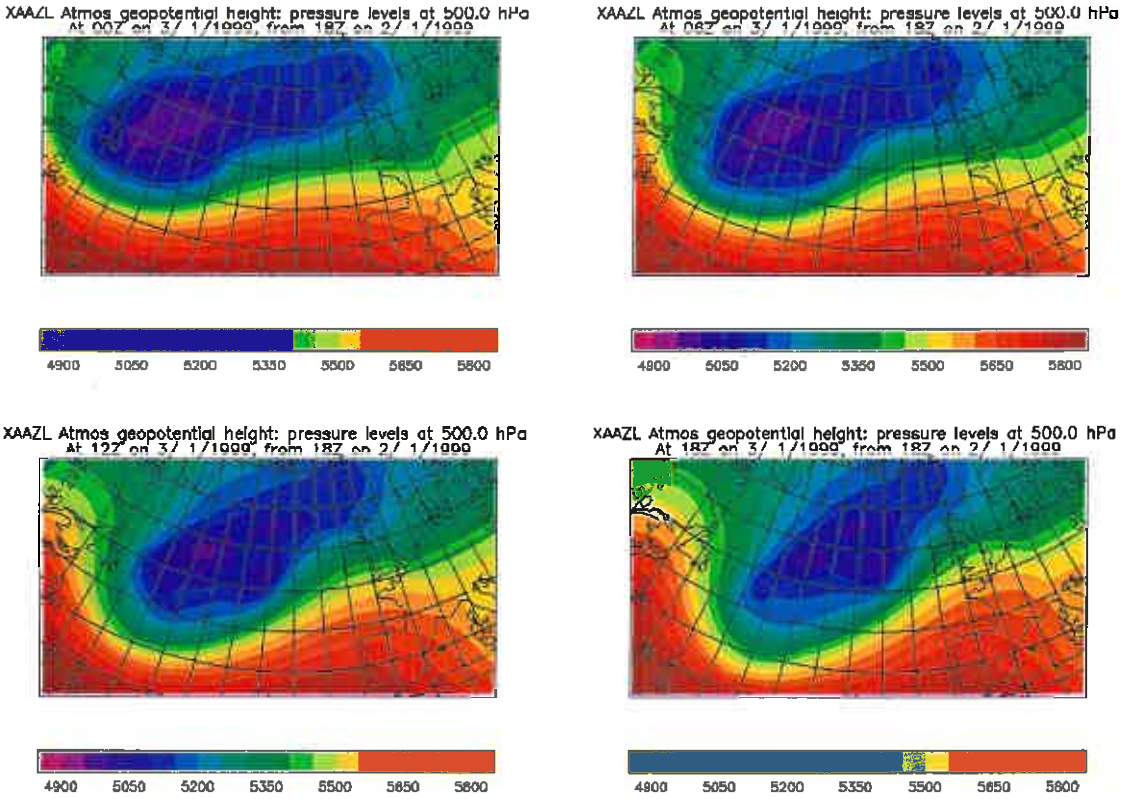

Fig. 4.1.6 Case 1: 500hPa height, forecast from background

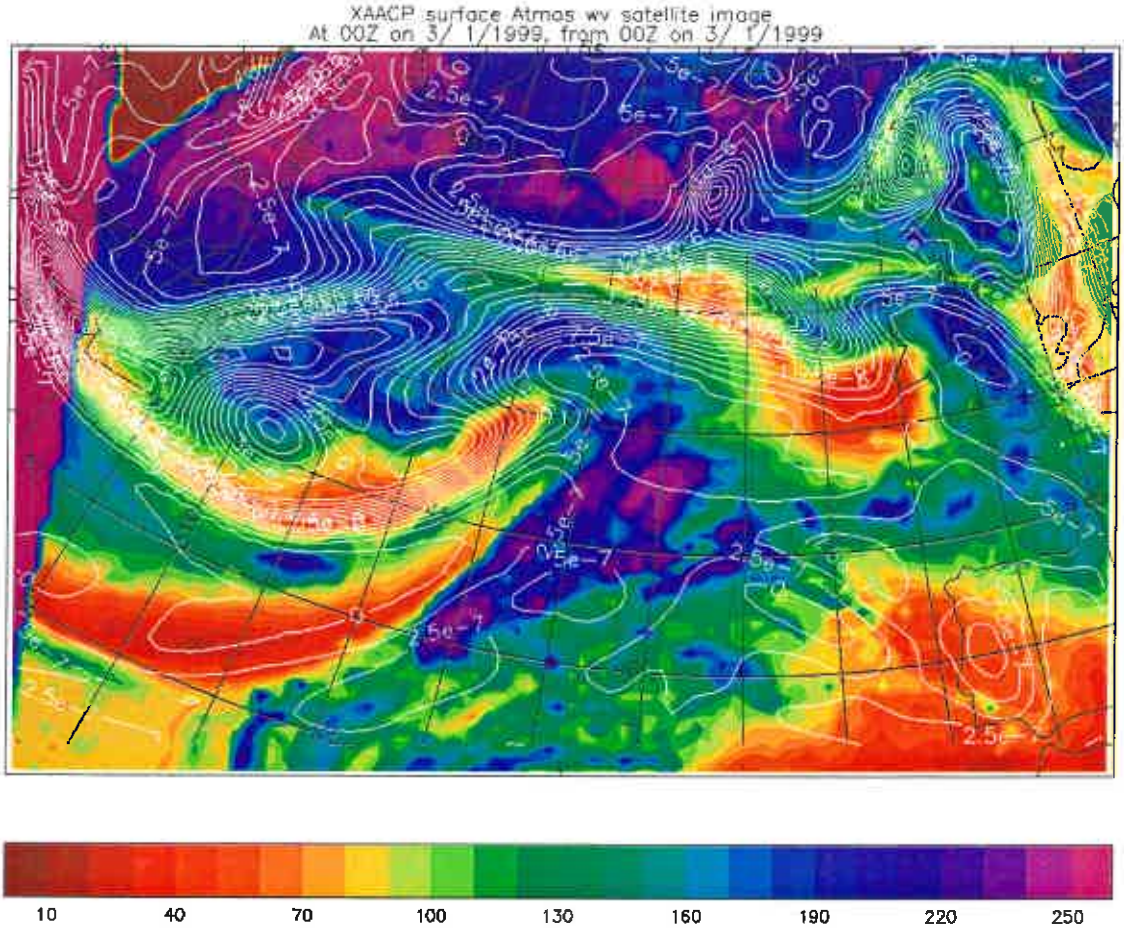

Figs. 4.1.7 Case 1: WV image with contours of analysed PV on 400hPa at T+0

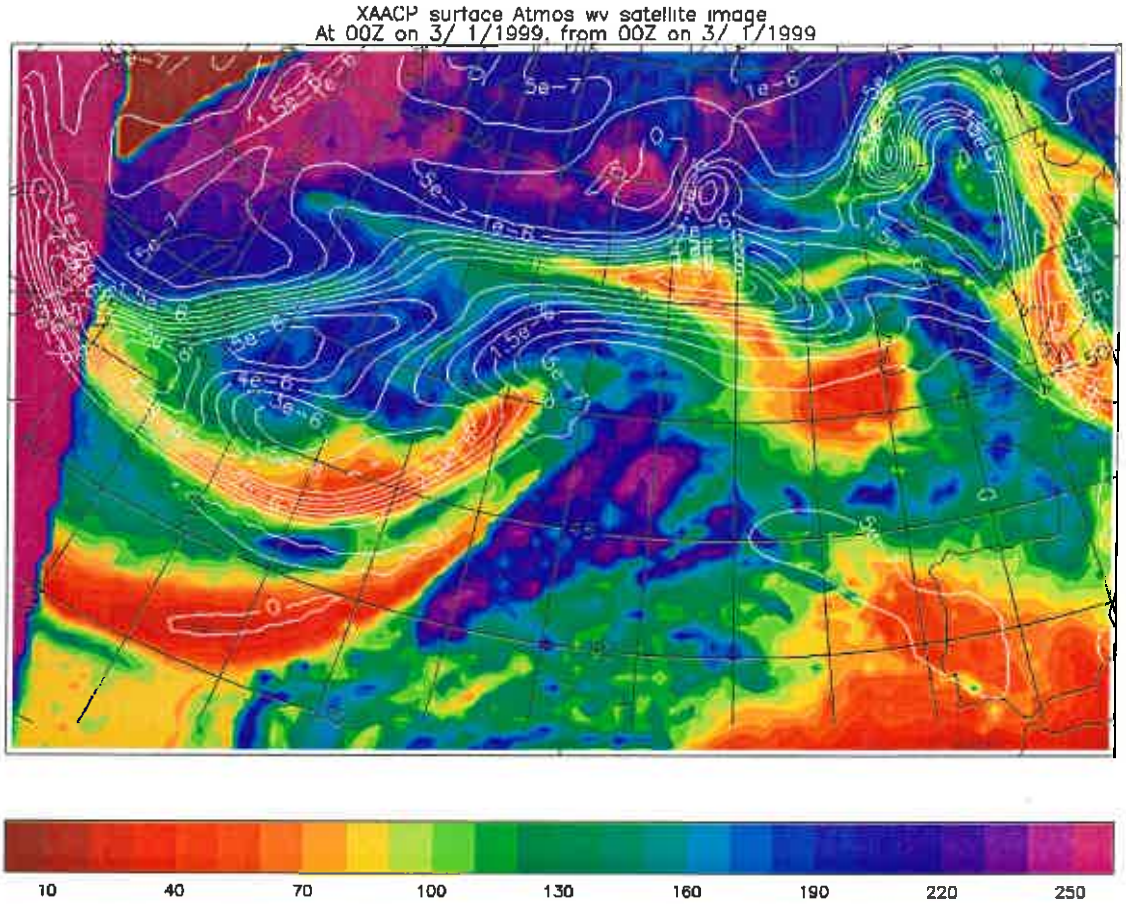

Figs. 4.1.8 Case 1: WV image with contours of background PV on 400hPa at T+0

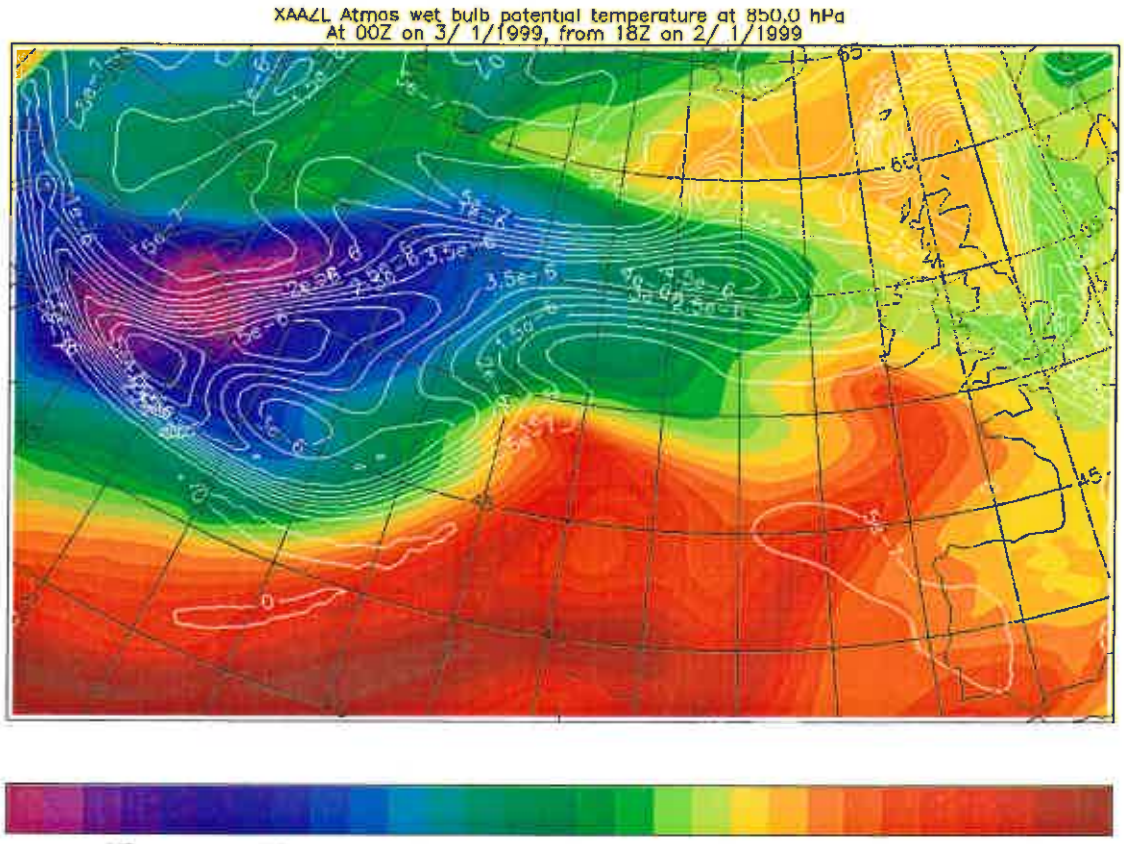

Fig. 4.1.9 Case 1: Background theta-w on 850hPa with 400hPa background PV contours at T+0

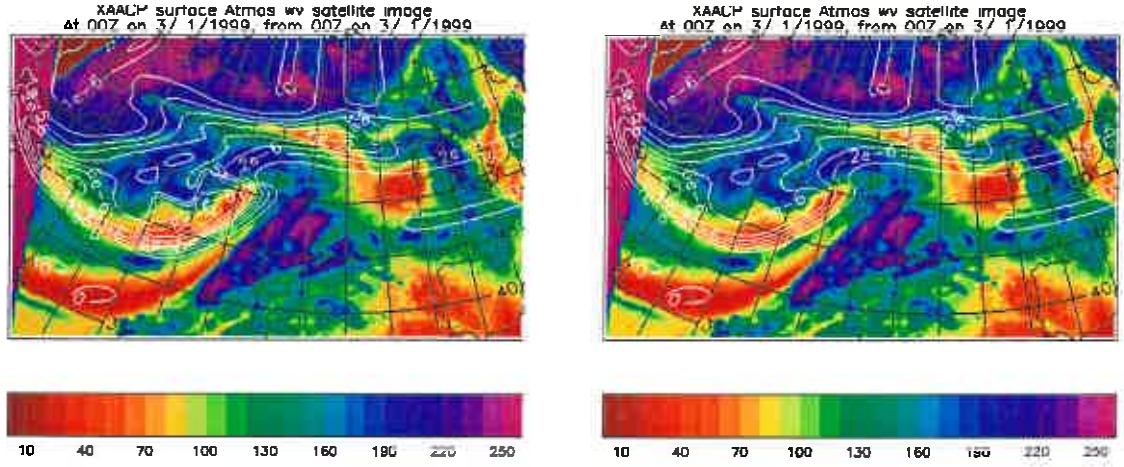

Fig.4.1.10 Case 1: Manually adjusted PV (LH frame) compared with original background PV (RH frame) at 380hPa

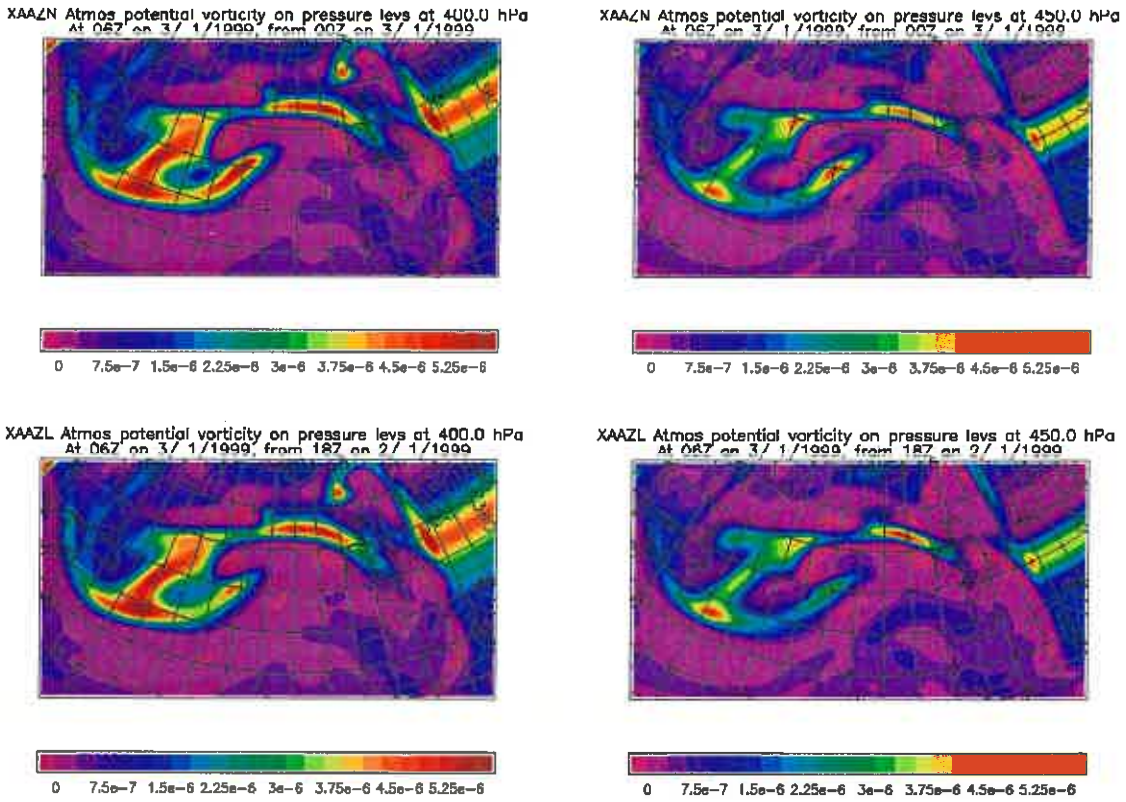

Fig. 4.1.11 Case 1: T+6 PV fields: forecast from background (lower frames) and forecast from adjusted background (upper frames) on 400 & 450hPa.

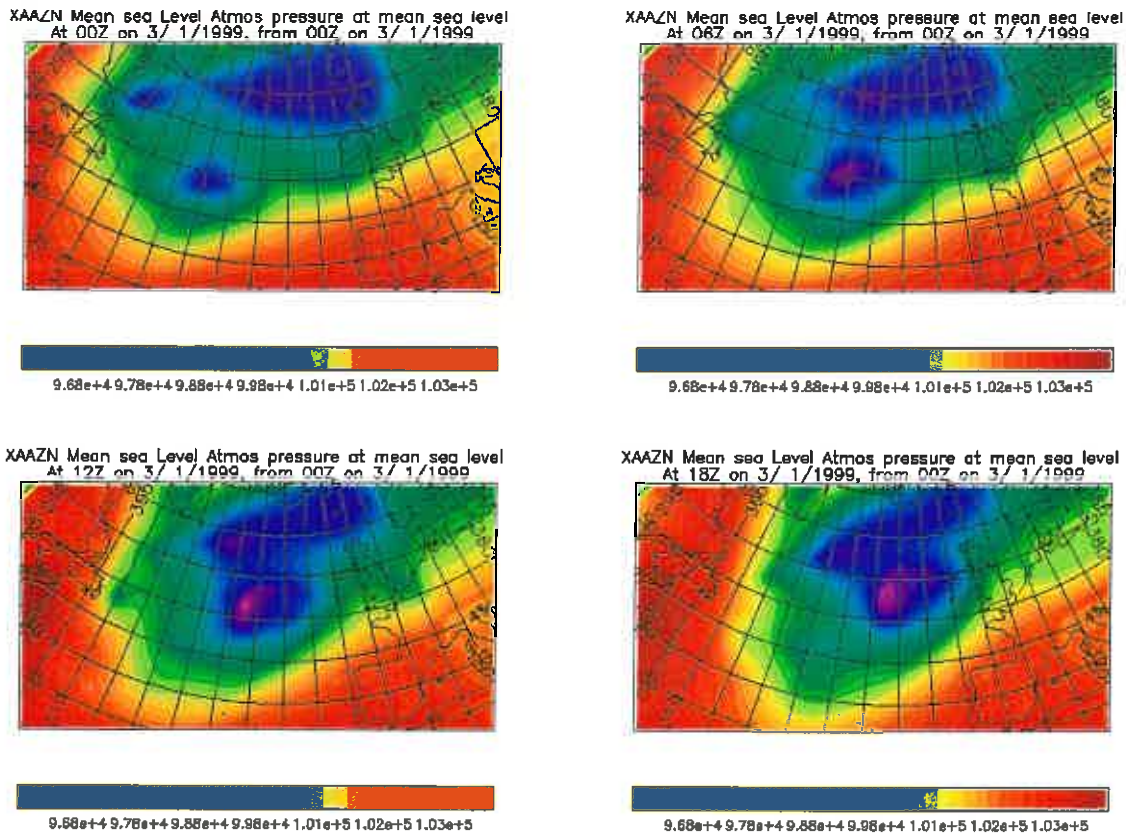

Fig. 4.1.12 Case 1: PMSL forecast from adjusted background

CASE 2: 06z 28/1/99 (40%, 5hPa)

Pmsl fields (figs. 4.2.1,2,3): This case concerned a cyclone in W Atlantic, moving NE and deepening. At T+12 the central pressure was ~5hPa too high and the location ~2 deg too far S in the forecast from analysis. The forecast from background showed larger errors.

WV image and PV fields (fig. 4.2.4): The WV image showed an associated dry intrusion. Analysed PV on 315K/300hPa showed two anomalies each located several degs from the dry intrusion - anomaly 1 to the N, and anomaly 2 to the NW.

850hPa theta-w field (fig. 4.2.5): This showed a strong baroclinic region colocated with the cloudy region just E of the dry intrusion. The warm conveyor belt appeared to be too far east in part, on the edge of the cloudy region rather than through the middle of it.

Pseudo water vapour image (fig. 4.2.6): The pseudo WV image was examined - it was not well matched with the satellite image - however this mismatch did not yield any guidance as to how the PV field should be adjusted.

Rerun 1: The PV adjustments were suggested by the PV/WV comparison referred to above. The two PV anomalies noted above were judged to be too far from the dry intrusion. The objective of the PV adjustment was thus to position a PV anomaly over the cold dry air just poleward of the dry intrusion. The anomaly should not encroach on the moist air. Anomaly 1 was moved several degs SE; anomaly 2 was not moved but reduced in intensity (fig. 4.2.7). The adjustments were made on levels 300-600hPa, every 20hPa. The adjustments were performed on the background PV fields.

Examination of the T+6 (fig. 4.2.8,9,10) PV fields indicates that the field adjustments input via the IAU are in fact manifested in the model fields, so the model has not rejected the adjustments. In the rerun forecast plot (fig. 4.2.10), the PV maximum just SE of Newfoundland can be seen, accompanied by a PV minimum just NW of Newfoundland, which is not visible in the original forecast fields. This minimum may be a diabatically-generated response to the introduced PV maximum, suggesting that the introduced maximum is having some effect.

The results of this rerun were compared against both the forecast from the original analysis and the forecast from the original background fields. Both comparisons showed a small negative impact, i.e., the position and intensity errors of the surface cyclone were increased slightly (fig. 4.2.11).

Dynamical Balance: Pstar tendency fields were plotted for the first few hours of the rerun in order to test whether dynamical balance was maintained. The rerun was carried out both with and without the IAU input mechanism, for comparison purposes. When inputting increments by the non-IAU method, the increments are simply added in full to the T+0 wind and temperature fields. When inputting them by the IAU method, they are input as equal sub-increments over 24 timesteps, from T-3 to T+3. The pstar tendency plots indicate that a great deal of spurious oscillation occurs in the non-IAU case, suggesting severe imbalance. When the IAU method is used, however, no such oscillations are seen.

Rerun 2: A second rerun was attempted, using a different PV adjustment to that carried out for rerun 1. A PV gradient region runs N-S across the field, passing about 5 deg E of Newfoundland. It passes over the E part of the dry intrusion lying SE of Newfoundland, but fails to follow the curve of the edge of the dry intrusion running southwards. The shape of this region was adjusted so that the PV contours did follow the curve of the dry intrusion reasonably well. Also, anomaly 2 (as referred to above) was reduced in intensity. The adjustments were made on levels 280-320hPa, every 20hPa. This was the total vertical extent of the PV gradient feature. The adjustments were performed on the background PV fields. The impact of these adjustments on the forecast was negligible.

Comparison with case 1: This case has the same position and pressure errors as case 1, but in this case the PV/WV comparison definitely does look wrong, whereas in case 1 the comparison was much less definite. In this case the relevant PV anomaly appears to be in the wrong place (rerun1), and the PV gradient does not follow the cloud edge (rerun 2). However, attempts to correct these mismatches in case 2 have not led to positive impacts on the forecast.

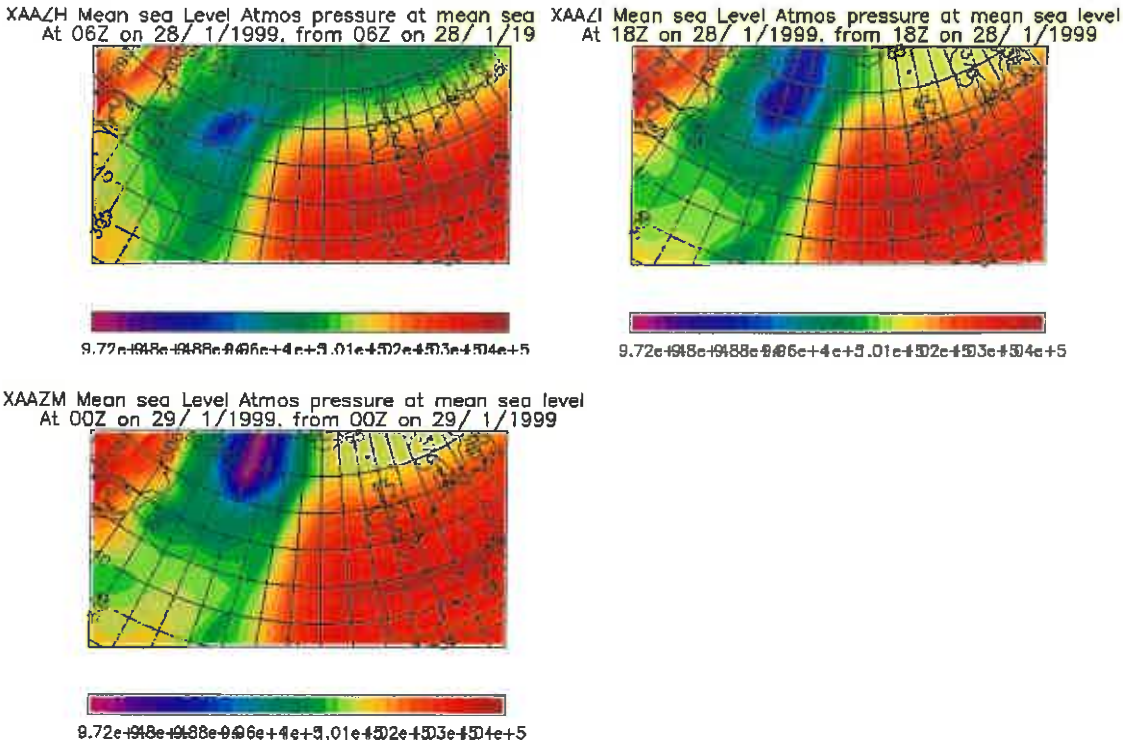

Fig. 4.2.1 Case 2: PMSL analyses

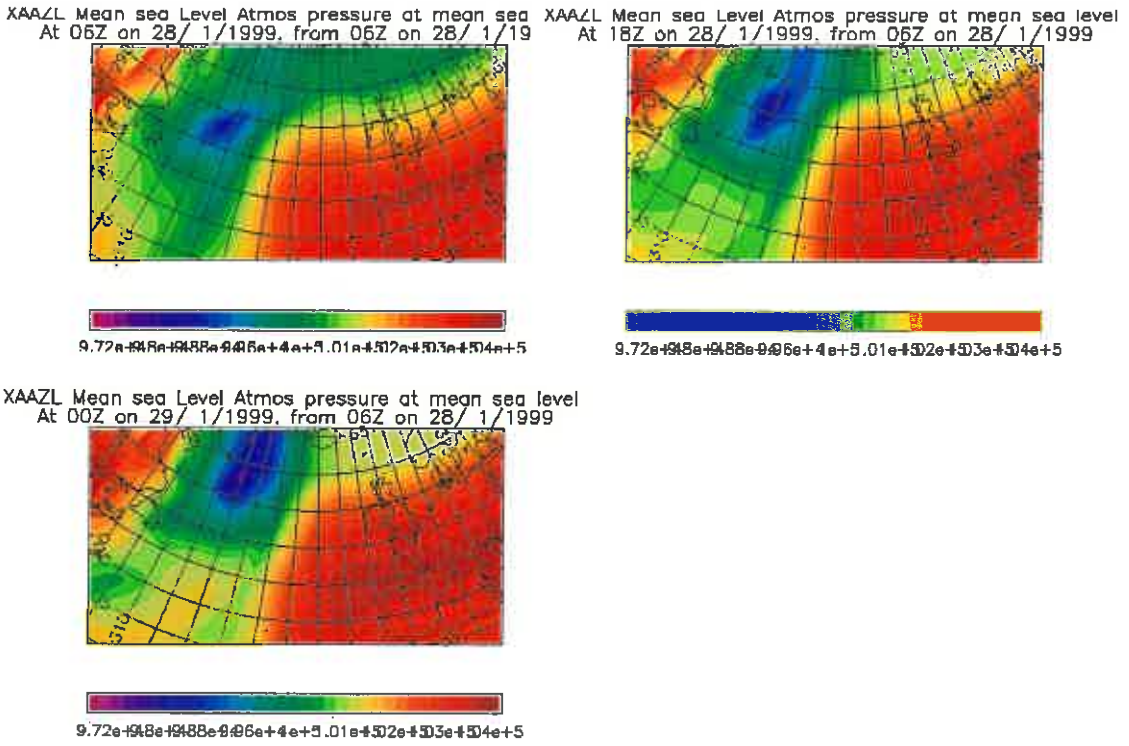

Fig. 4.2.2 Case 2: PMSL forecast from analysis

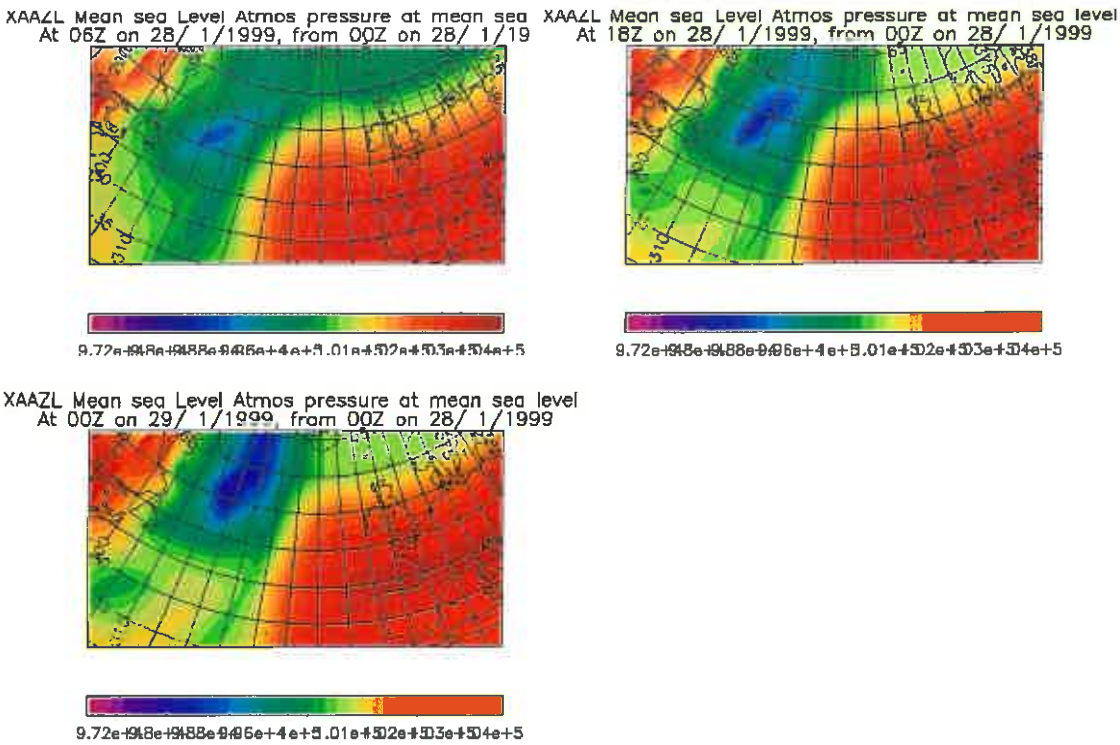

Fig. 4.2.3 Case 2: PMSL forecast from background

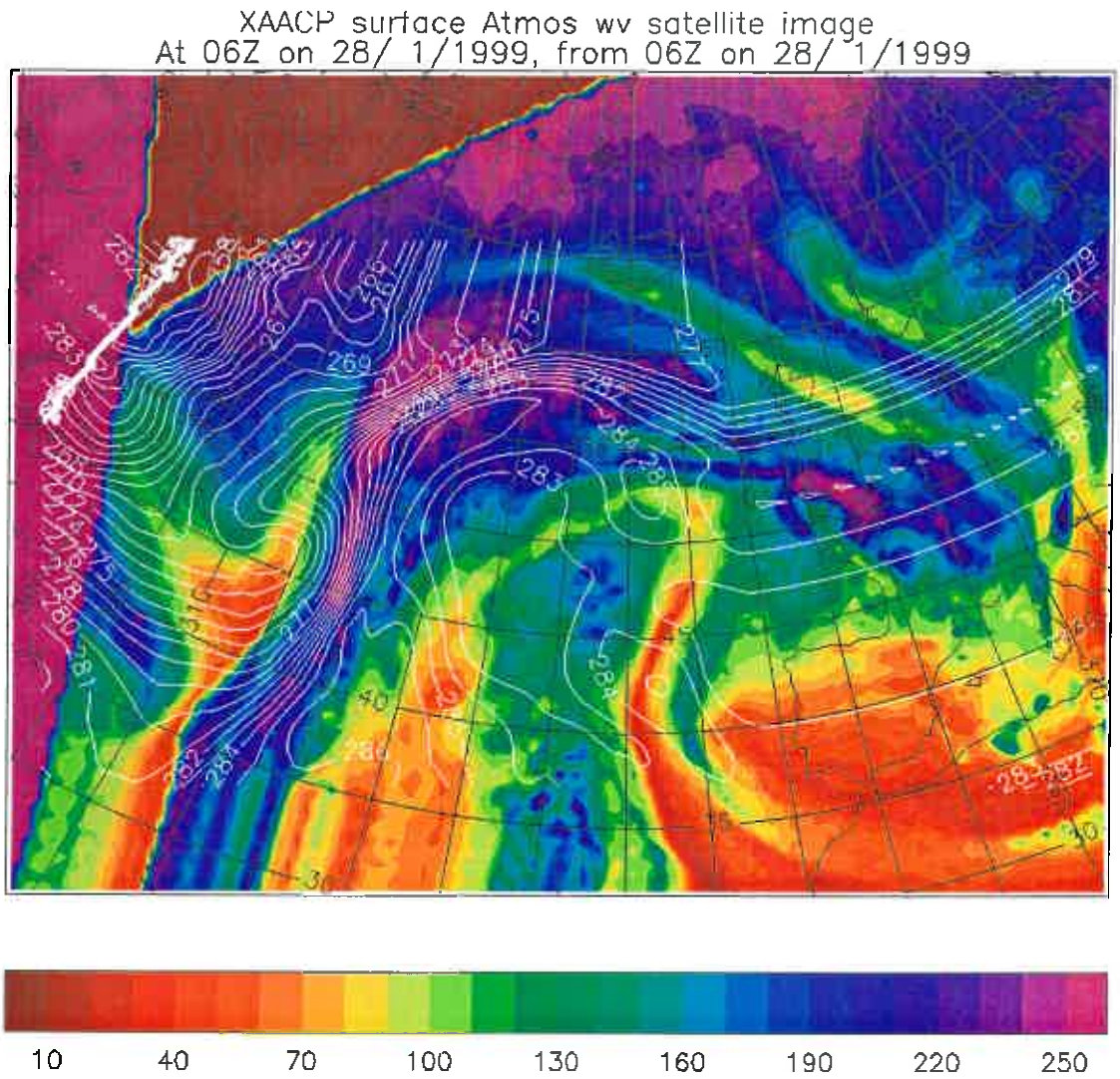

Fig. 4.2.4 Case 2: WV image with contours of PV on 300hPa at T+0

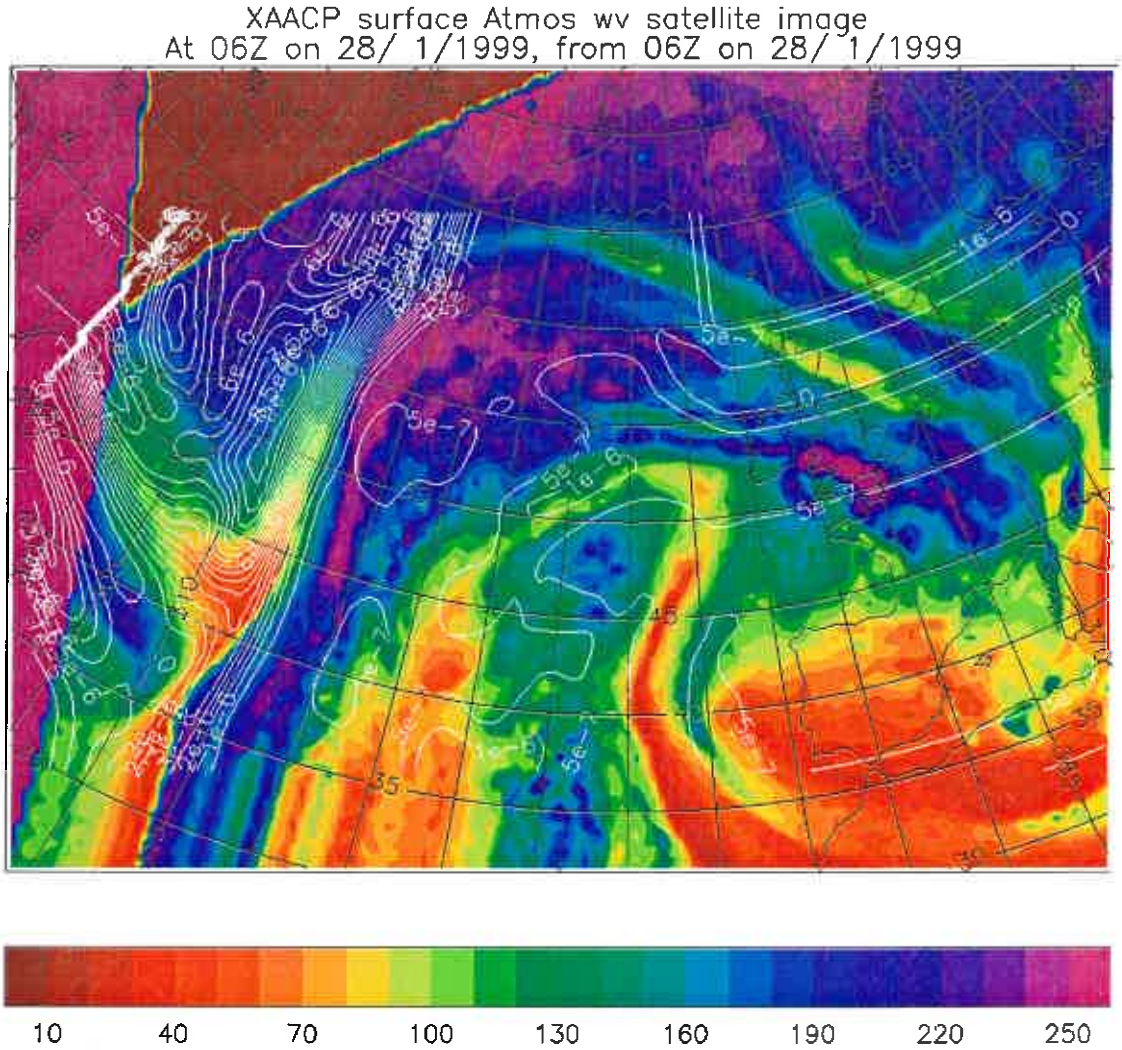

Fig. 4.2.5 Case 2: WV image with contours of theta-w on 850hPa at T+0

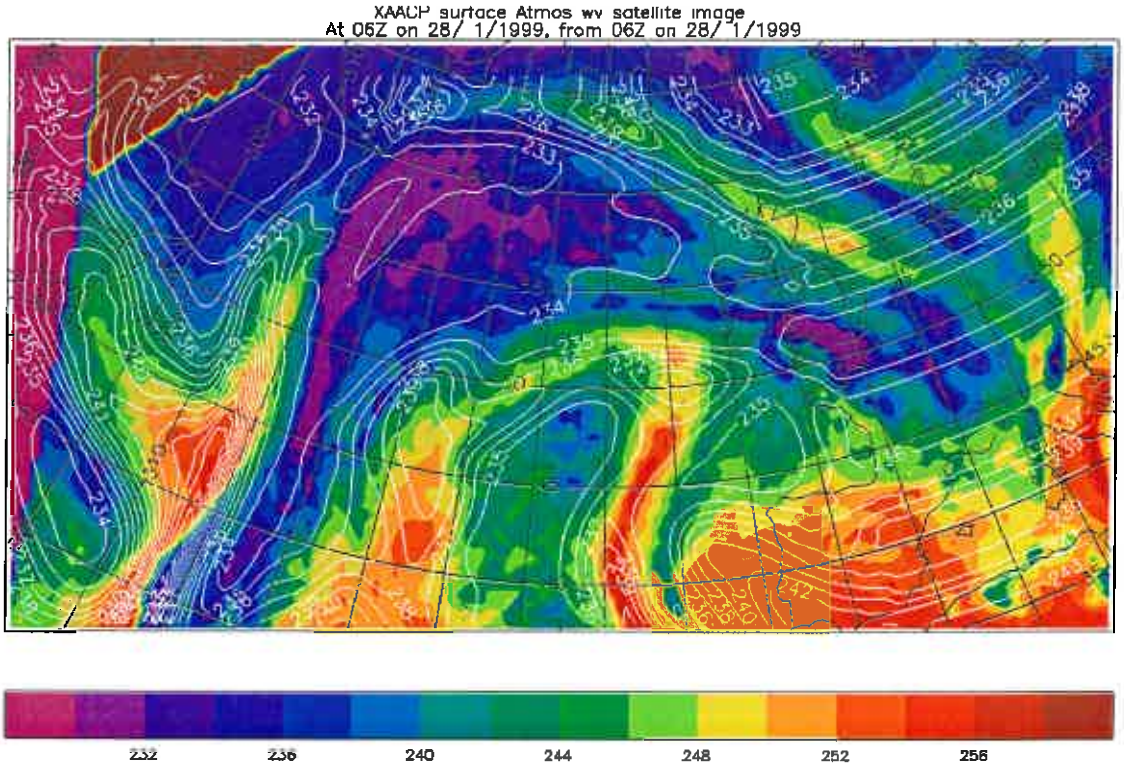

Fig. 4.2.6 Case 2: WV image with contours of pseudo-WV image at T+0

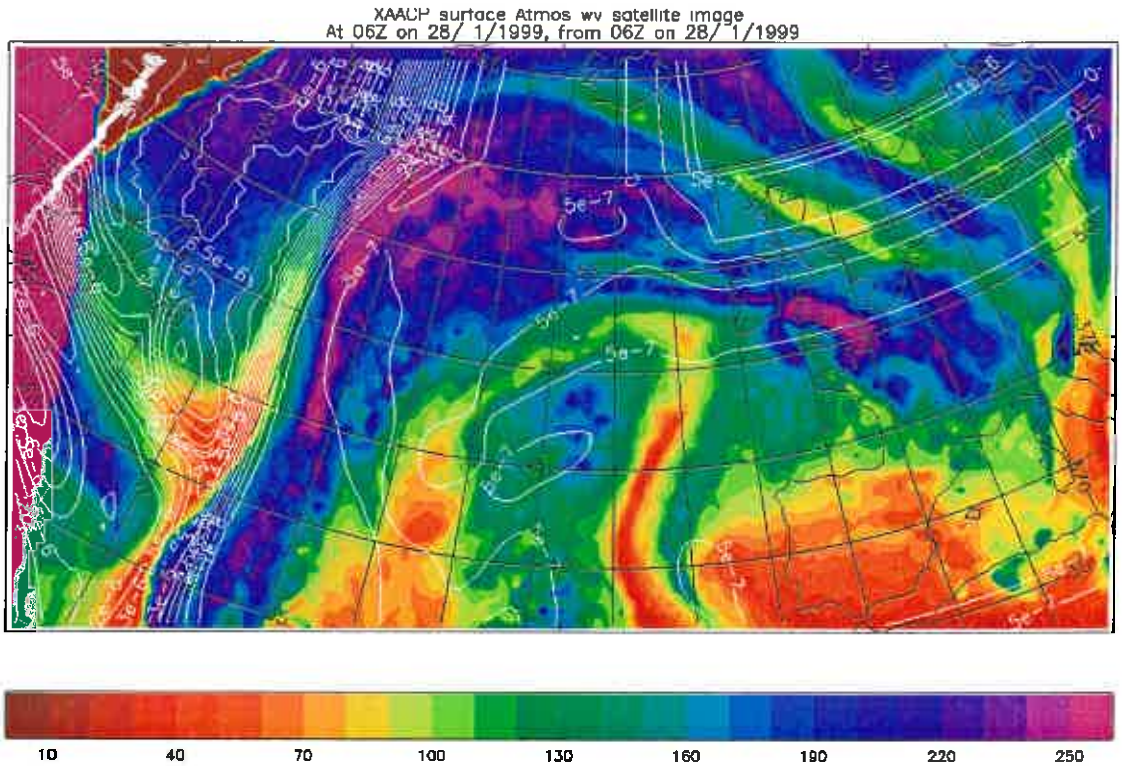

Fig. 4.2.7 Case 2: WV image with contours of manually edited PV field on 300hPa (input to PV inversion). The manually edited region is just SE of Newfoundland.

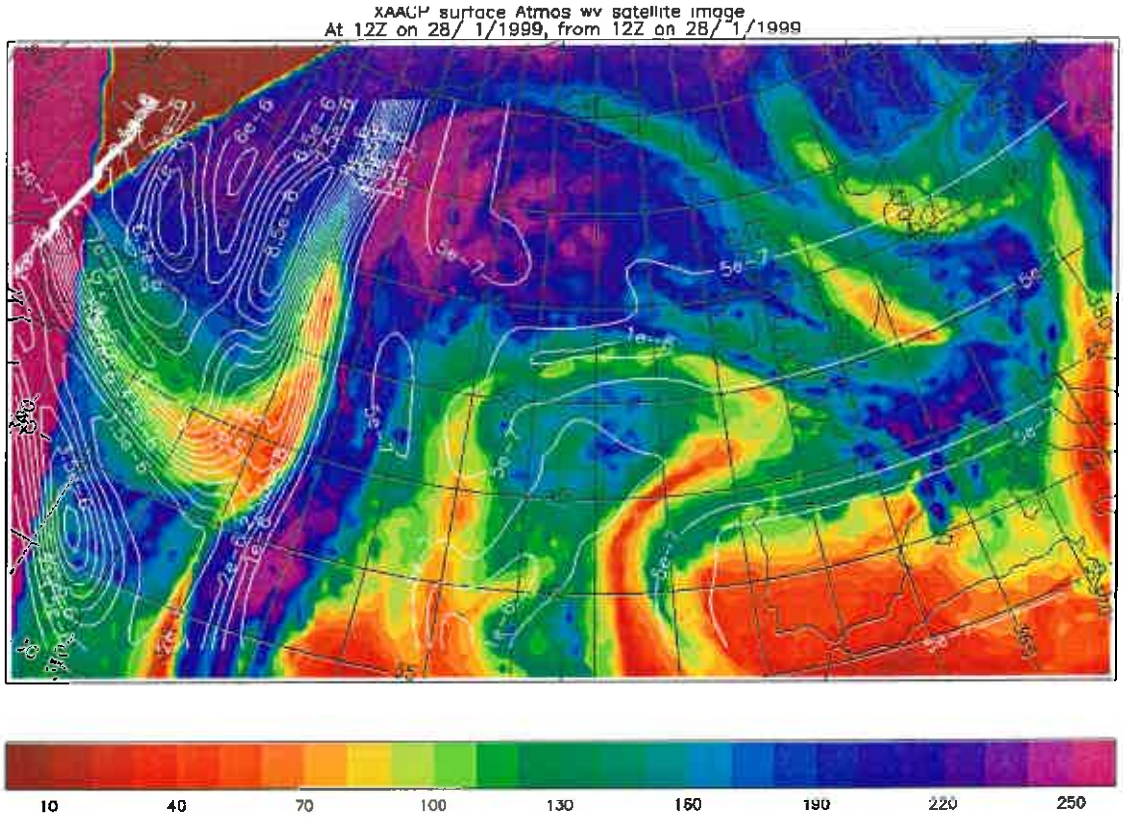

Fig. 4.2.8 Case 2: Sat WV image 12z 28/1/99 with contours of T+6 PV on 300hPa, forecast from analysis

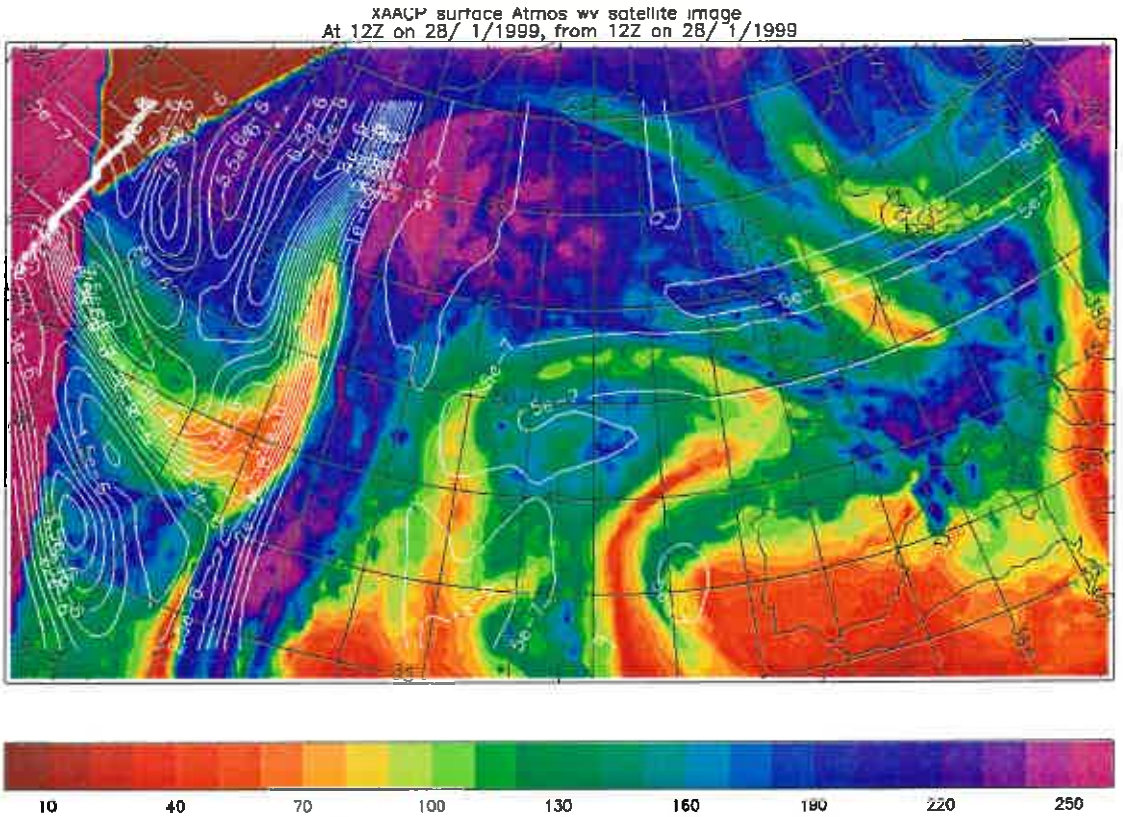

Fig. 4.2.9 Case 2: Sat WV image 12z 280199 with contours of T+6 PV on 300hPa, forecast from background

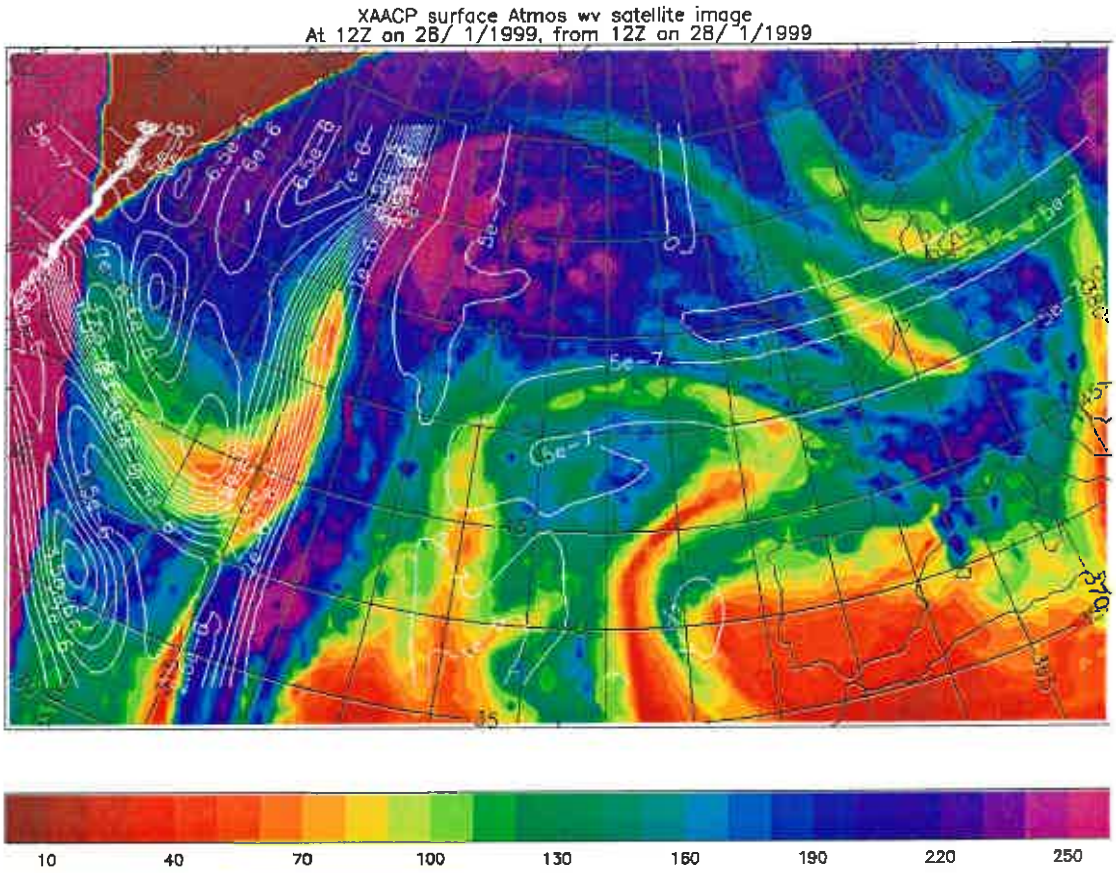

Fig. 4.2.10 Case 2: Sat WV image 12z 280199 with contours of T+6 PV on 300hPa, rerun forecast

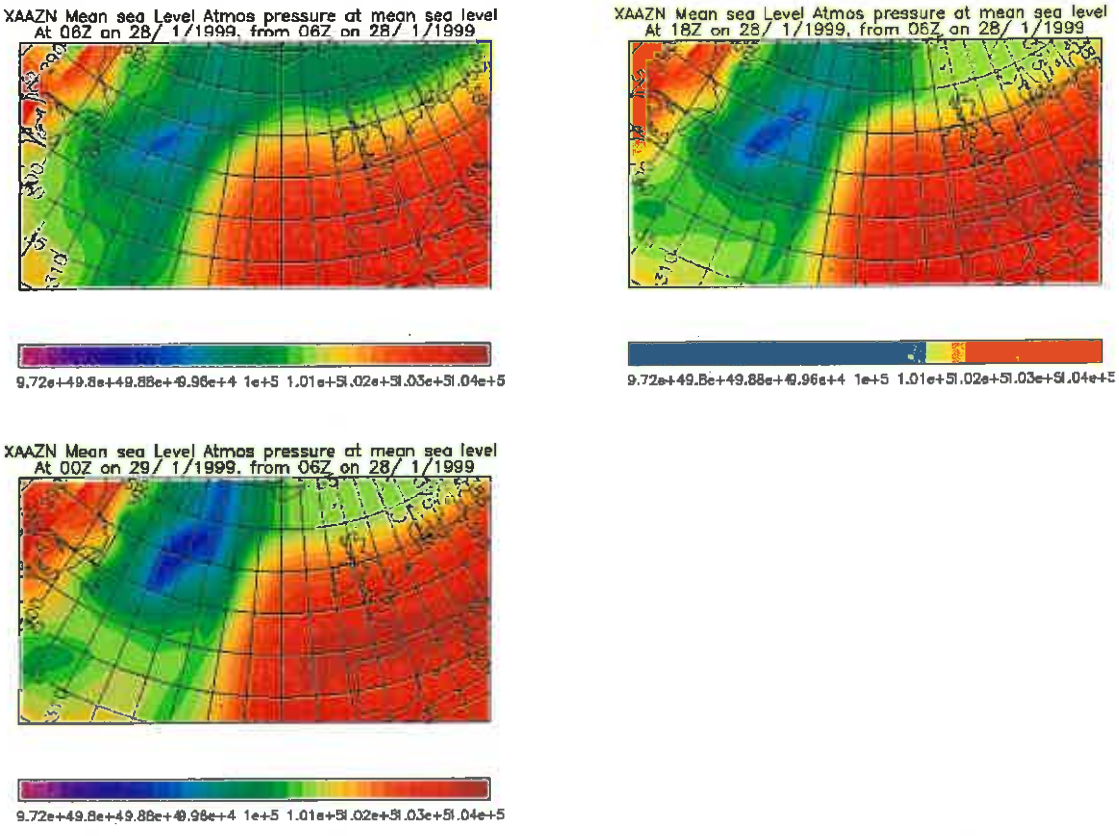

Fig. 4.2.11 Case 2: PMSL rerun forecast from adjusted background

CASE 3: 06z 5/2/99 (25%, 3hPa)

Pmsl fields (figs. 4.3.1,2,3): This case concerned a cyclone in W Atlantic, which remained almost stationary (since it was adjacent to a large high pressure area). It deepened from 1012 to 1002 up to 18z 5/2/99, then started to fill. At T+12 the forecast cyclone had central pressure about 3hPa too high. The forecast from background followed the same general trend as the forecast from analysis, but the central pressure of the cyclone was 6-10 hPa too high throughout the forecast.

500hPa height fields (fig. 4.3.4) : At 500hPa, the system appeared as a minimum feature in the height field. The forecast from analysis had this feature about correct, except at T+12 when it was a little too deep. The forecast from background had this feature a little deeper than the analyses throughout the forecast.

WV image & PV at 300hPa (fig.4.3.7): The WV image for 06z 050299 shows a curving dry intrusion feature over the W Atlantic, apparently associated with the cyclonic system in question. The analysed PV field at 300hPa shows a large intense PV anomaly apparently well matched with this dry intrusion.

850hPa theta-w field (fig.4.3.8): The 850hPa theta-w field, both analysed and background, also appears to be well matched with the satellite image. The WCB appears to be in about the correct location, corresponding with the cloudy region just E of the dry intrusion. The fact that these low-level structures appear to be correctly disposed relative to the satellite image suggests that any forecast errors are likely to be due to errors in the upper-level fields.

Rerun 1: The original forecast had very little error and so offered little scope for improvement. (It may be argued that this case was not a very useful one to study, but this was not appreciated a priori). However, there was a significant difference between the forecast from analysis and the forecast from background. The background PV fields were therefore modified and the forecast rerun from the modified background without data assimilation. The objective was to see if the PV modification could act as a substitute for data assimilation. The PV anomaly in the background fields was scaled up by a factor of 1.3 on pressure levels 300-420hPa, every 20hPa (fig. 4.3.9). This PV modification was based on past experience rather than on the PV/WV comparison.

The result of this adjustment was to deepen the surface cyclone to a value close to that of the forecast from analysis (figs. 4.3.10).

The effect on the 500hPa height field (fig 4.3.11) was to increase the error, i.e. it made the minimum height lower rather than increasing it.

Rerun 2: In this rerun, an attempt was made to improve the fit of the PV anomaly to the WV image by displacing just the central portion of the anomaly (PV > 5 units at 300hPa) by about 2 degrees to the SE. Unfortunately, the rerun crashed with a floating point exception on UM timestep 12, in a routine which computes the theta-w diagnostic. This crash was not investigated, apart from carrying out some basic checks to ensure that the reason for the crash was non-trivial. It appears that the UM could not cope with the PV adjustment which was made in this rerun.

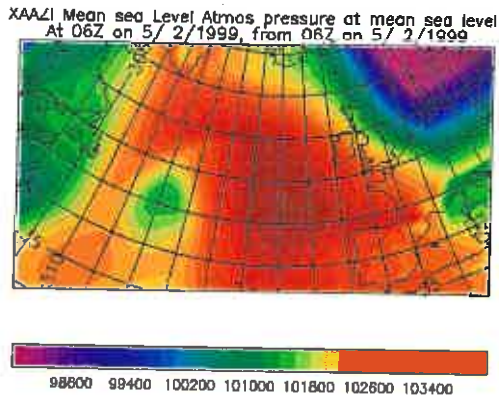

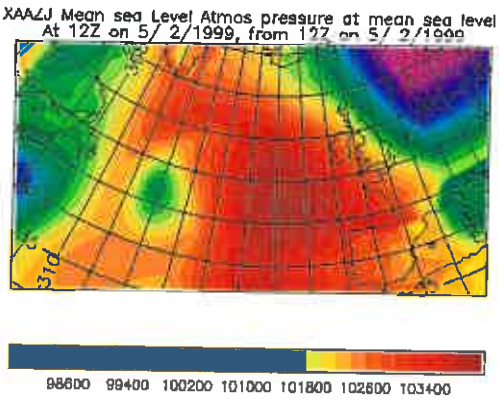

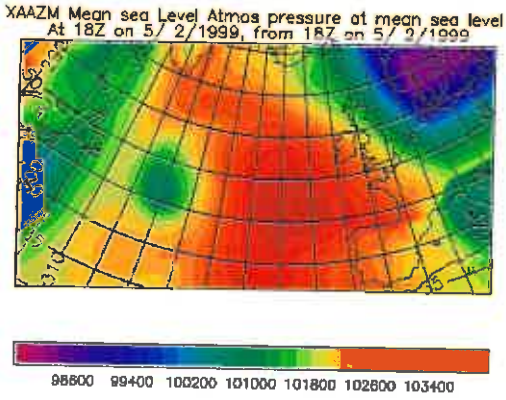

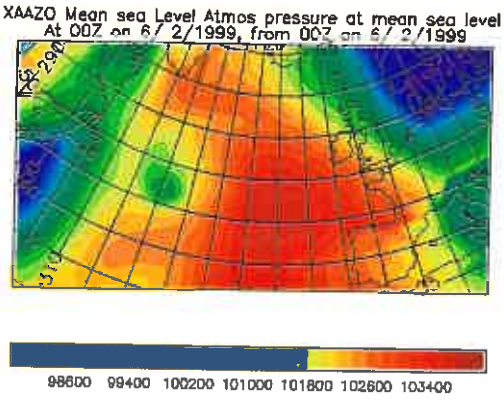

Fig. 4.3.1 Case 3: PMSL analyses

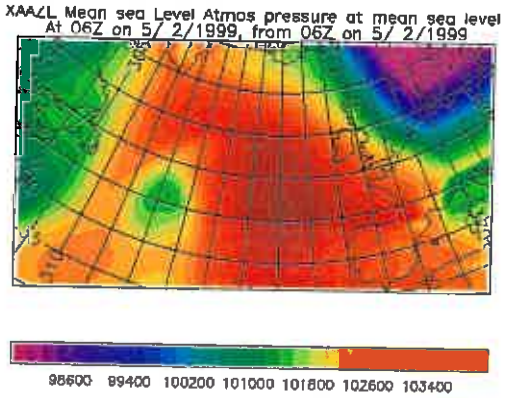

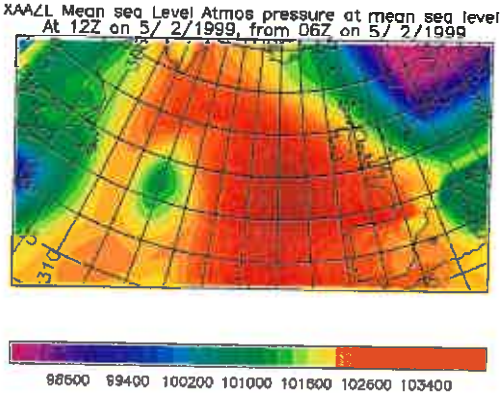

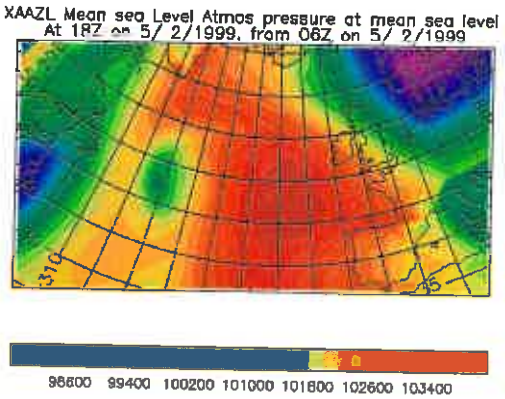

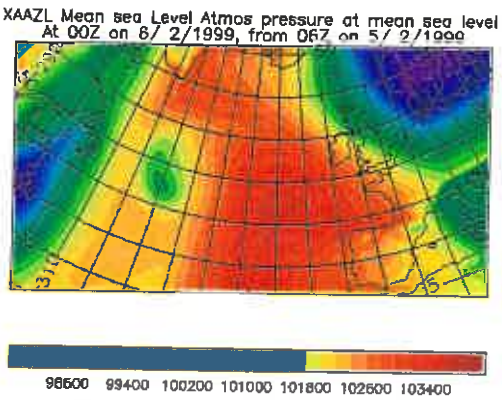

Fig. 4.3.2 Case 3: PMSL forecast from analysis

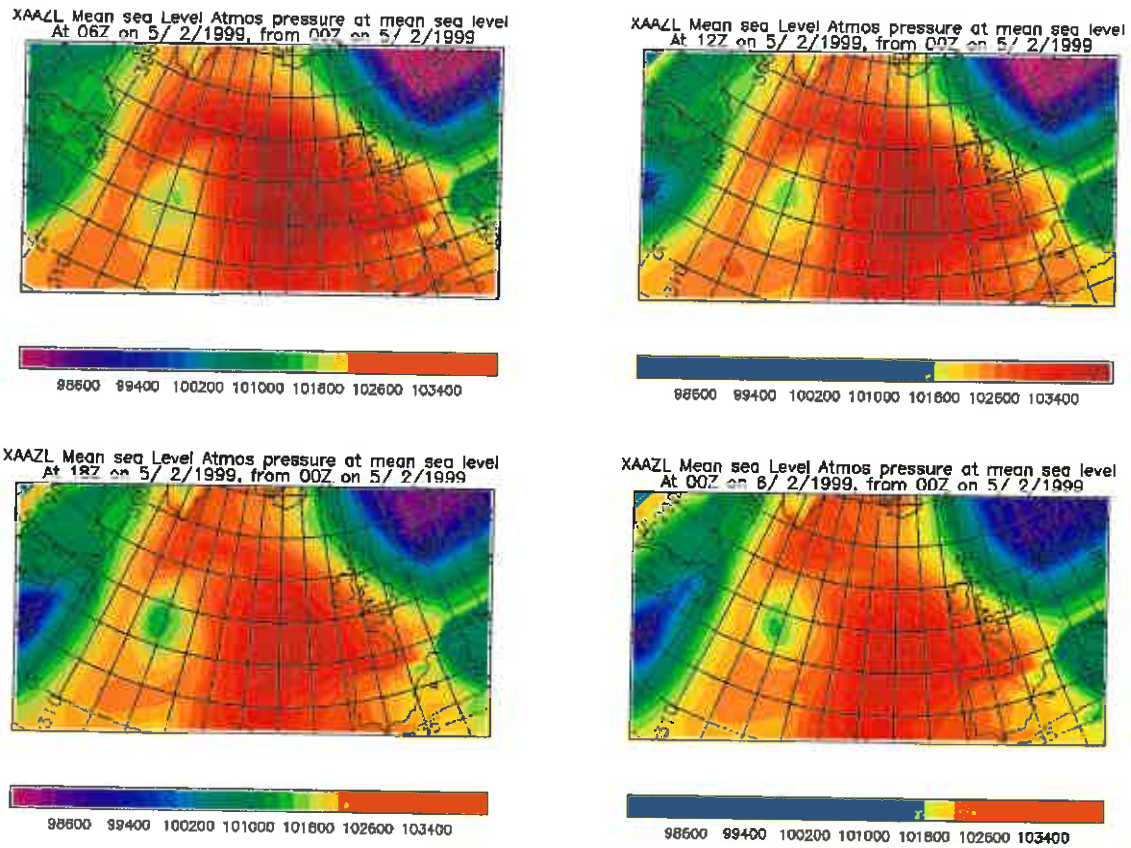

Fig. 4.3.3 Case 3: PMSL forecast from background

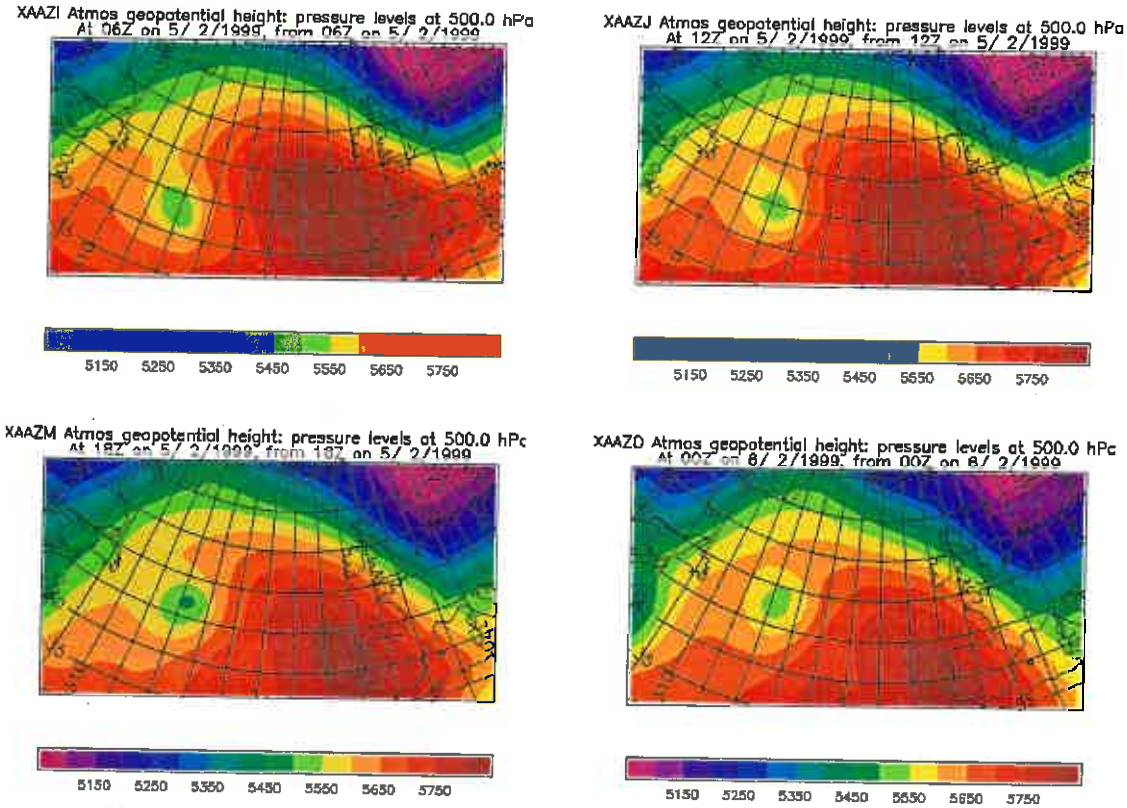

Fig. 4.3.4 Case 3: 500hPa height analyses

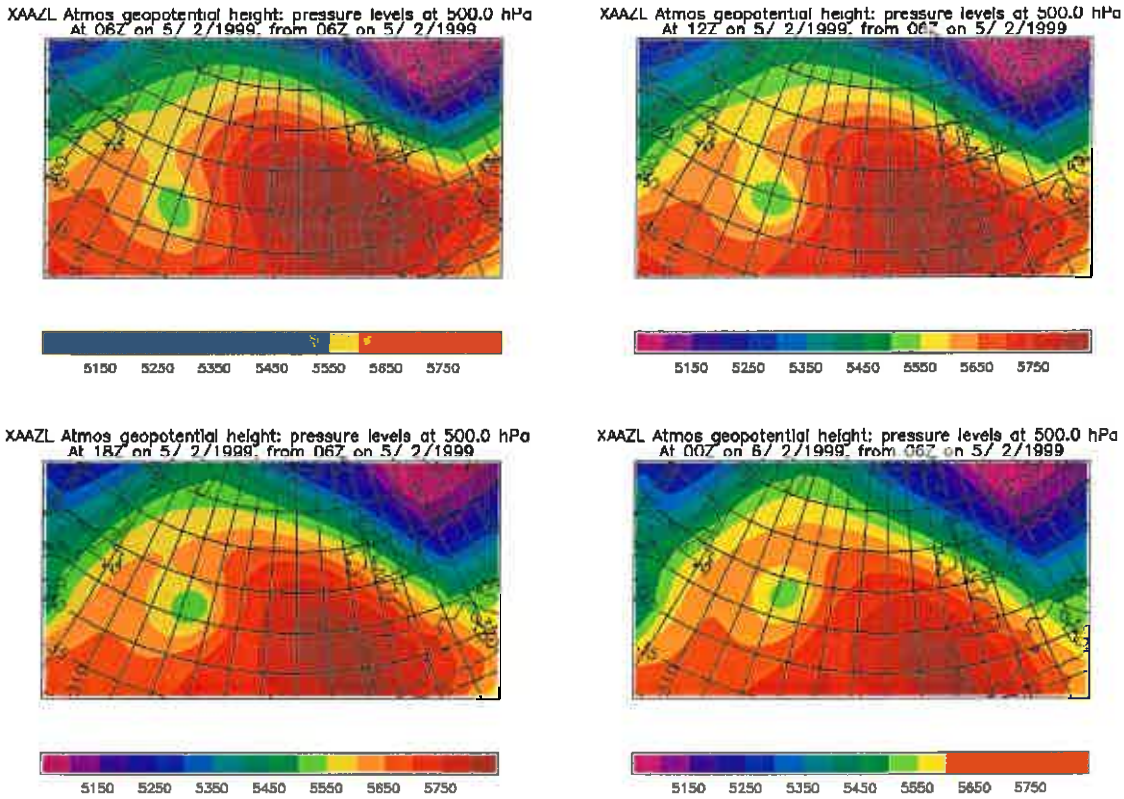

Fig. 4.3.5 Case 3: 500hPa height forecast from analysis

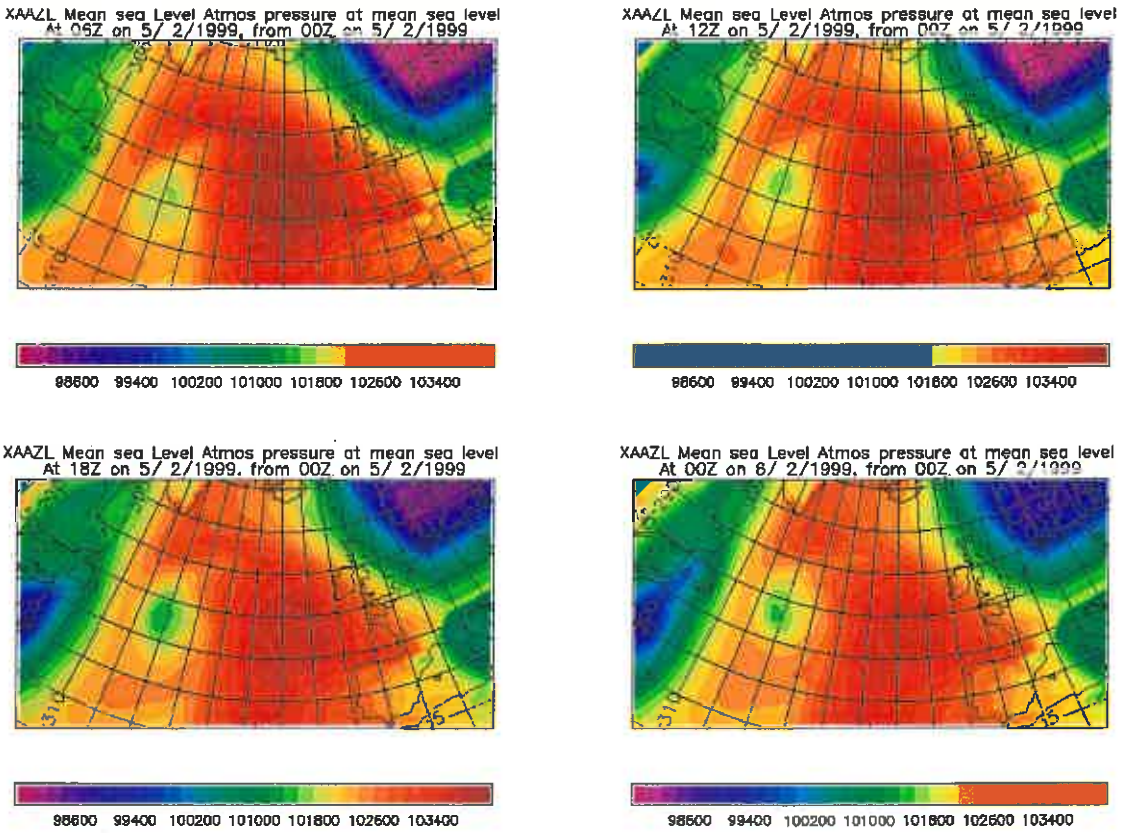

Fig. 4.3.6 Case 3: 500hPa height forecast from background

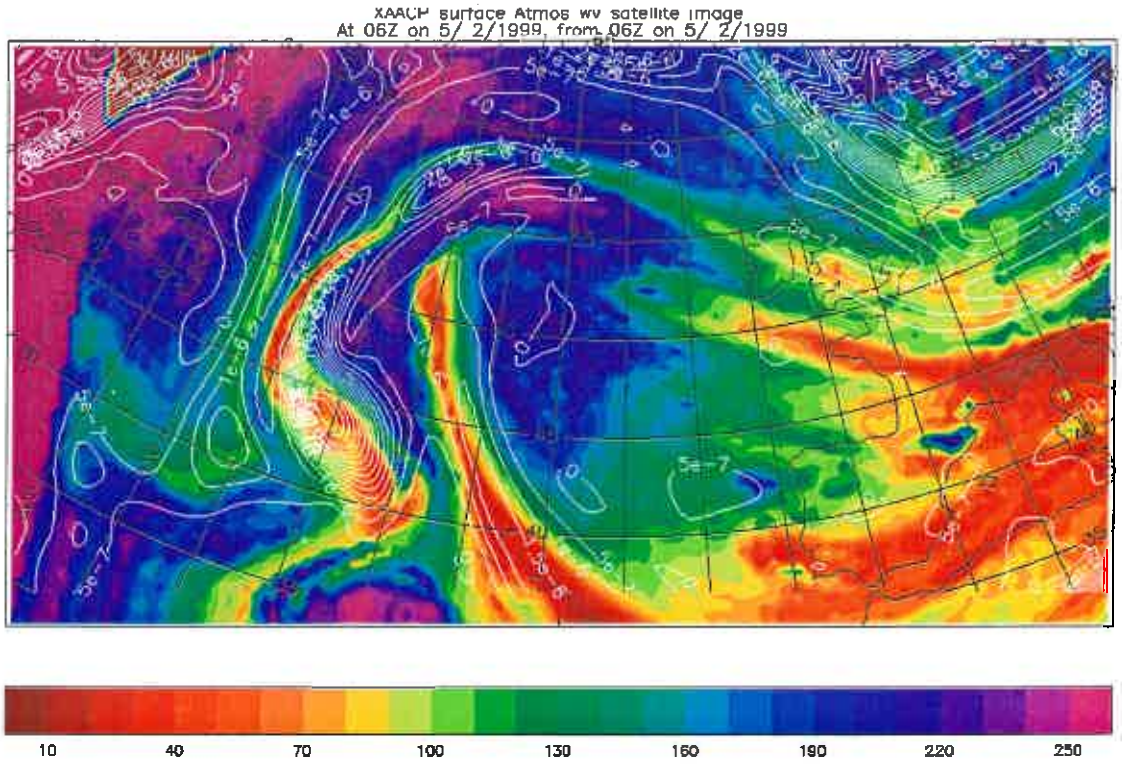

Fig. 4.3.7 Case 3: WV image with contours of background PV on 300hPa at T+0

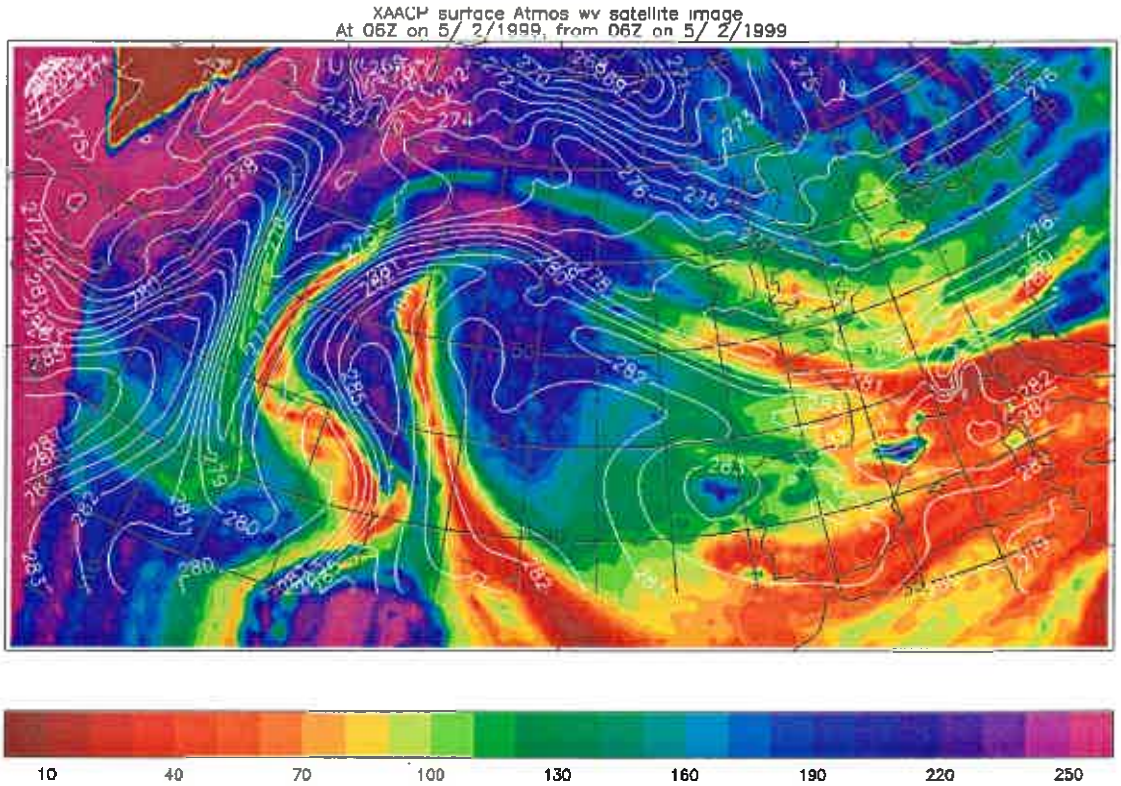

Fig. 4.3.8 Case 3: WV image with contours of analysed theta-w on 850hPa at T+0

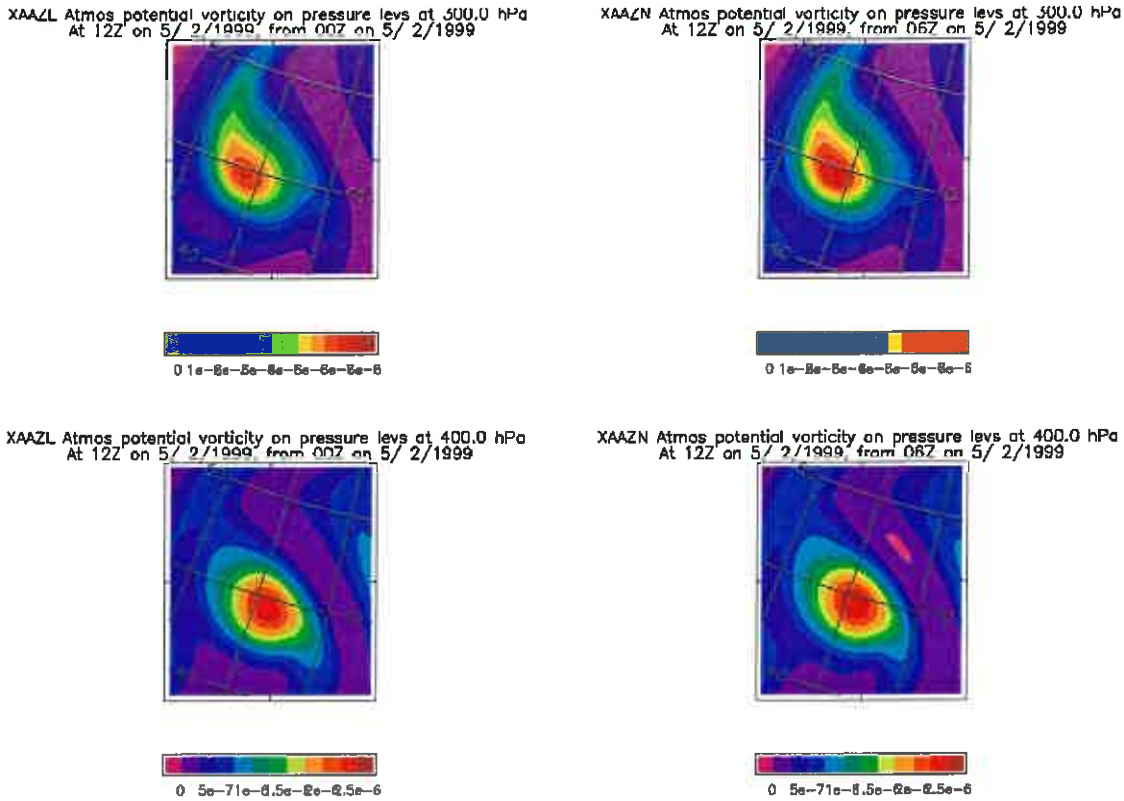

Fig. 4.3.9 Case3: T+6 PV fields: forecast from background (lhs) and forecast from adjusted background (rhs)

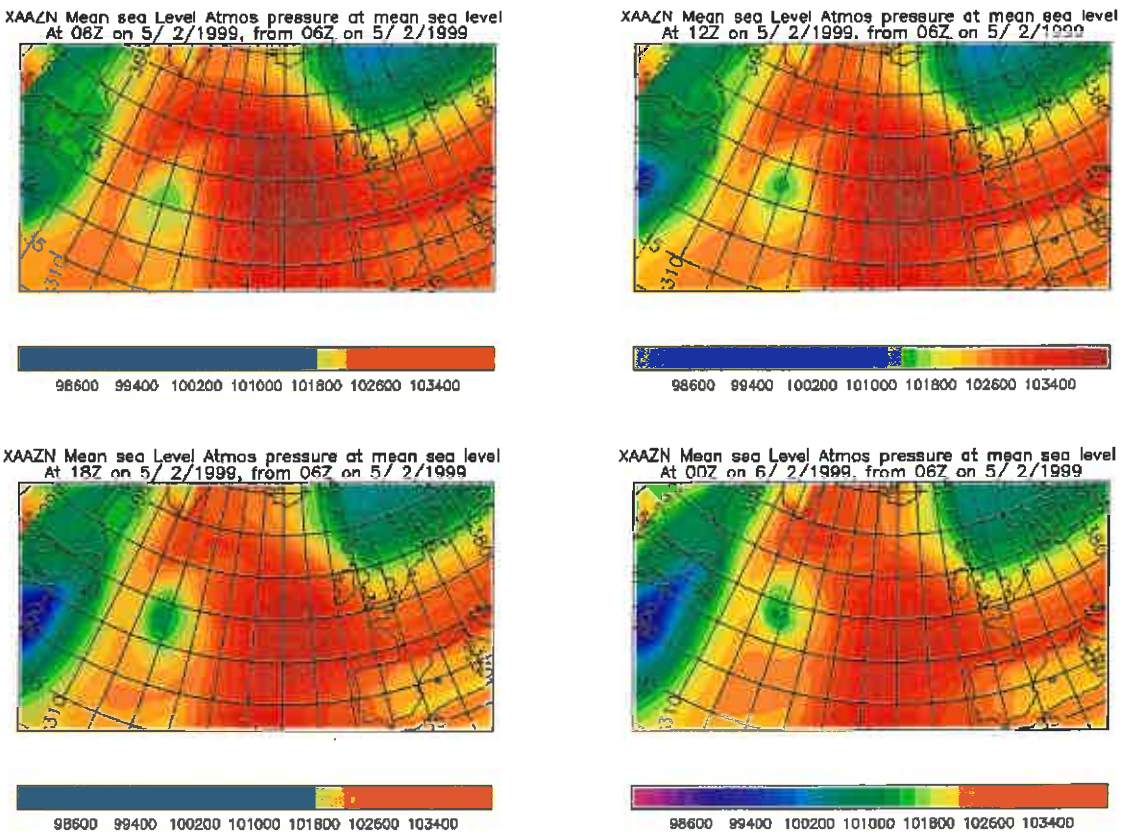

Fig. 4.3.10 Case 3: PMSL forecast from adjusted background

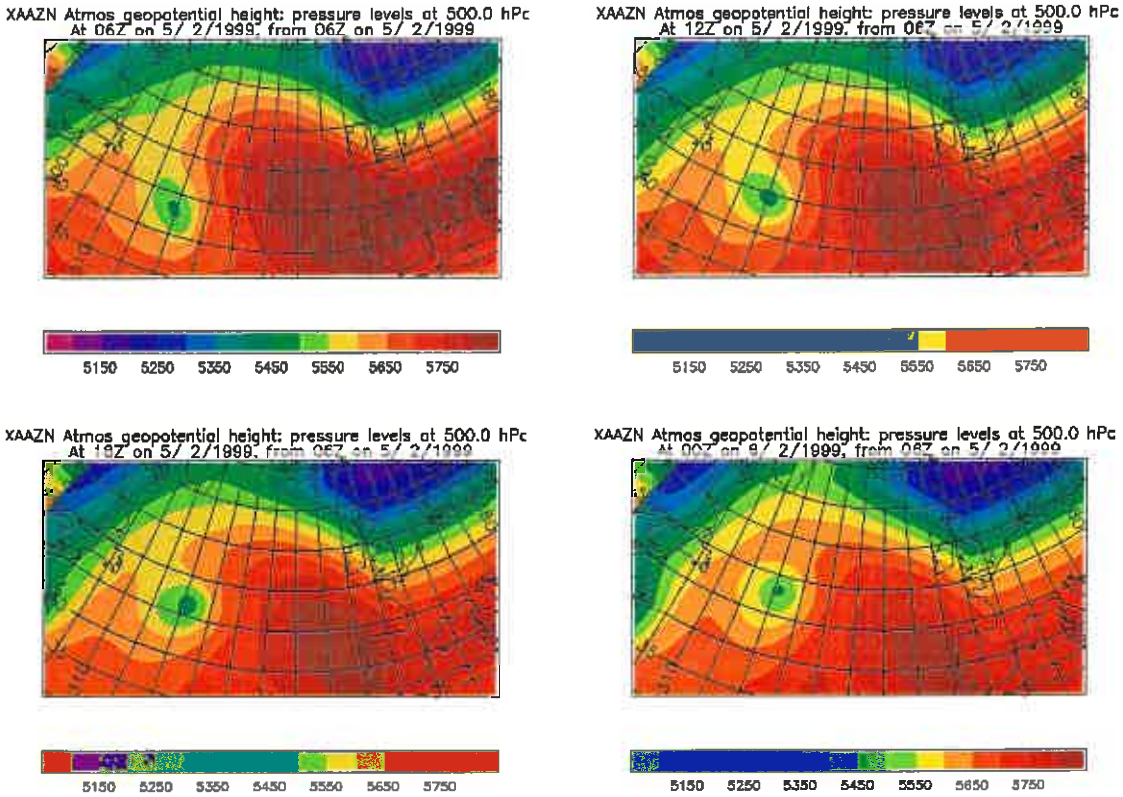

Fig. 4.3.11 Case 3: 500hPa height forecast from adjusted background

CASE 4: 12z 23/4/99 (45%, 1hPa)

Pmsl fields: This case, like the others, was selected from the Semple review of cyclonic forecasts, although it does not appear to be a very suitable case for the PV-water vapour approach. The system is a large mature quasi-stationary mid-Atlantic cyclone. At T+12 the forecast error according to Semple's assessment was 45% location error and virtually no pressure error. However, at T+18 it appears that there is a significant pressure error (about 4hPa too high) and virtually no location error. This may be because the low is rather broad and so the position of the low centre is actually difficult to locate precisely. The change in pressure error seems to suggest that the forecast failed to develop the deepening after T+12 which the real system actually underwent. (See figs. 4.4.1,2,3). There is very little difference between the forecast from analysis and the forecast from background.

PV fields & water vapour image: Figs. 4.4.4 & 5 show the 300 & 400hPa PV fields for 12z 23/4/99 overlaid on the water vapour image. There is little difference between the analysed and background fields. A prominent dry intrusion feature can be seen starting just S of Newfoundland and curving out into the mid-Atlantic. Associated with this is a similarly curving PV anomaly which appears to be well matched with the dry intrusion feature. The level-by-level PV field plots (fig. 4.4.6) show that this PV anomaly does not have a very great vertical extent.

850hPa theta-w fields: Fig. 4.4.7 shows that the PV anomaly referred to above is apparently coupled to a low level baroclinic zone. There is little difference between the analysed and background fields. This apparent coupling suggests that the forecast cyclone development is likely to be sensitive to adjustments of this particular PV anomaly.

Rerun: The PV/water vapour image comparison for this case does not appear to give any useful guidance; as already noted, the cyclone is too mature for PV/WV analysis to be meaningful anyway. However, a sensitivity study was carried out, in which the PV anomaly referred to above was scaled up by 1.2 (fig. 4.4.8). Its effect on the cyclone was to deepen it slightly, and also to move the position of the low centre slightly to the NW. Overall, this represents a small reduction in the forecast error (fig. 4.4.7).

Convergence difficulties: This case presented some interesting difficulties with convergence of the PV inverter. Initially, PV inversion on the unmodified background PV fields failed – the error parameters became effectively infinite on the second iteration. N. Keeley suggested changing the PV inverter's horizontal length scale parameter from 2500km (its usual value) to 3500km. (See appendix for the significance of this parameter in the formulation). This was successful – convergence was achieved in 42 iterations (with both convergence thresholds at 0.05). Convergence with the modified PV fields was rather more difficult, taking 249 iterations. It appears that stability of the PV inversion for this case is remarkably sensitive to both the input data and the formulation of the algorithm.

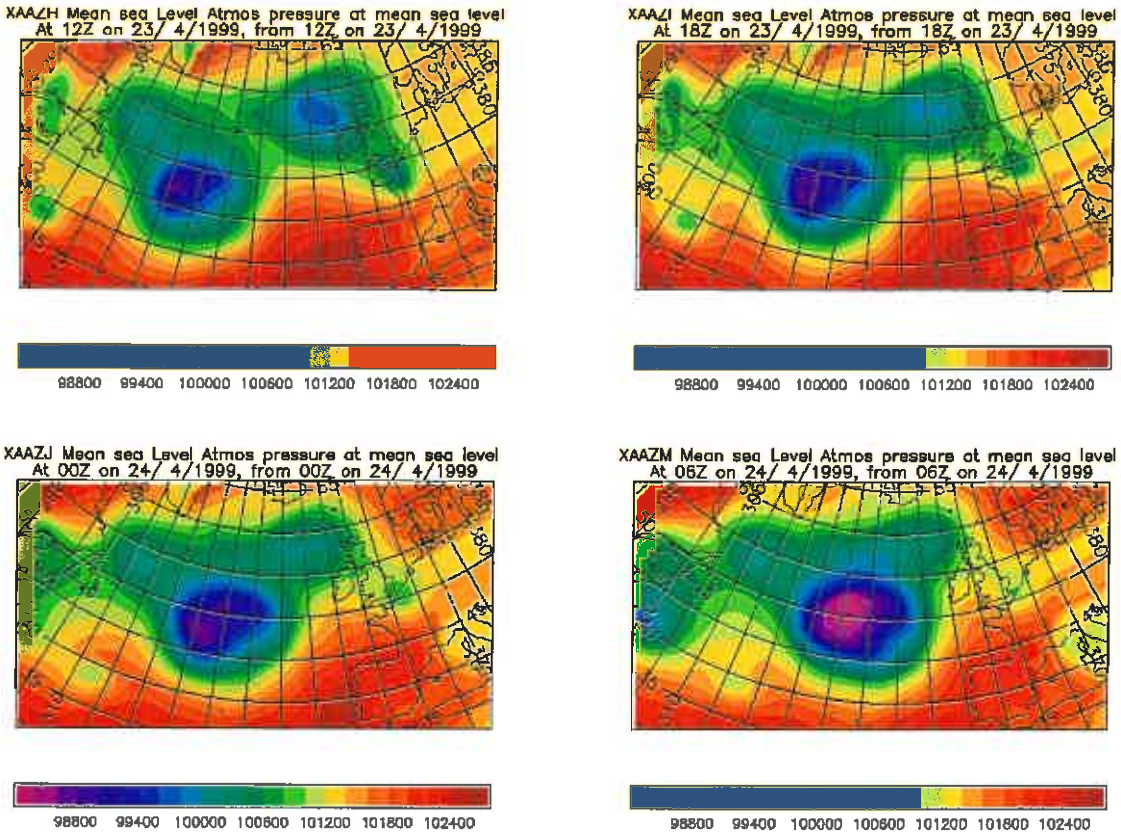

Fig. 4.4.1 Case 4: PMSL analyses

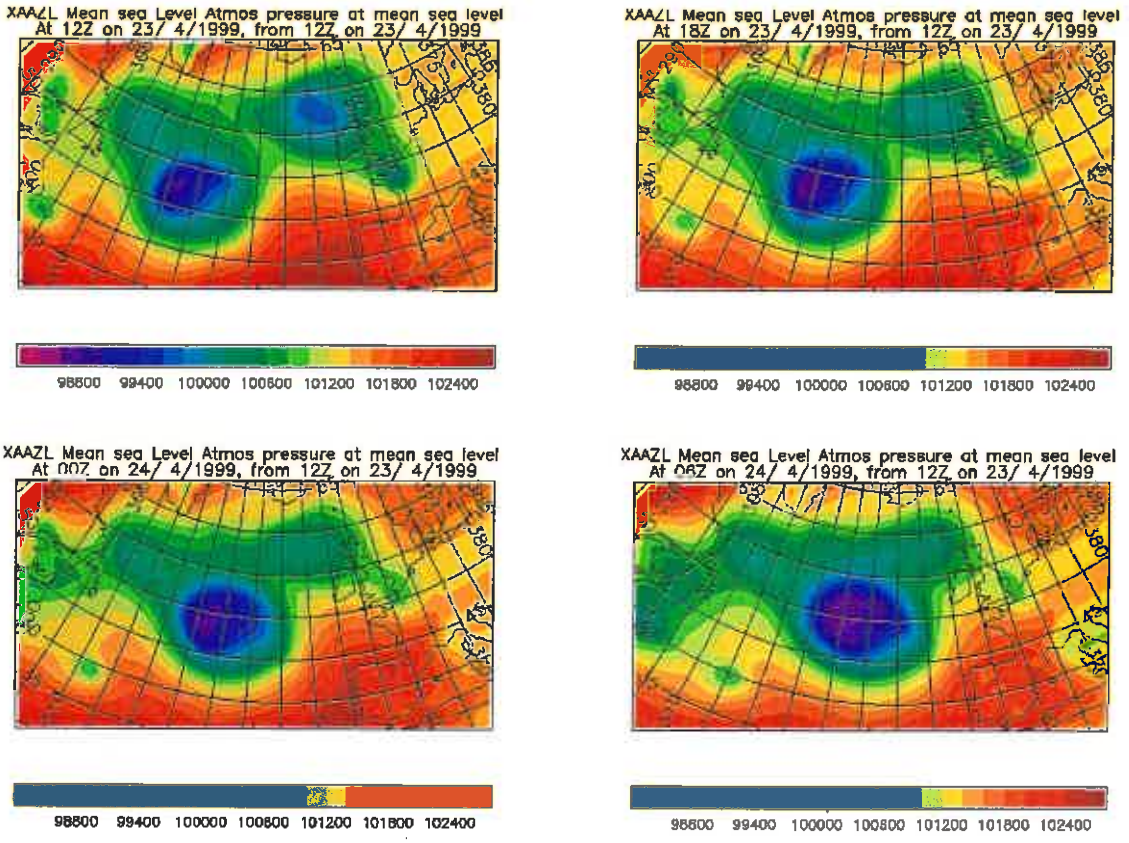

Fig. 4.4.2 Case 4: PMSL forecast from analysis

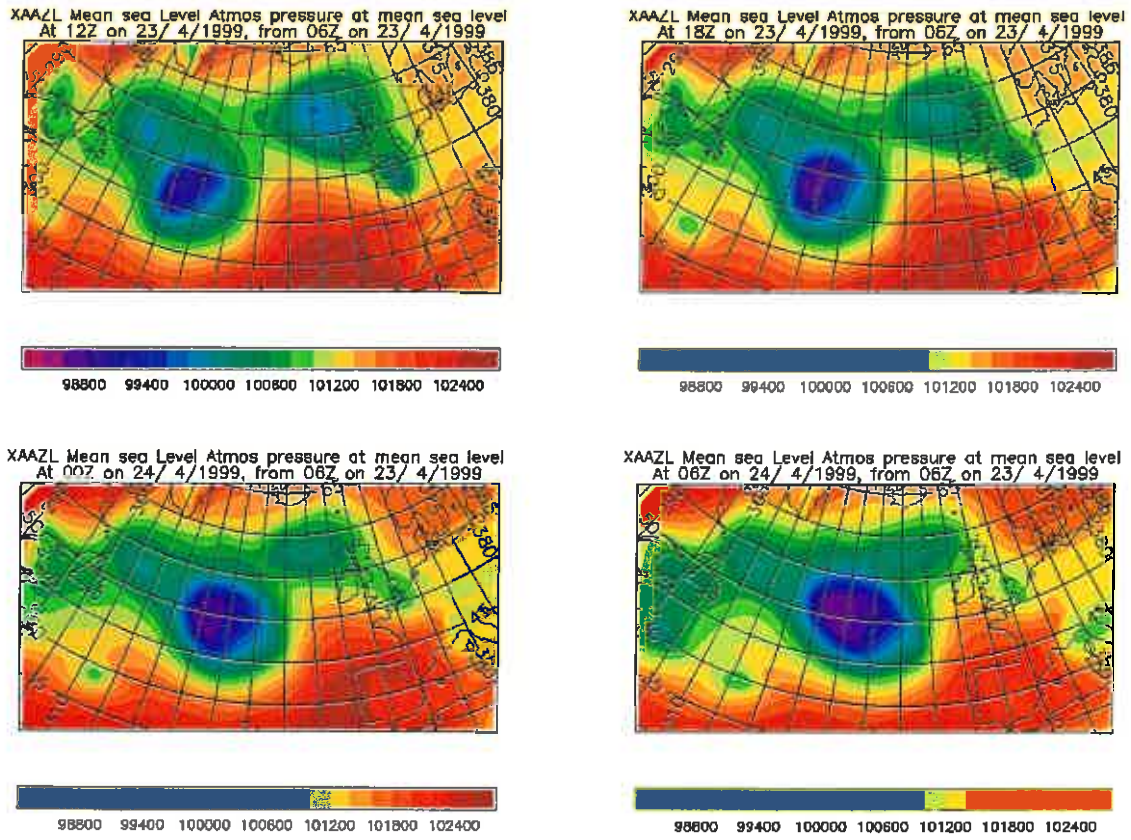

Fig. 4.4.3 Case 4: PMSL forecast from background

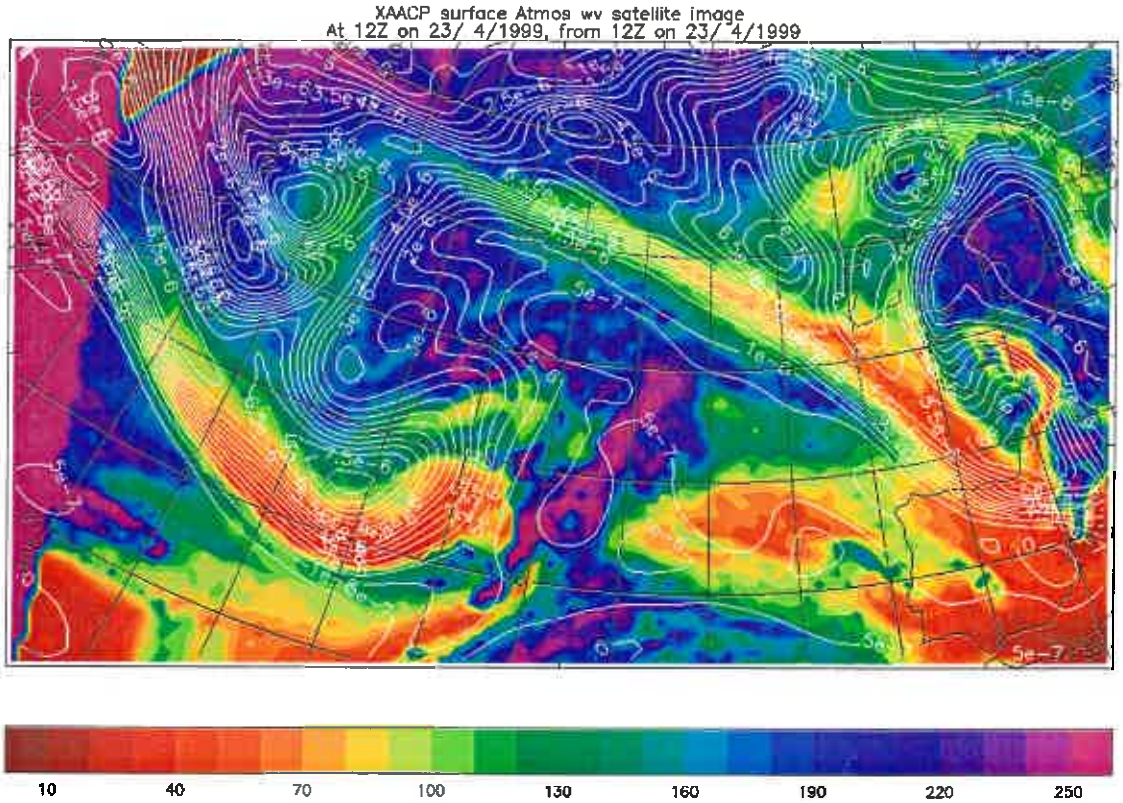

Fig. 4.4.4 Case 4: WV image with contours of background PV on 300hPa at 12z 23/4/99

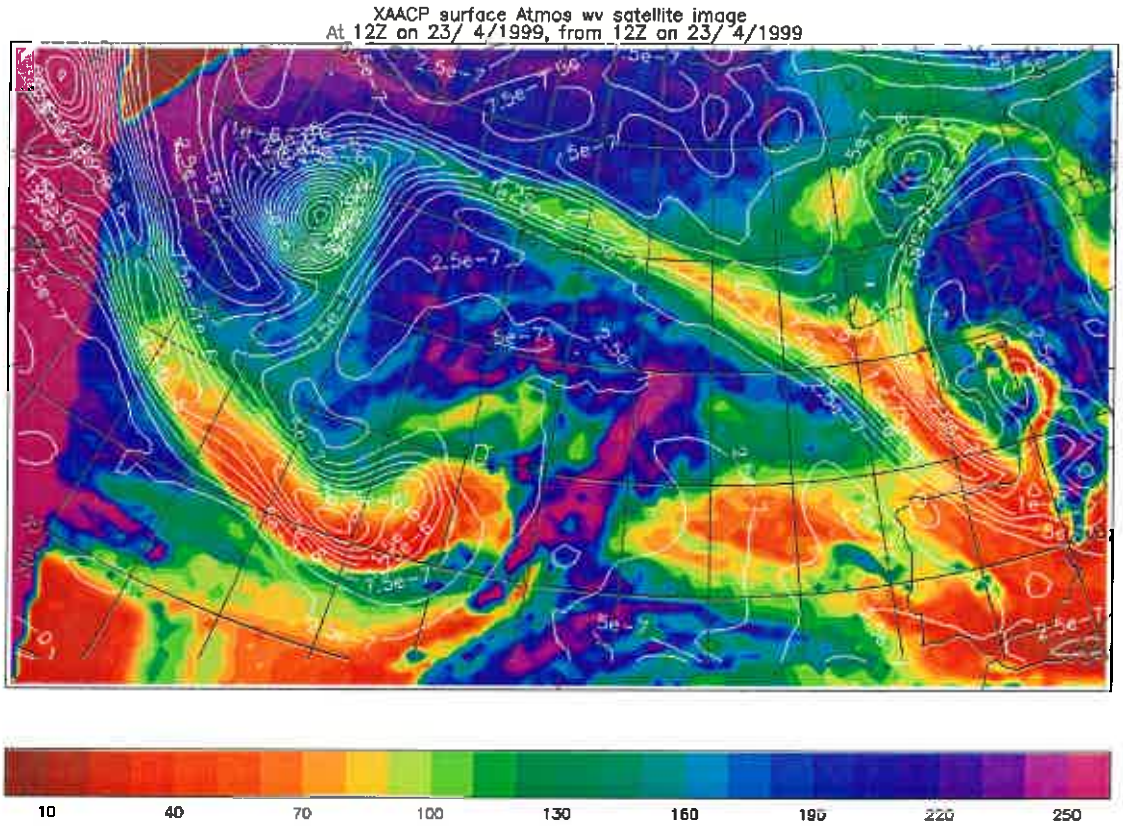

Fig. 4.4.5 Case 4: WV image with contours of background PV on 400hPa at 12z 23/4/99

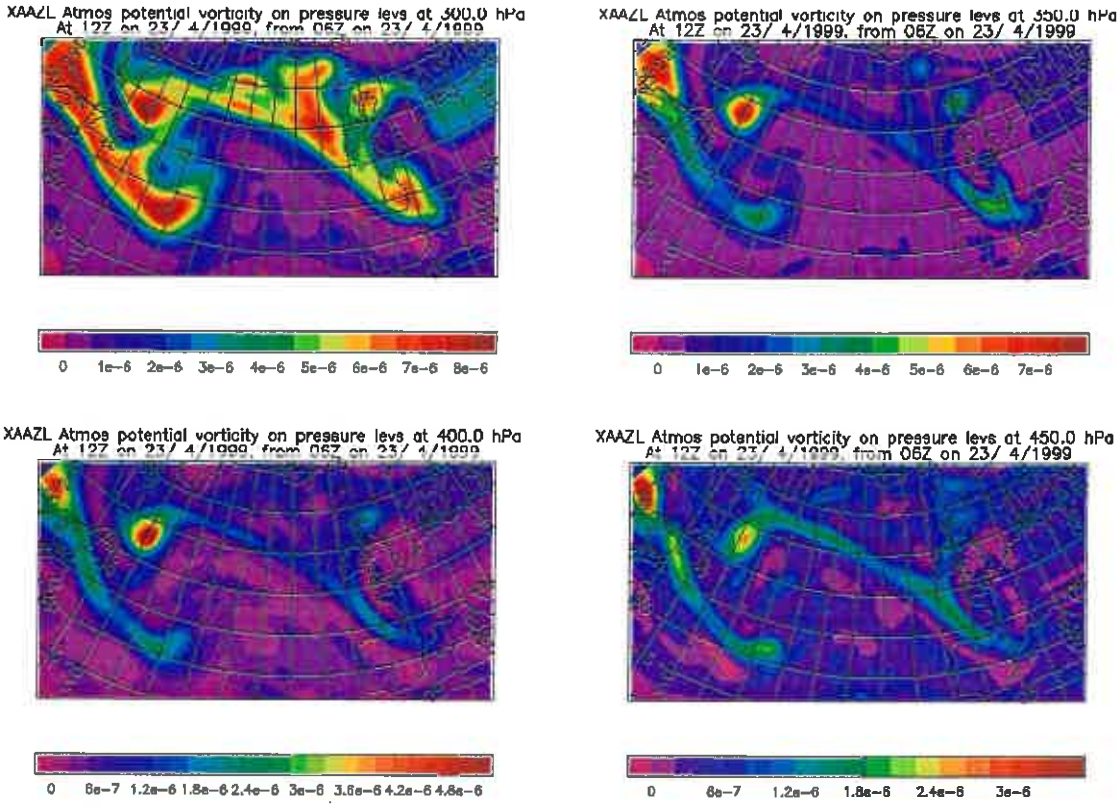

Fig. 4.4.6 Case 4: Background PV fields at 12z 23/4/99 on levels 300-450hPa

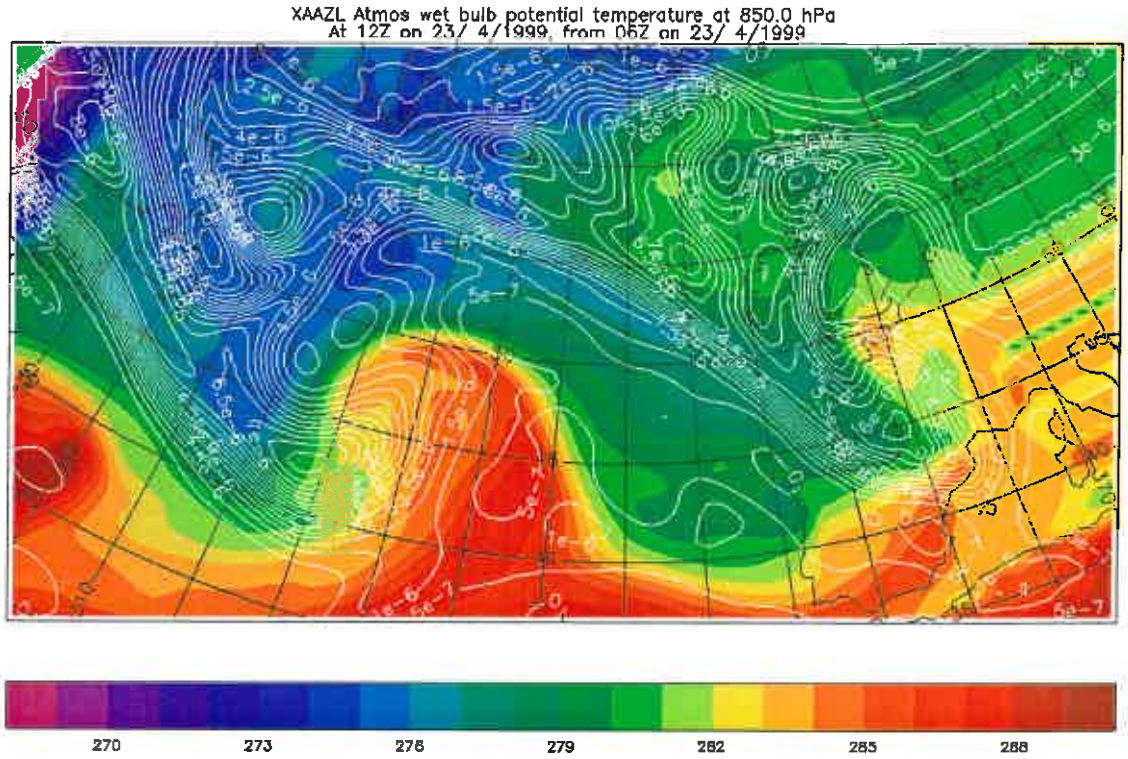

Fig. 4.4.7 Case 4: PV at 300hPa with contours of background theta-w on 850hPa at 12z 23/4/99

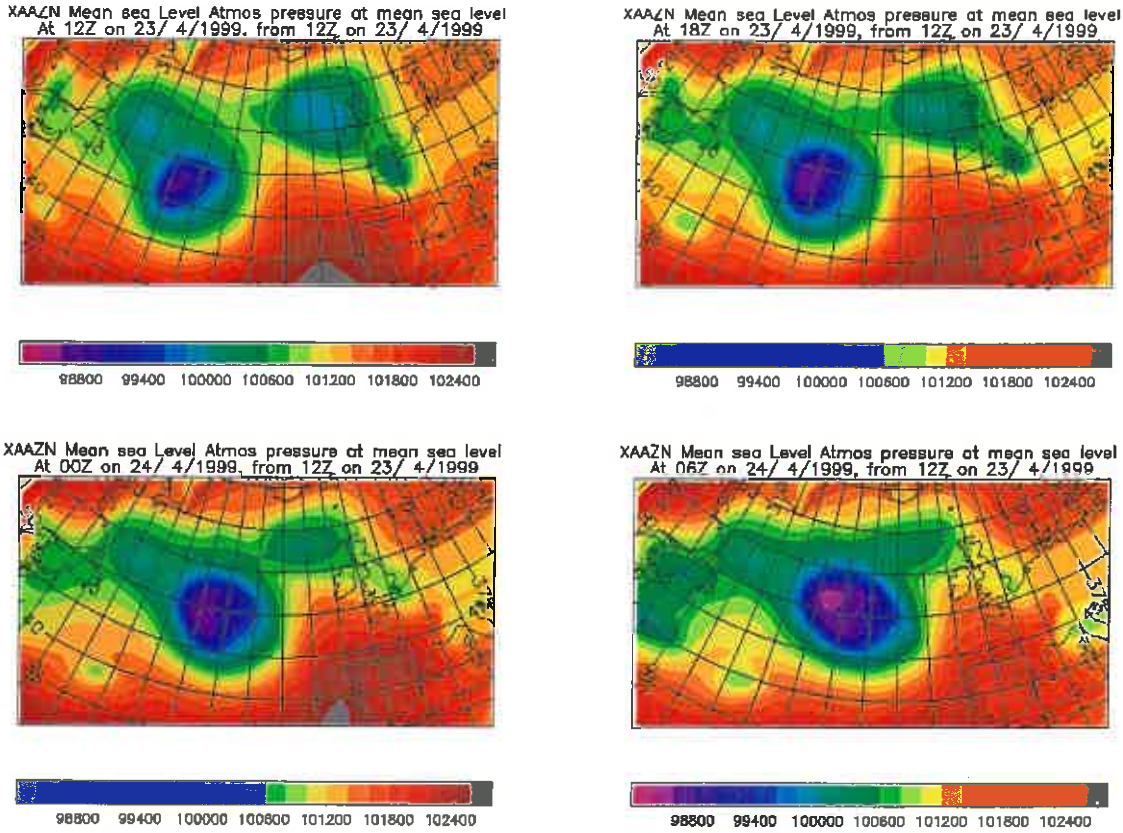

Fig. 4.4.8 Case 4: PMSL for rerun forecast

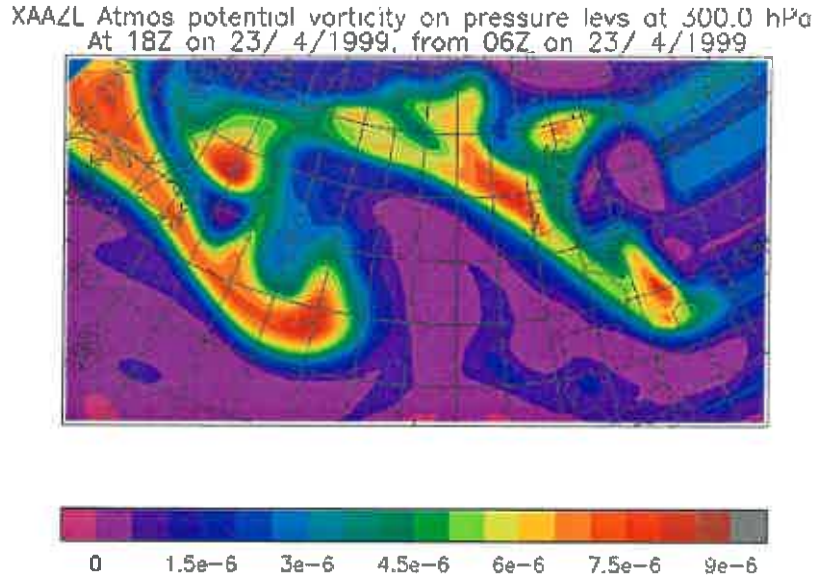

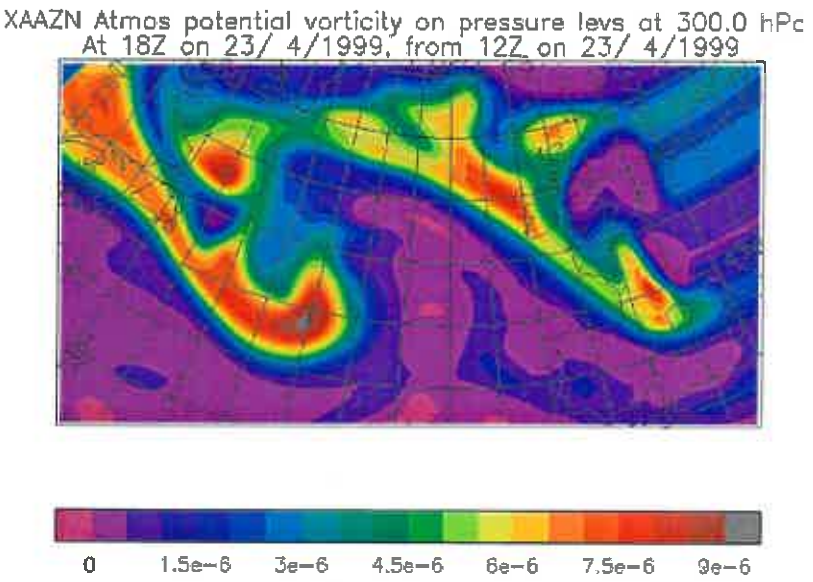

Fig. 4.4.9 Case 4: PV on 300hPa at 18z 23/4/99: forecast from background (upper) and rerun (lower)

CASE 5: 00z 06/07/99 (40%, 5hPa)

Pmsl fields (figs. 4.5.1,2,3): The analysis for 0z 6/7/99 shows mid-atlantic cyclone centred about 46N, 295W (latitude of mid-France, longitude of Greenland), which is part of a complex low system with three low centres. The central pressure is about 994hPa. This low moves NE over the subsequent 18 hours, while deepening to about 982hPa and merging with the adjacent low centres.

The forecast from analysis and forecast from background are very similar – in both of them the forecast cyclone is under developed by about 4hPa and lags behind the analysed cyclone by 2-3 degrees.

500 hPa height fields (fig.4.5.4,5,6) : The forecast error at 500hPa is rather less marked than the pmsl error, but the cyclone is again a little under developed.

WV image and PV fields (figs. 4.5.7,8): There appears to be a mismatch between the 300hpa PV field and the WV image in the vicinity of 55N, 40W, i.e. where the PV contours cross over the cloudy region The level-by-level PV distribution (fig. 4.5.9) shows that the upper-level anomalies do not extend significantly below 400hPa. However, significant PV anomalies (2.5-3 PVU) are present at 800hPa (particularly the one between Canada and Greenland).

850 hPa theta-w fields (fig. 4.5.10): The 850hPa theta-w field seems not to manifest any coupling with the 300hPa PV field, although this is simply because the cyclone is at an early stage of development. The PV gradient region does run parallel to the polar front baroclinic zone, and a warm conveyor belt is apparent in the vicinity of 25-30W, 50-60N. It would therefore be expected that coupling would follow. The lack of vertical extent in the PV anomalies is probably also due to the fact that the system is at an early stage of development.

Rerun: It would be of interest to adjust the PV field so that the contours curve around the edge of the cloudy region. Unfortunately, an adjustment of this type is impossible to carry out manually without a very great deal of tedious labour, and even then the result would be crude and unsatisfactory. It was therefore decided to perform a sensitivity study instead. The more southerly of the two upper level PV anomalies was scaled up by a factor of 1.5, from 300hPa to 400hPa. The anomaly does not extend below 400hPa. The scaling can be seen in the T+6 PV fields (fig. 4.5.11)

The impact of this adjustment on the forecast at both sea level and 500hPa was negligible. There is no point in displaying the rerun forecast fields as they did not differ significantly from the original forecast. This lack of sensitivity suggests a lack of coupling between this upper-level PV anomaly and the lower level development, but, as noted above, this is presumably because the system is at an early stage of development and such coupling has not yet had time to develop.

Further work: This case is in fact of considerable interest, in view of the PV/WV mismatch noted above. The correction of this mismatch is practically beyond the technical means available to this project, because it would involve re-shaping PV contours, which is a much more difficult operation than simply displacing blocks of PV. However, such reshaping is possible using the "Fieldmod" software referred to in section 2.5 of this report. A.T.Semple of JCMM is proposing to pursue this case using the Fieldmod software.

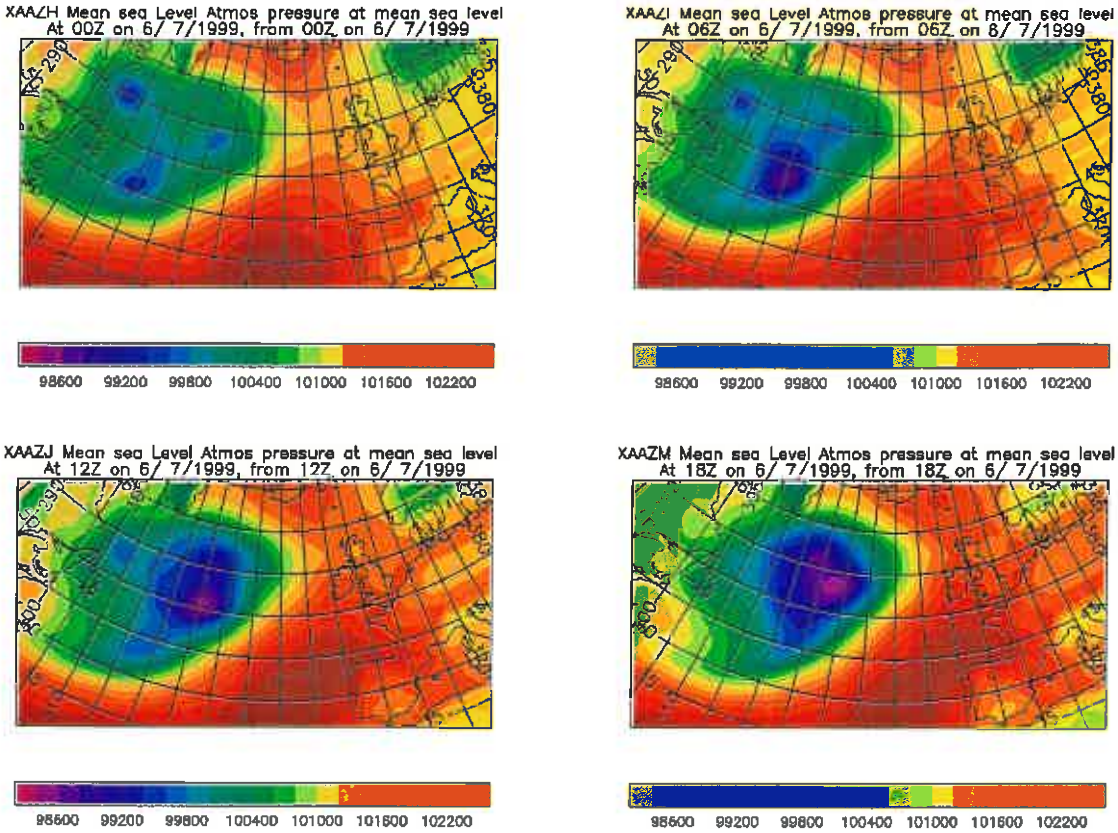

Fig. 4.5.1 Case 5: PMSL analyses

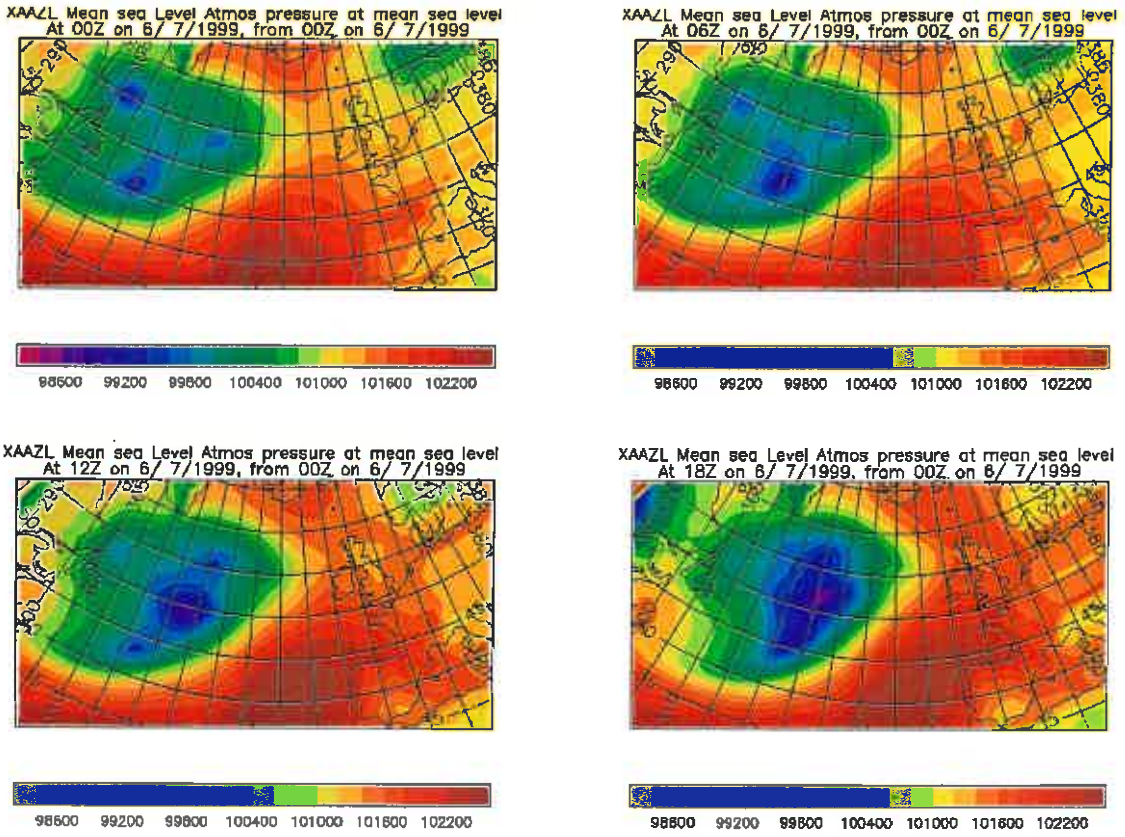

Fig. 4.5.2 Case 5: PMSL forecast from analysis

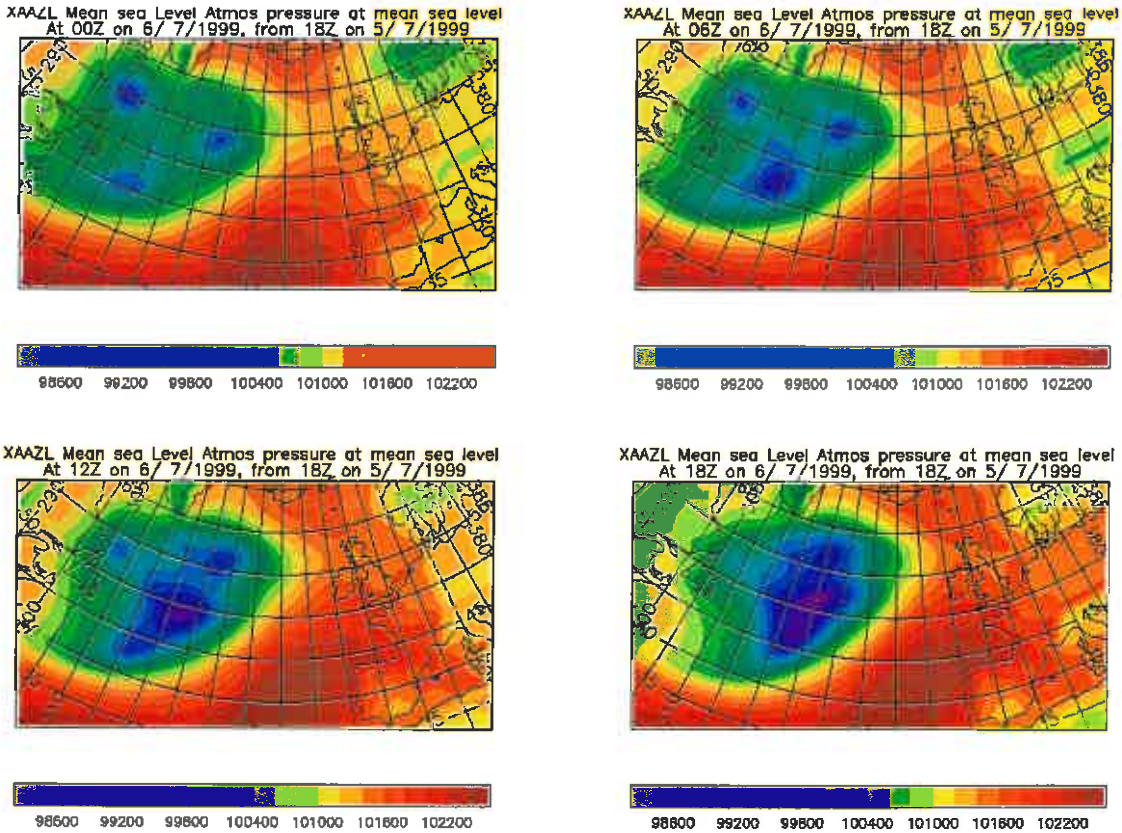

Fig. 4.5.3 Case 5: PMSL forecast from background

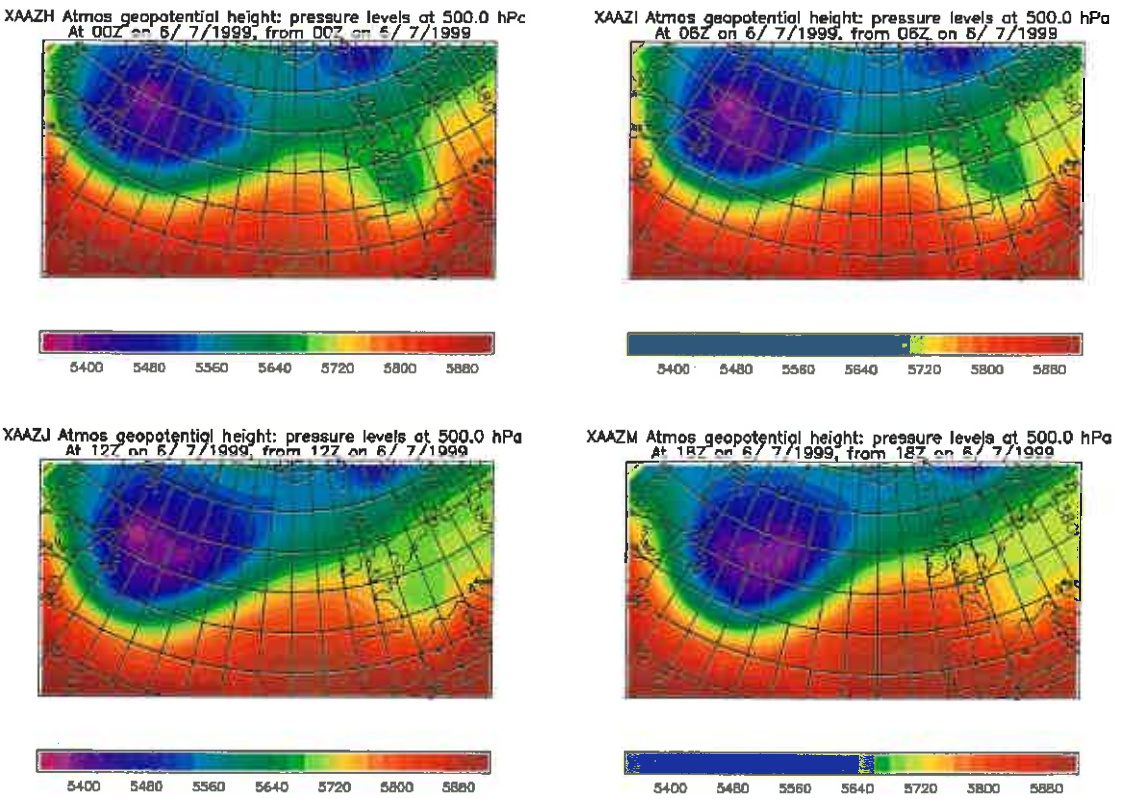

Fig. 4.5.4 Case 5: 500hPa height analyses

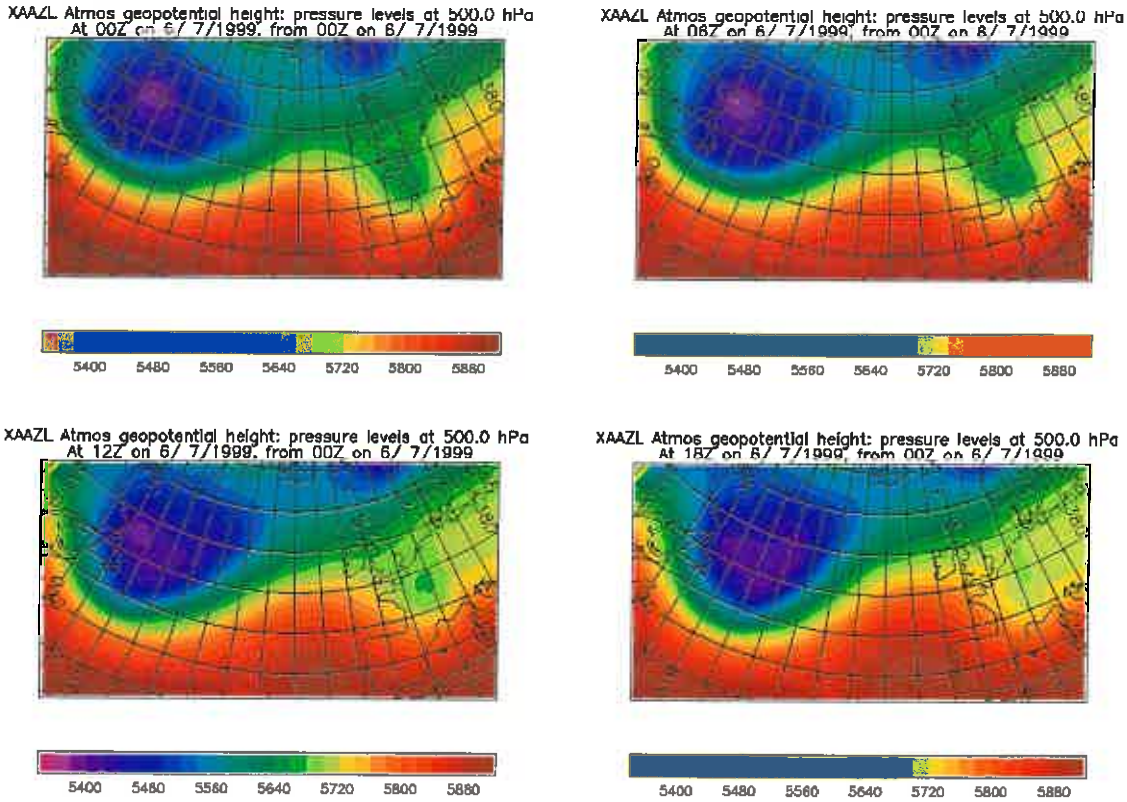

Fig. 4.5.5 Case 5: 500hPa height forecast from analysis

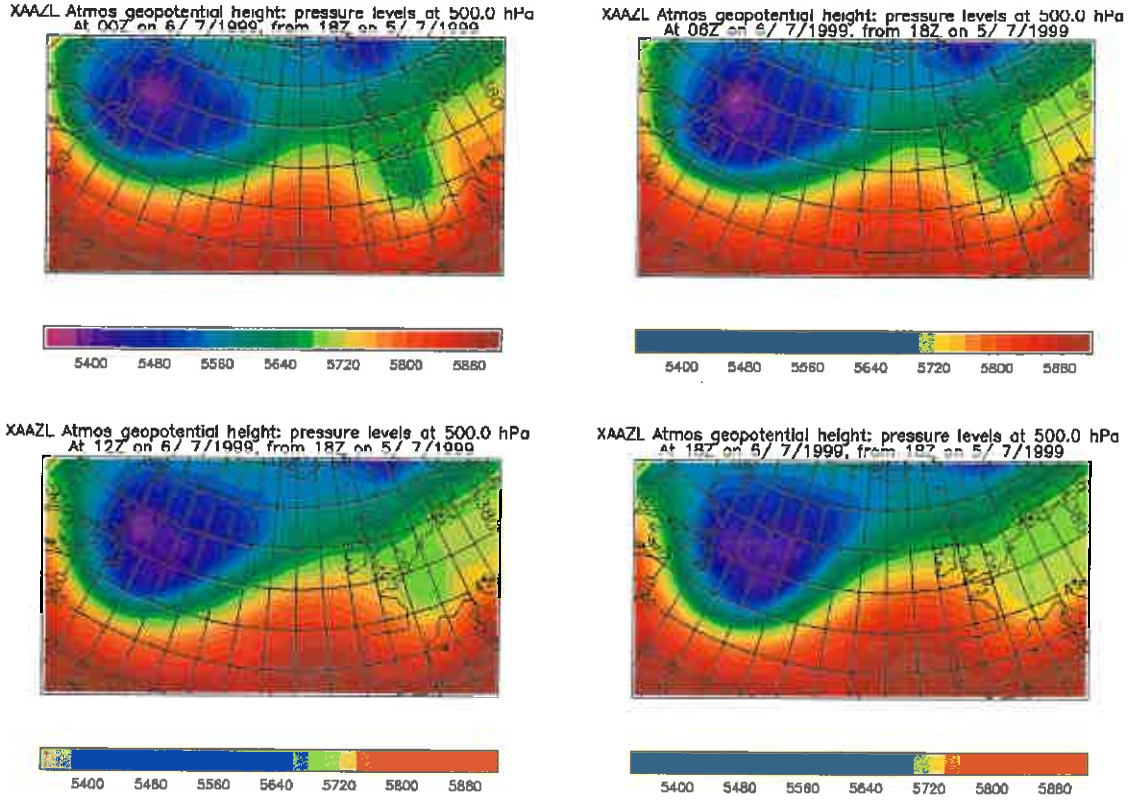

Fig. 4.5.6 Case 5: 500hPa height forecast from background

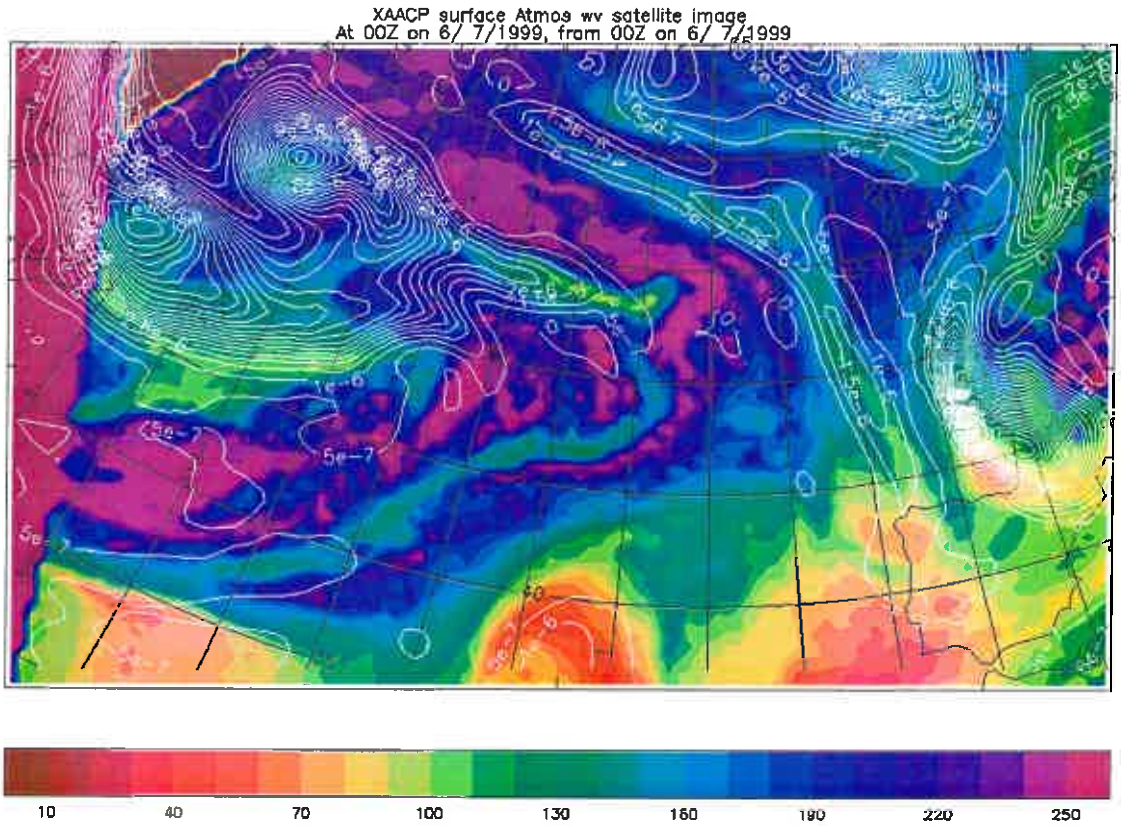

Fig. 4.5.7 Case 5: WV image with contours of analysed PV on 300hPa at 0z

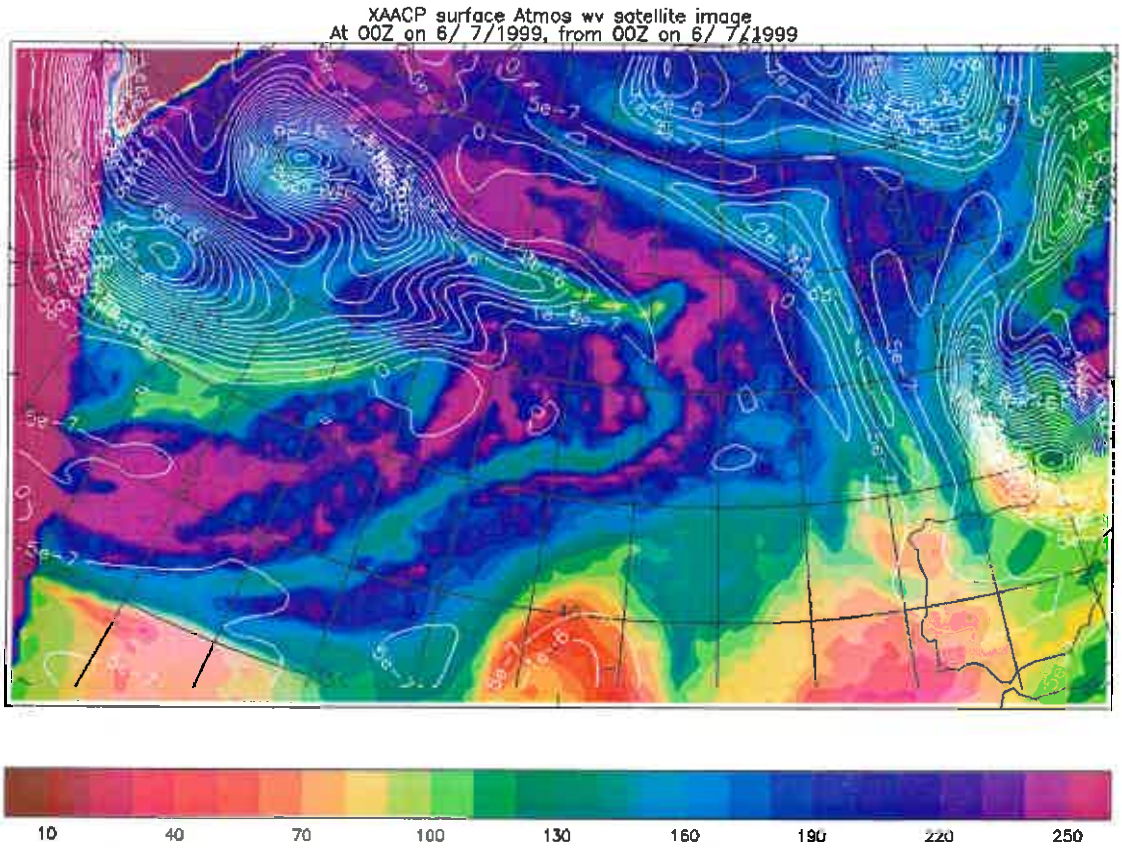

Fig. 4.5.8 Case 5: WV image with contours of background PV on 300hPa 0z

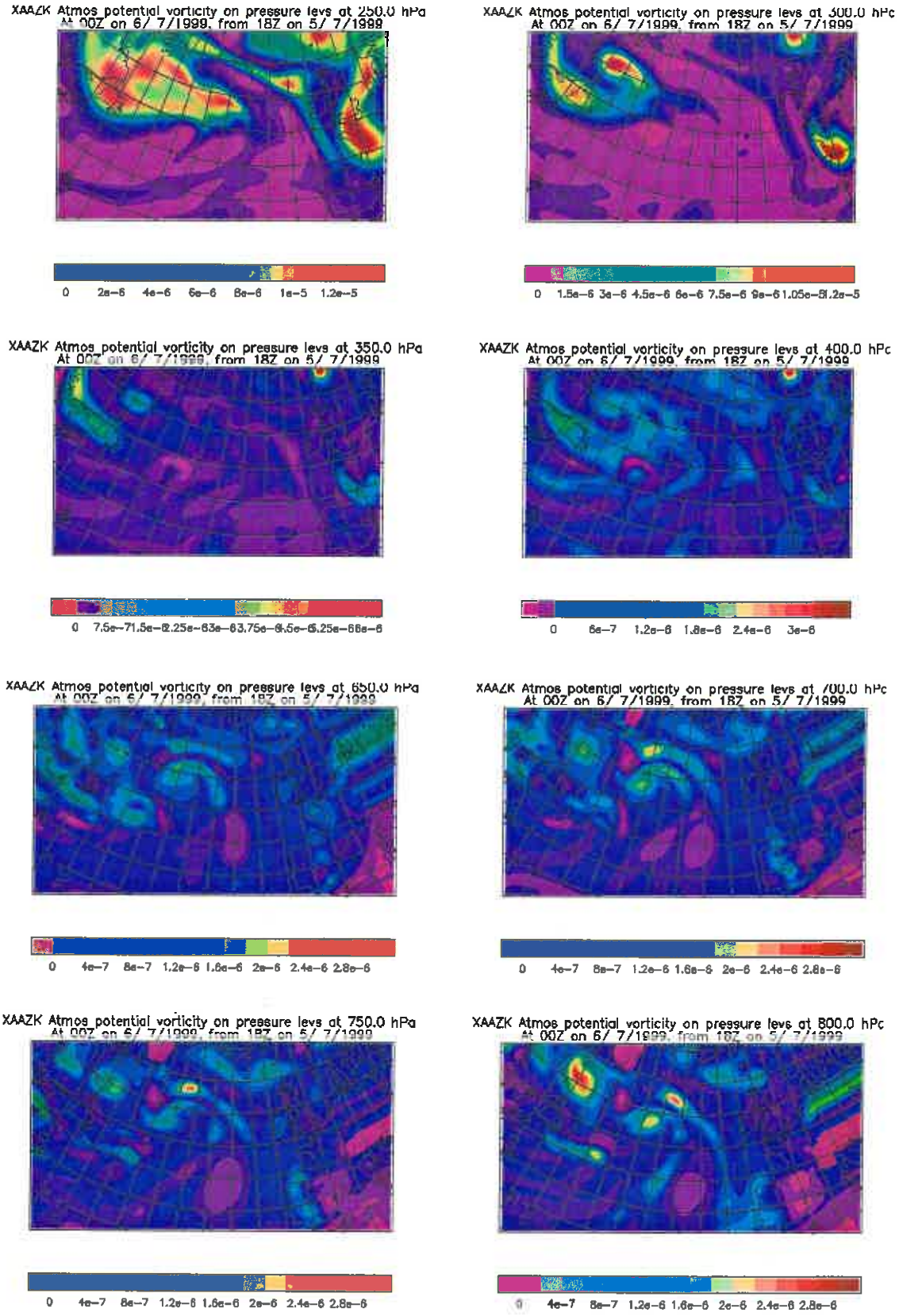

Fig. 4.5.9 Case 5: Background PV on various levels at 0z

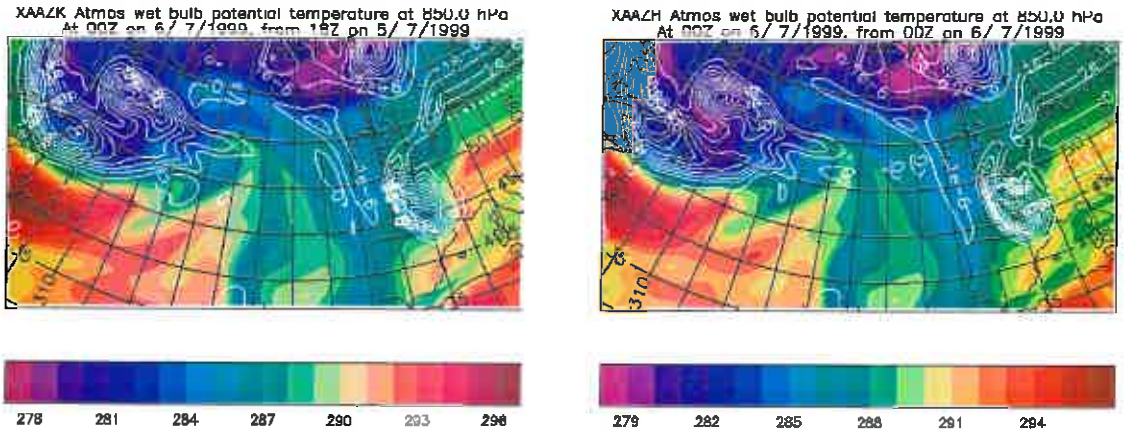

Fig. 4.5.10 Case 5: 850hPa theta-w with contours of PV on 300hPa at 0z
(Analysed lh frame, background rh frame)

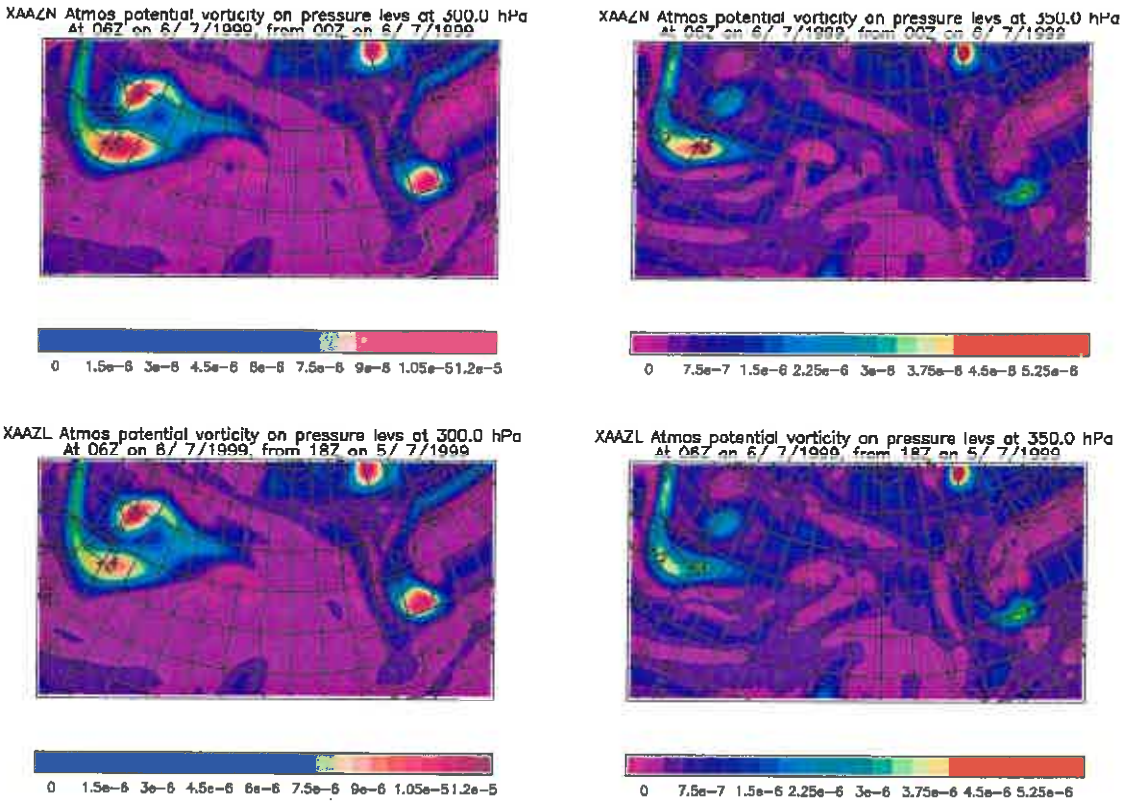

Fig. 4.5.11 Case 5: Rerun PV (upper frames) and original forecast PV (lower frames) at T+6

5. A 'DRY EYE' CASE (courtesy of N. Keeley, JCMM)

This section describes a short case-study of a so-called "dry eye" event (Browning & Roberts, 1999) using the high resolution global Unified Model. The time period covered is from 00z on 22/6/1999 to 18z on 22/6/1999. Figure 5.1 shows Meteosat water vapour images at six-hourly intervals from 00z on 22/6/1999. Dry areas are coloured yellow/red while moist areas are coloured purple/blue. The "dry eye" is the roughly circular feature at 17 W, 56N at 00z on 22/6/1999. It can be seen to move South-Eastwards throughout the 18 hour period until it is located over Northern Ireland.

Dry eye features are of interest as thunderstorms are frequently associated with them. In addition, the dry eye feature is usually associated with a potential vorticity anomaly. Figure 5.2 below shows close ups of the water vapour images overlaid with PV on the 400 hPa surface (white contours) obtained from the appropriate UM global analyses.

Rain rates: Figure 5.3 shows UM analysed convective rain rates for 6, 12, & 18z on 22/6/99. Figure 5.4 shows the 'analysed' large-scale rain rates. Note that the rainfall is mostly non-convective in origin in this case, the convective rain rate being considerably smaller than the large-scale rain rate.

Figure 5.5 shows radar images for 06z, 12z and 18z on 22/6/1999 which show where the rainfall was actually occurring. Fig. 5.6 shows the total analysed rain rates for these times. Figures 5.7, 5.8 show the convective and large scale rain rates as forecast from the background fields (i.e with data assimilation switched off).

It can be seen that the position of the model analysed rainfall is in reasonable agreement with the radar images, although it is much less structured (most probably due to the limitations of the model resolution). It is not possible to comment on how accurate the model is in terms of the magnitude of the rainfall rate, due to the problem of extracting absolute information from radar imagery.

Sensitivity tests were carried out to investigate the effect on the forecast rain rate of removing some or all of the PV anomaly associated with the dry eye system. The PV adjustments were carried out on the background PV fields and the reruns were performed without data assimilation. The methodology employed was the same as that used for the case studies outlined in section 4, i.e. it made use of PV inversion to obtain wind and temperature increments, and the IAU input mechanism.

The fact that the analysed and background/forecast PV distributions match rather well, both in position and magnitude, while the forecast and analysed convective rainfall rates are significantly different suggests that the model convection scheme is rather sensitive to the PV distribution associated with the dry eye. The forecast large-scale rain rate is also significantly different from the analysed one, being considerably more intense.

Rerun 1: The central maximum of the PV anomaly associated with the dry eye was levelled off to 4 PVU; this was done on levels 340, 320, 300 & 280 hPa. At T+6, the effect of this adjustment on the PV field was only just detectable, as figure 5.10 shows. The effect on the forecast convective and large scale rain rates is shown in figures 5.11, 5.12. Figs. 5.11,12 show that there is a marked effect on the convective rain rate but much less of an effect on the large scale rain rate. Figure 5.13 shows vertical velocity on 650hPa for the original and rerun forecasts. Fig. 5.13 shows that the ascent associated with the dry eye has been markedly reduced, which is consistent with the reduction in convective rain rate. Surface pressure, temperature and humidity fields were also examined and all show very little change.

Rerun 2: In this rerun the PV anomaly associated with the dry eye was removed completely. Figure 5.14 compares the PV on 400hPa at T+6 in the original and rerun 2 forecasts. Figures 5.15, 5.16 compare the convective and large scale rain rates between the original and rerun 2 forecasts. There is a reduction of the large-scale rain rate while its distribution is unaltered. However, the most striking change is the complete absence of convective rain associated with the dry eye in the re-run forecast. It would appear that removing the PV anomaly associated with the dry eye switches off the convection.

Figure 5.17 compares omega on the 650 hPa level for the two forecasts. It can be seen that ascent associated with the dry eye system (negative omega values) is greatly reduced, which is consistent with the reduction in convective rain rate. It is evident that convective ascent for this dry eye system is very sensitive to alteration of the associated PV anomaly.

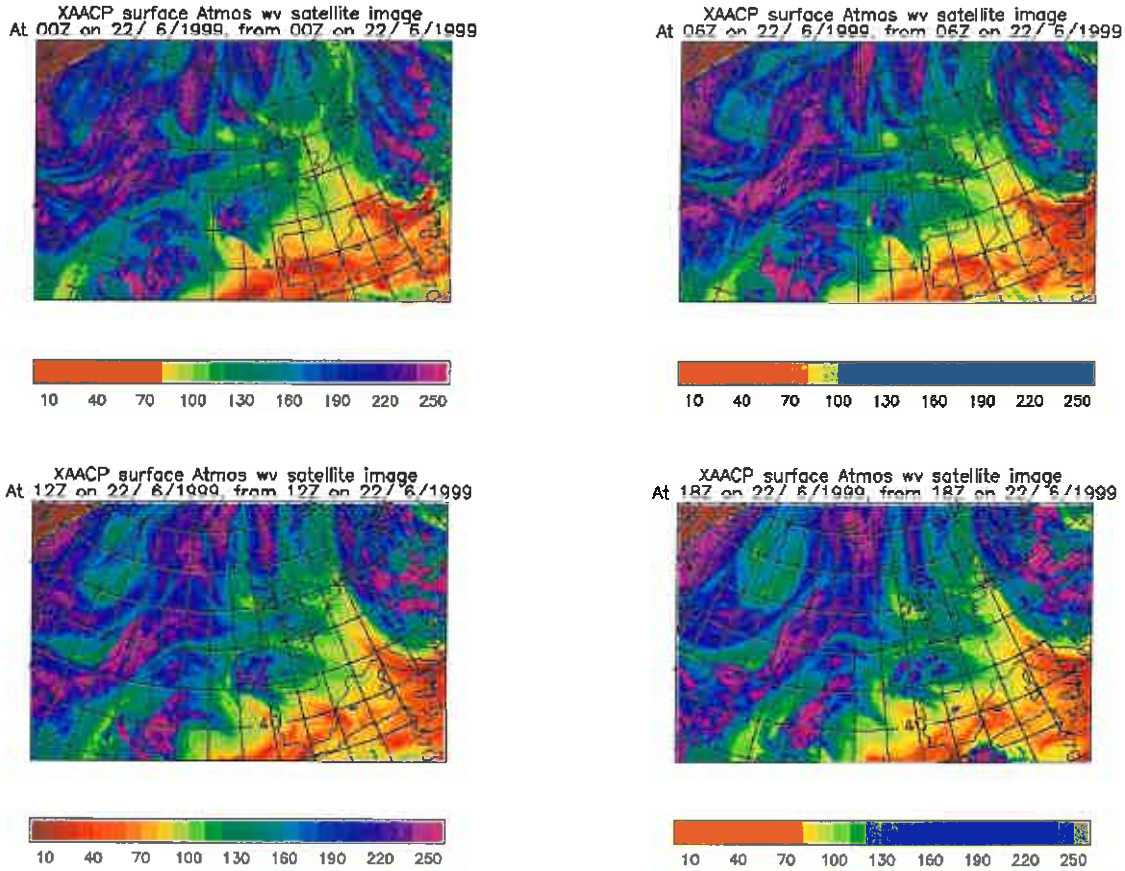

Fig. 5.1 Meteosat WV images showing dry eye system

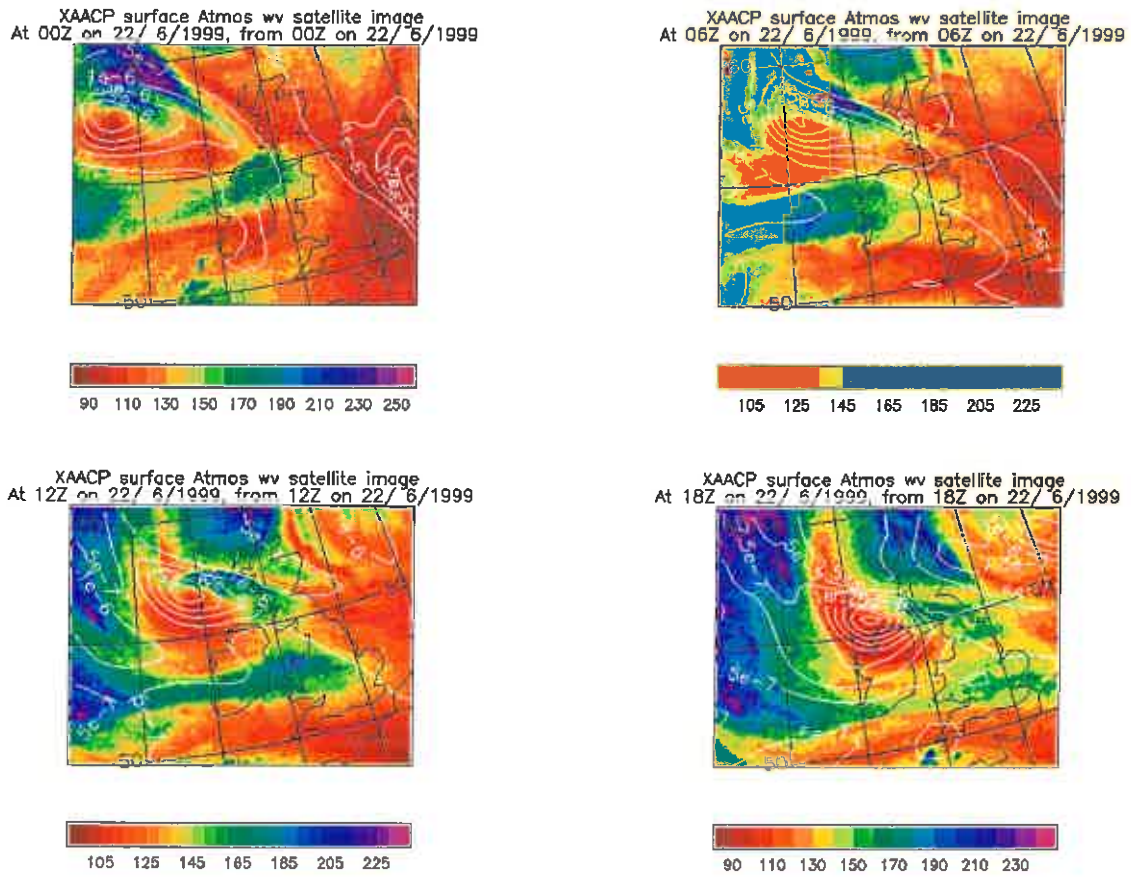

Fig. 5.2 WV images overlaid with PV on 400hPa

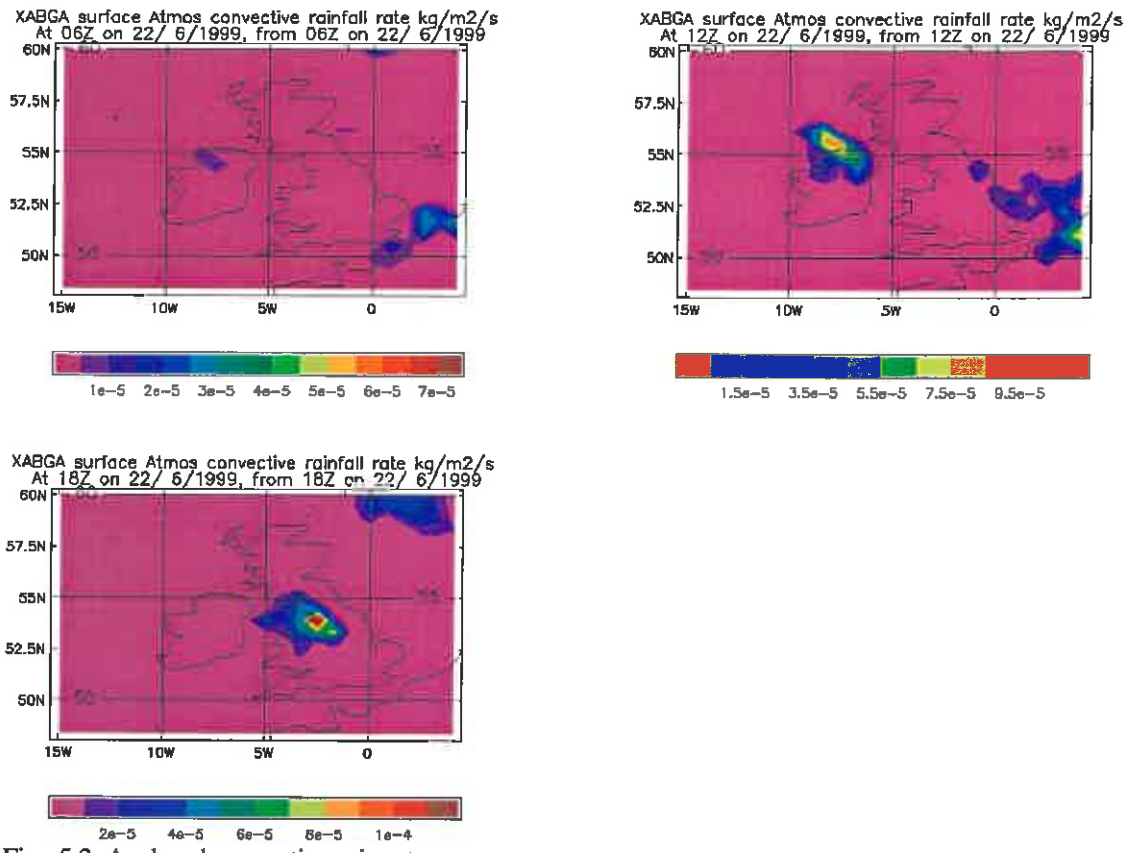

Fig. 5.3 Analysed convective rain rates

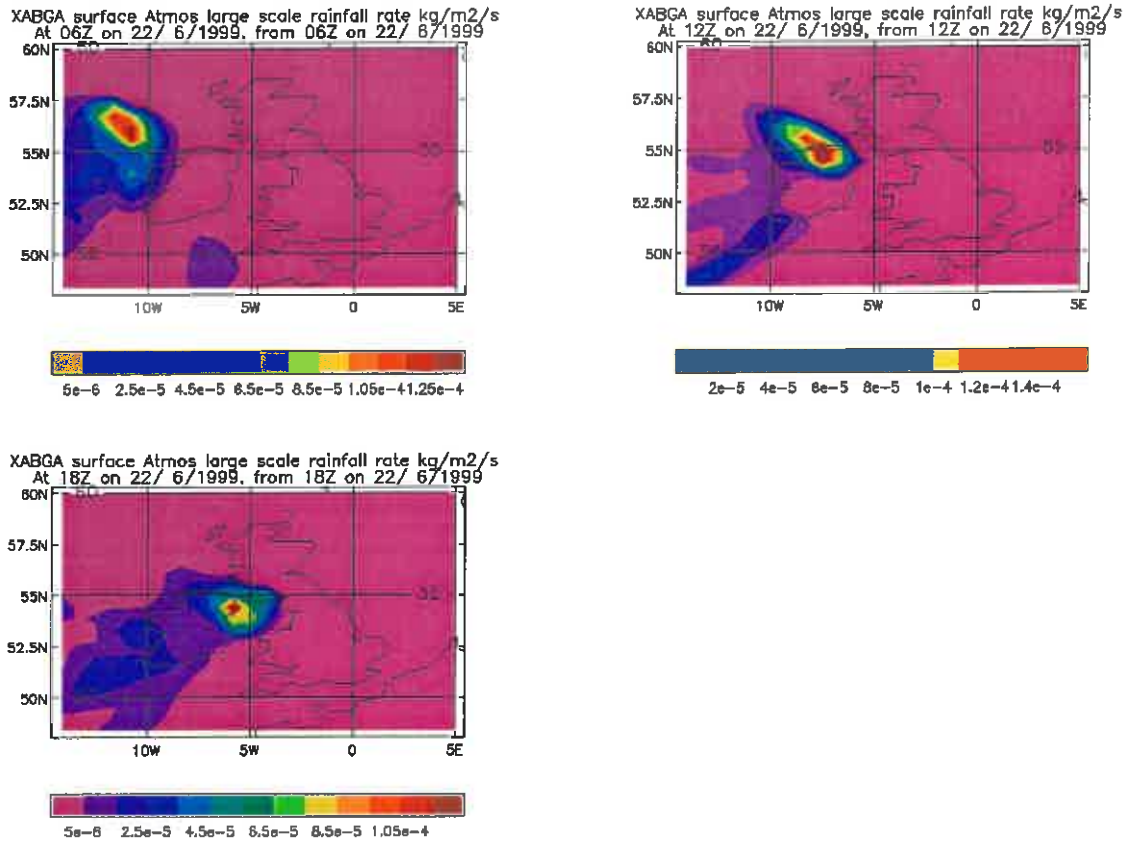

Fig. 5.4 Analysed large scale rain rates

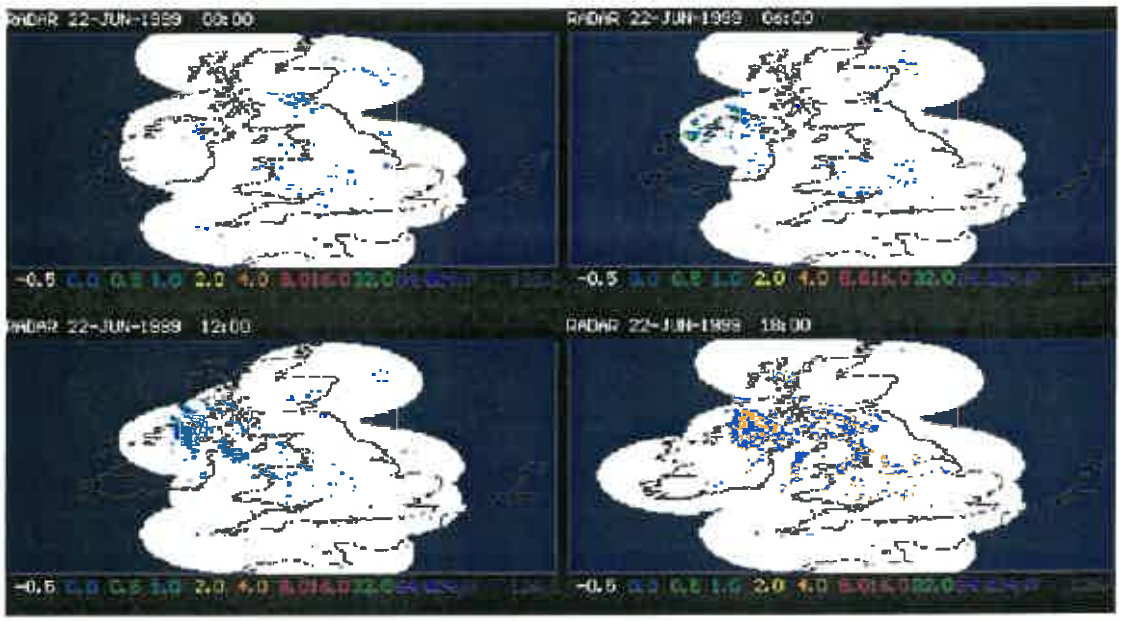

Fig. 5.5 Radar images for 22/6/99

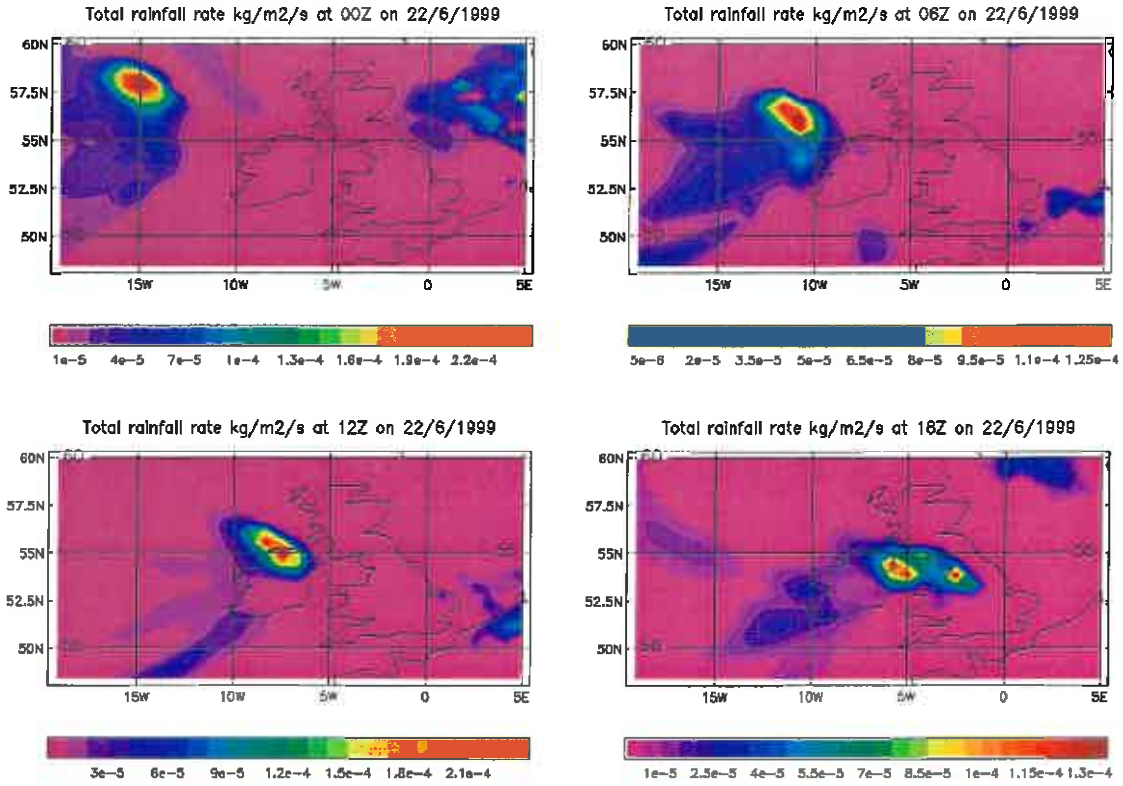

Fig. 5.6 Analysed total rain rates

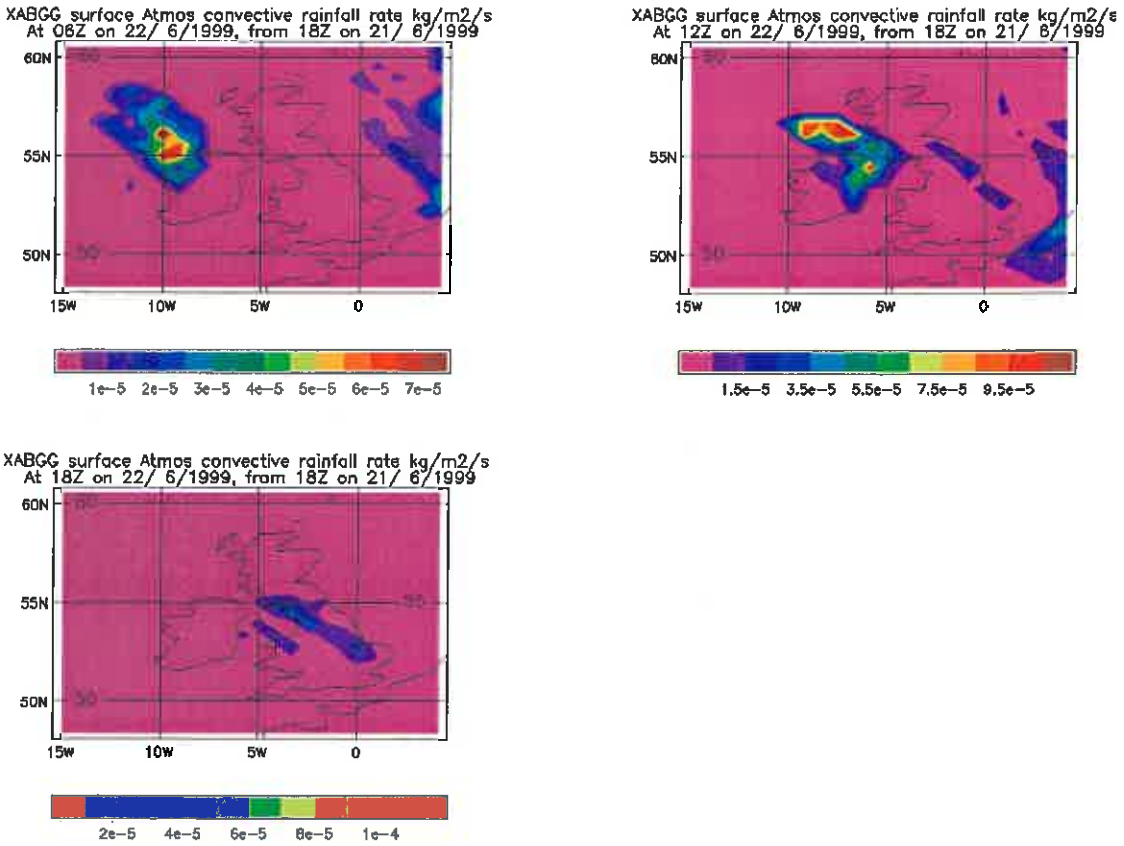

Fig. 5.7 Convective rain rate – forecast from background

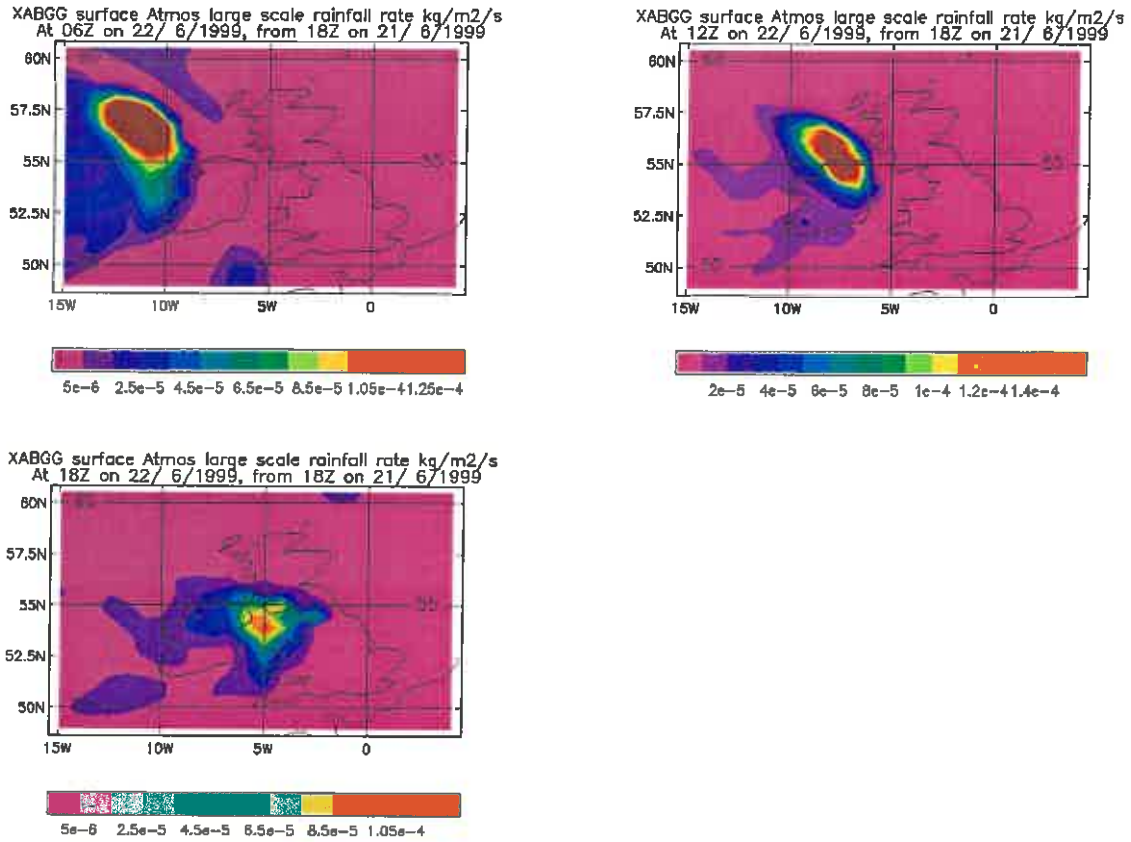

Fig. 5.8 Large scale rain rate – forecast from background

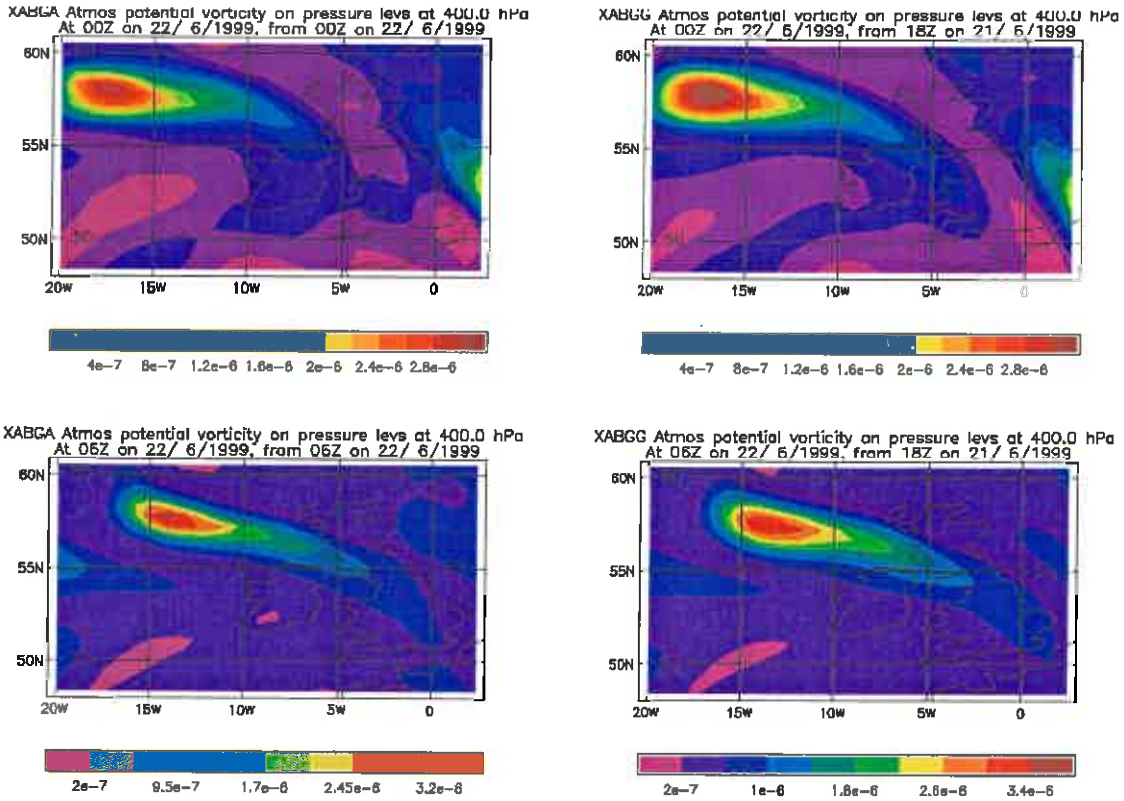

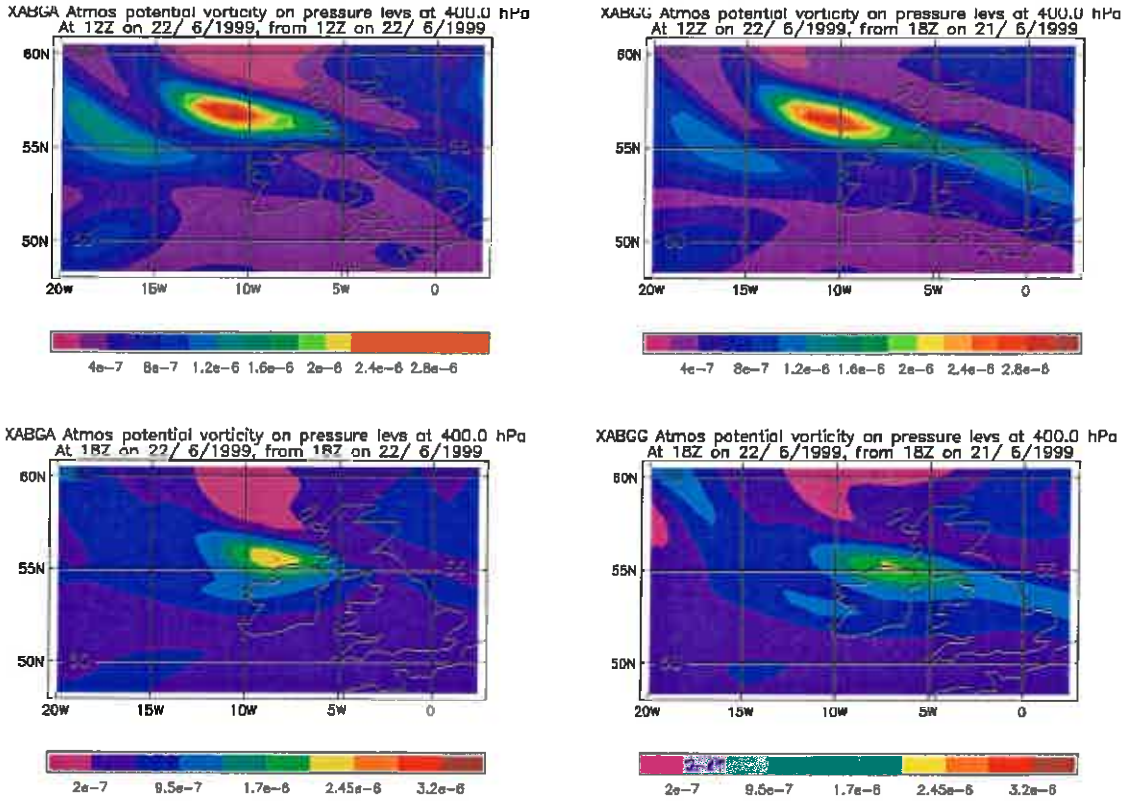

Fig. 5.9 LH frames: analysed PV on 400hPa RH frames: PV on 400hPa forecast from background

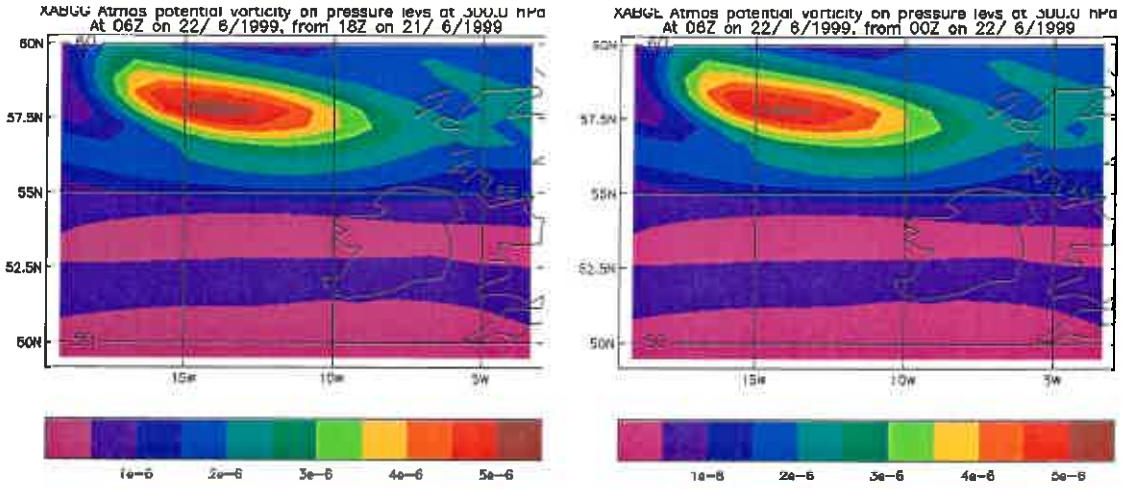

Fig. 5.10 PV on 300hPa at T+6; LH frame - original forecast; RH frame – rerun 1 forecast.

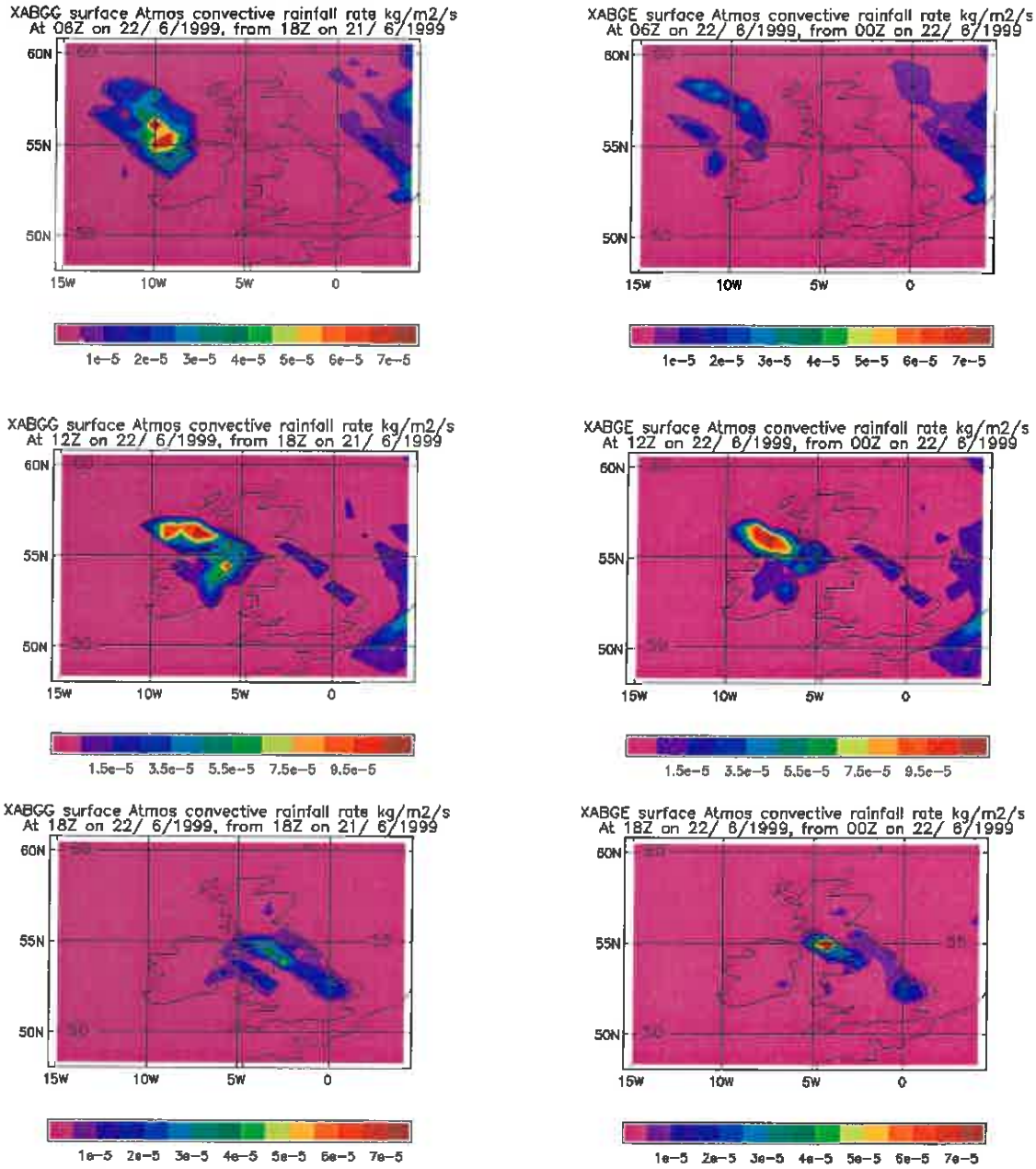

Fig. 5.11 Convective rain rate; LH frames – original forecast; RH frames – rerun 1 forecast

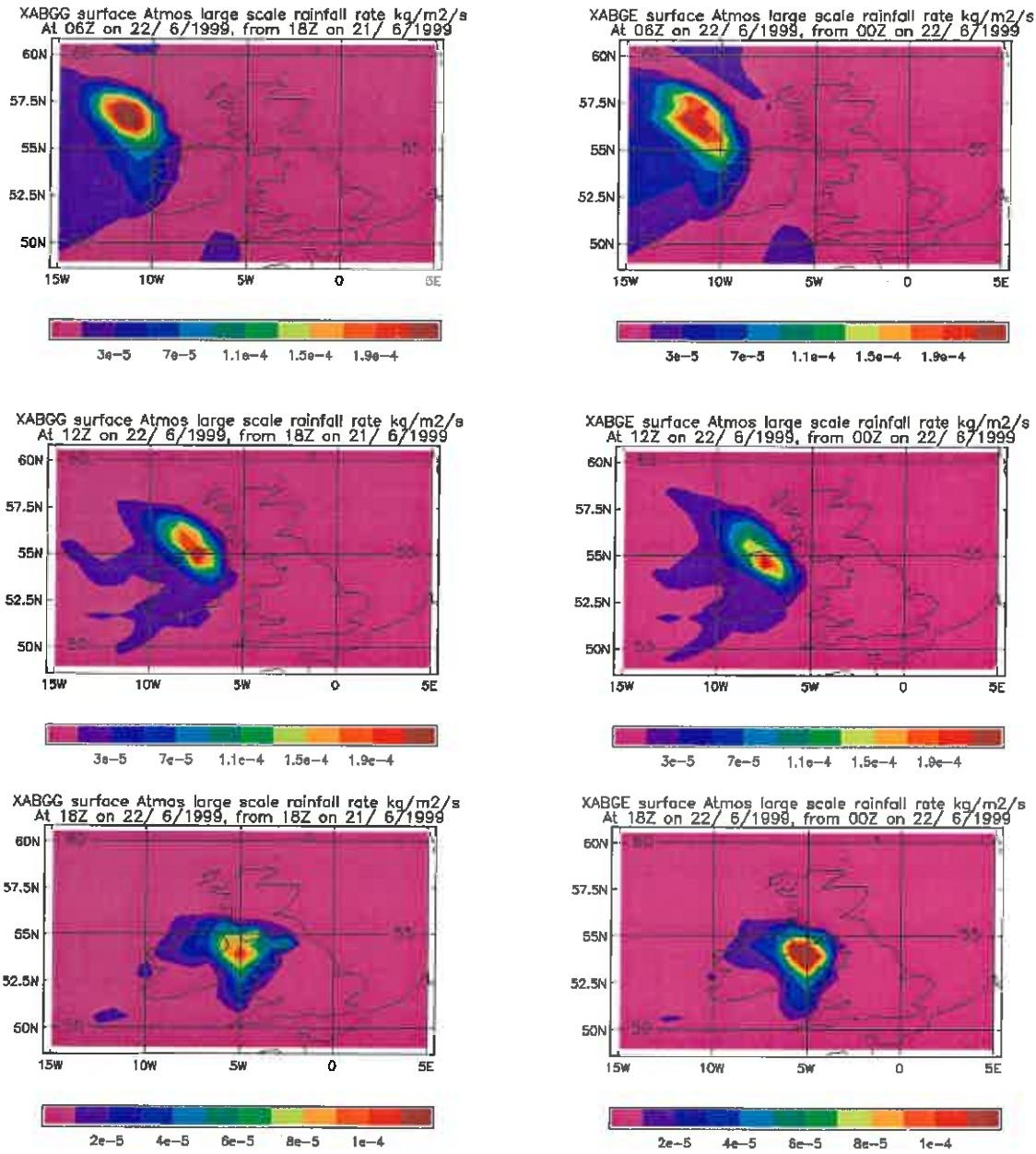

Fig. 5.12 Large scale rain rate; LH frames – original forecast; RH frames – rerun 1 forecast

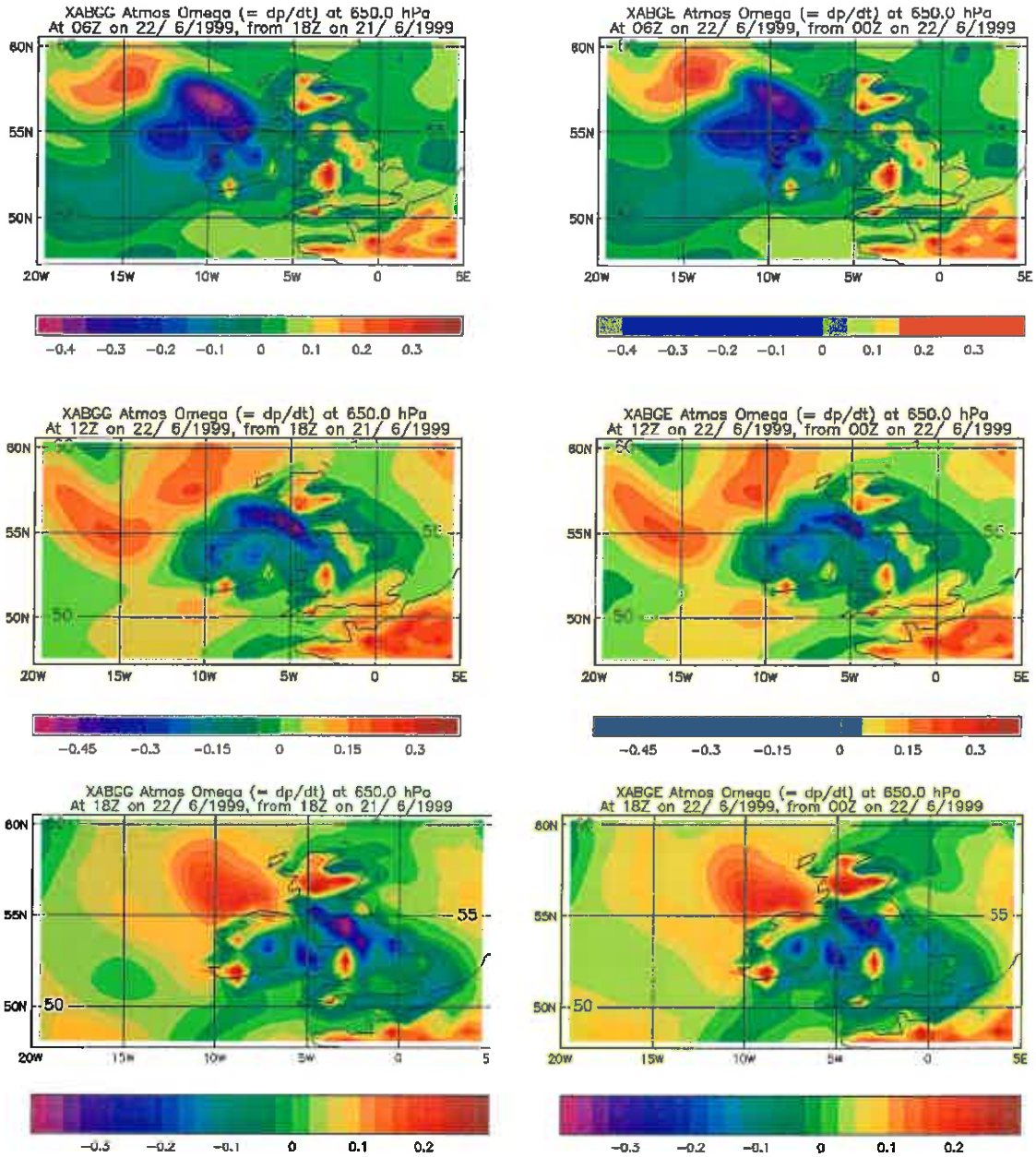

Fig. 5.13 Omega on 650hPa; LH frames – original forecast; RH frames – rerun 1 forecast.

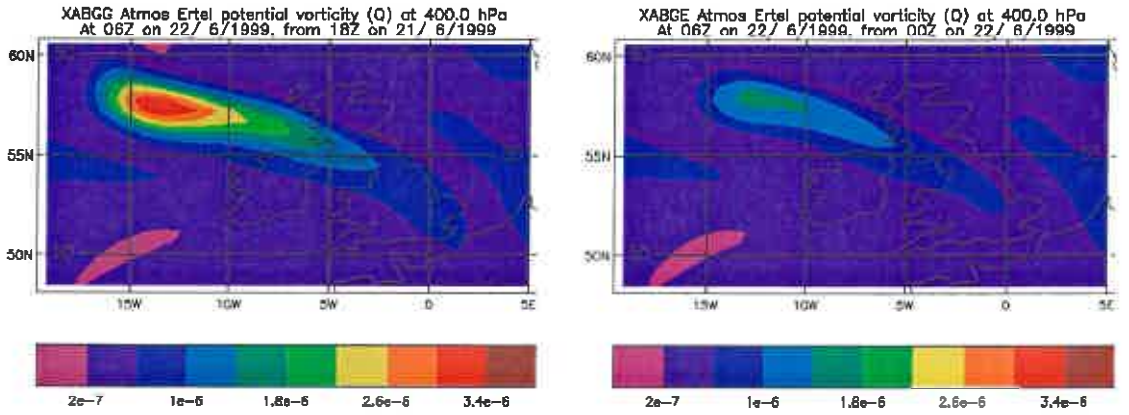

Fig. 5.14 PV on 400hPa at T+6; LH frames – original forecast, RH frames – rerun 2 forecast

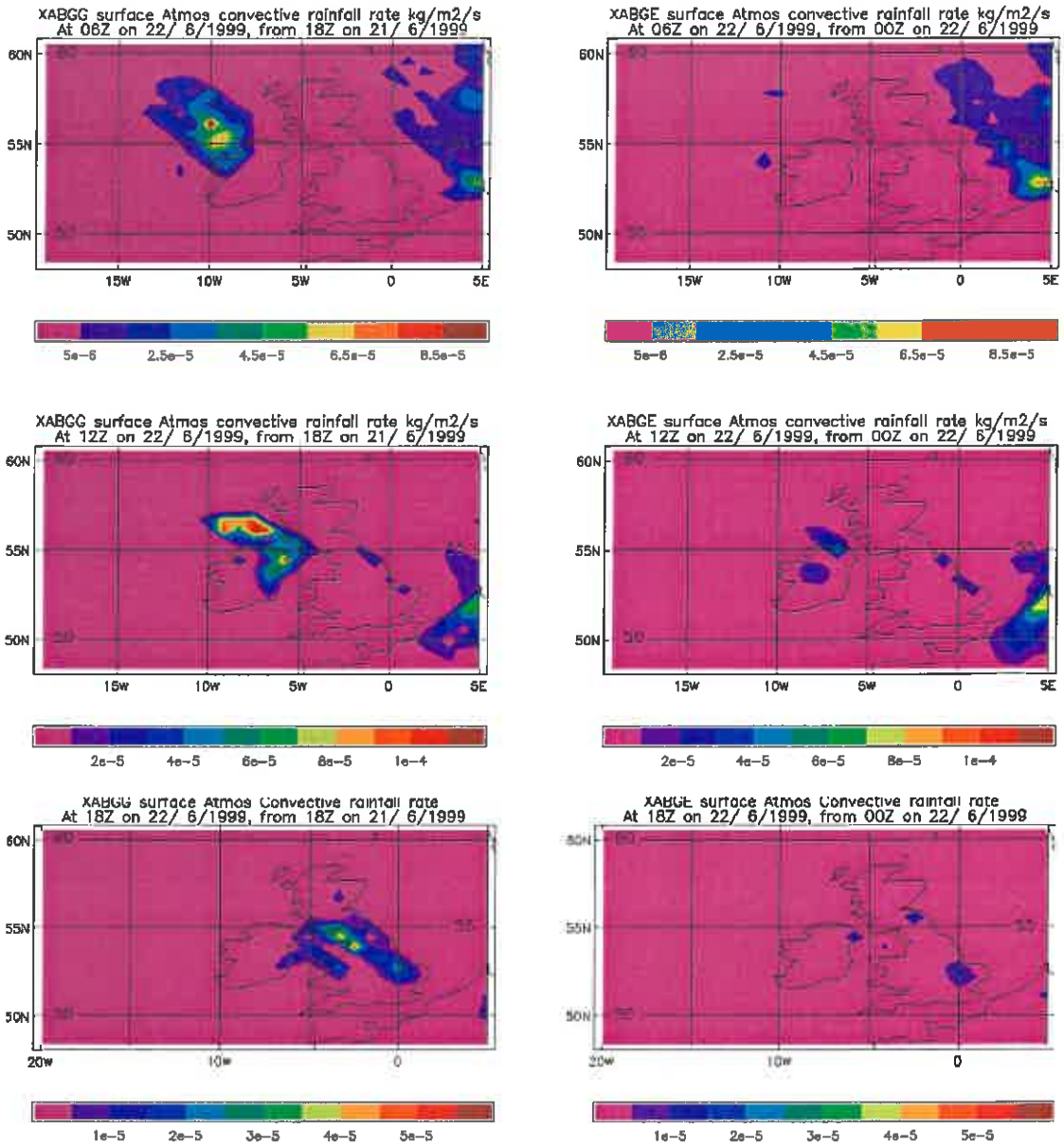

Fig. 5.15 Convective rain rate; LH frames – original forecast, RH frames – rerun 2 forecast

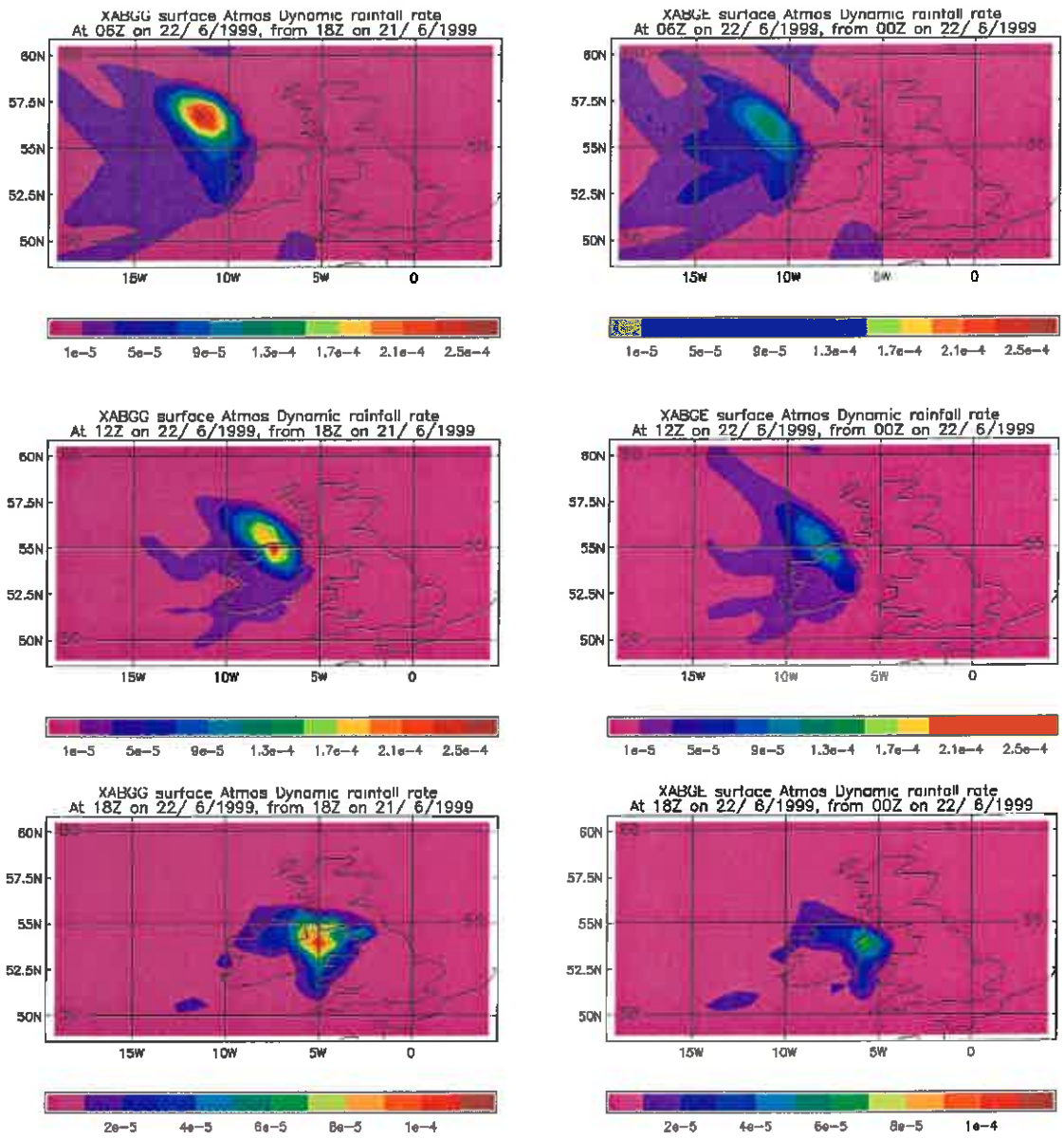

Fig. 5.16 Large scale rain rate; LH frames – original forecast, RH frames – rerun 2 forecast

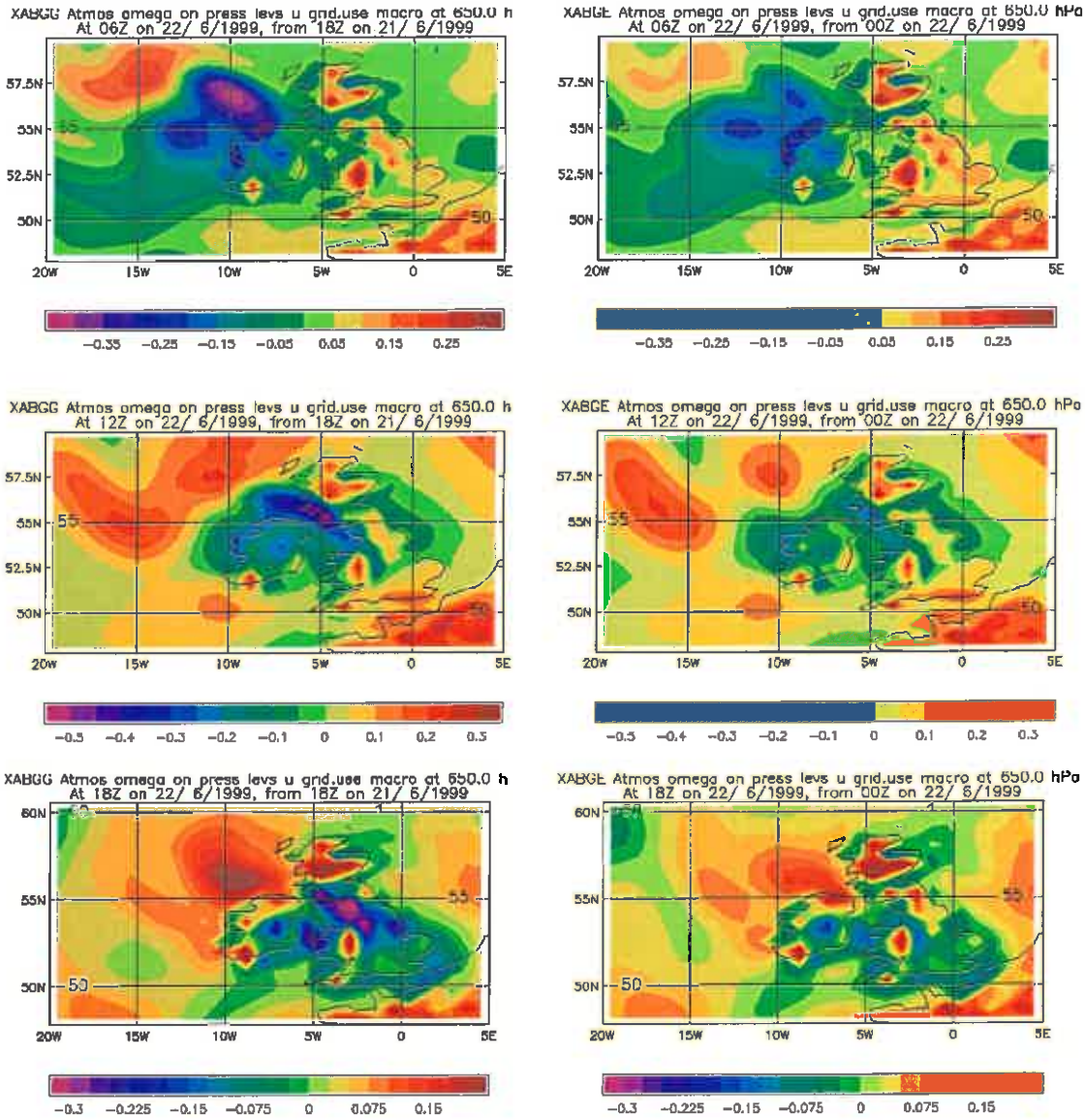

Fig. 5.17 Omega on 650hPa; LH frames – original forecast, RH frames – rerun 2 forecast

6. CONCLUSIONS

The project has established a methodology for investigating the feasibility of using the PV – water vapour image relation as a tool for the adjustment of initial states in NWP. This methodology was partially established in the first phase of the project (which was reported in JCMM internal report 102, Swarbrick 1999). The methodology has been improved upon in the second phase of the project; in particular, the use of the UM vn4.4 high-resolution global configuration has made it possible to employ the IAU mechanism for introducing field increments to the initial state, and this has largely eliminated the problem of spurious gravity wave activity which was an unavoidable consequence of the instantaneous initial field adjustment mechanism employed in phase 1 of the project.

Six case studies have been undertaken in the second phase of this project. One of these was in fact a sensitivity study on the role of PV anomalies in a so-called dry-eye system, and did not aim to improve the forecast. Of the other five cases, none yielded a clear positive impact on the forecast. Cases 1 & 3 showed a significant impact, but in each case it was partially positive and partially negative. Case 4 showed a small positive impact but this was achieved without using guidance from the PV/water vapour comparison. Case 2 showed a small negative impact and case 5 showed no impact.

The case studies in both phases of the project have established that there is often a direct relationship between the strength of an upper-tropospheric PV anomaly and the depth of the corresponding surface low; scaling up the anomaly will invariably deepen the low. Positional adjustments applied to a PV anomaly will affect the trajectory of the surface low, but the relation between position adjustments and trajectory appears to be quite unpredictable.

The overall message from the case study results, in both phases of the project, is clearly negative, although some cases have shown positive impacts in certain respects. It is clearly worthwhile to pursue the PV – water vapour relation as an academic exercise, but its potential usefulness as an operational initialisation tool has not been clearly demonstrated by this project.

Possible reasons for the lack of positive results – in order of importance

- The essentially manual technique for PV field adjustment which this project has had to rely on is hopelessly crude and impossibly laborious. It is easy to *imagine* the sort of adjustment one would like to make, but to actually carry it out by manual editing of pp files is generally impractical. This has placed a severe limitation on the kind of PV adjustment which can be performed. This is by far the most significant difficulty which has impeded progress in this project.

- As shown by the survey of cyclonic forecasts carried out by A.T. Semple (see section 1 of this report), suitable cases of misforecast cyclonic systems are quite rare. A "suitable case" would require a reasonably large forecast error (say, greater than 50% location error) which could be attributed mainly to clearly identifiable errors in the upper level PV field. In practice, such errors are rare for N Atlantic cyclones, and when they do occur it appears that their cause is complex and likely to involve a subtle combination of upper and lower level factors.

- The PV – water vapour relation is not yet precise enough. Mansfield (1996,97) has been able to obtain useful insights from the PV/WV relation which help to explain forecast errors in a number of cyclonic cases. The case studies undertaken in this project attempted to apply the same kind of analysis to the adjustment of initial conditions. It appears however that the qualitative understanding of the PV/WV relation demonstrated by Mansfield, which can indeed be useful for subjective verification purposes, is not sufficiently well-defined to enable meaningful judgements to be made as to how initial fields should be adjusted a priori in any particular case. In order for this to be feasible, a well-defined quantitative relation between PV and water vapour would be required. Some progress has been made towards this (eg. Hoffman, Pankiewicz, Georgiev), but these studies have not yet yielded any results of practical use (although their results are at least of academic interest).

- The PV inverter is rather erratic and unreliable. In some cases convergence can be very rapid, but in others it can be extremely slow. Adjustment of parameters such as the vertical length scale can be helpful in cases of convergence failure – some cases (eg. case 4) are extremely sensitive to this sort of adjustment. However there is no apparent way of knowing a priori what convergence difficulties may arise in any given case. Another consideration which *may* be significant is that the PV inversion

domain cannot usually be extended below 850hPa, for practical reasons, and in any case, surface pressure is not adjusted by the PV inversion technique. This implies that the influence of any PV adjustments cannot be extended right down to the surface.

It may be that cases could be found in which it would be possible to demonstrate a positive impact on forecasts cyclonic development by upper-level PV adjustment guided by water vapour imagery, but in order to find such cases it would be necessary to carry out a very large number of case studies, which is clearly not feasible with the current methodology. A much more efficient, robust and automated methodology would have to be developed to make such a study possible; to overcome the technical difficulties which such a development would present would require a significant project in itself.

Reassessment of the Demirtas results (Demirtas 1996, Demirtas & Thorpe 1997)

The work carried out by M Demirtas (see above refs.) provided the scientific basis and motivation for this project, so it is of interest to reconsider the Demirtas results in the light of this project's results. The title of the Demirtas reports "Sensitivity of short range forecasts to local PV modifications" does not mention water vapour imagery. Although WV imagery did play a significant part in Demirtas' work, Demirtas does not claim that the PV/WV comparison alone is likely to lead to improved forecast accuracy; the conclusions reached in those reports are in fact more general, that "local PV modifications" can lead to more accurate forecasts. The PV modifications in general are not guided solely by the PV/WV comparison, but also by other considerations.

Demirtas reports on three case studies, which are 0z 16/02/95, 0z 27/04/97, and 6z 28/09/95. The first of these actually did use the PV/WV comparison explicitly to guide PV field adjustments at analysis time, and achieved a significant positive impact on the forecast intensity and trajectory of a cyclonic system. The second used the PV/WV comparison in a rather less explicit way, and the PV adjustments actually involved "transplanting" PV elements from the analysis 12 hours earlier, which had a better PV/WV comparison (and had produced a better forecast). The third case study involved PV adjustments at lower tropospheric levels only, and so did not use the PV/WV comparison at all to guide the actual adjustments. In all three cases, the approach was partly guided by a priori knowledge of the forecast errors, derived from comparison with the subsequent analyses.

So, in the Demirtas results there is only *one* case in which a positive impact was obtained by upper-level PV adjustment guided by the PV/WV comparison, and even in that case the precise nature of the forecast errors was known a priori. It should also be stressed that Demirtas does not claim that the PV/WV comparison alone could lead to better forecasts – the claims made are rather more general than that.

In view of the generally negative results obtained by this project, it appears that Demirtas was very fortunate to find a case which was apparently amenable to improvement by upper level PV adjustment alone. The results of this project and of the Semple survey of cyclonic forecasts (fig. 1.1) suggest that such cases are likely to be rare, although many more case studies would have to be attempted to be sure of this conclusion.

APPENDIX: Formulation of the PV inversion algorithm

This appendix gives a brief but complete account of the PV inversion program used in this project. More details of this PV inversion algorithm are to be found in Zemianski (1994), Demirtas (1996), Griffiths et al. (1998), and Davis and Emanuel (1991). The PV inverter described here was derived from that created originally by Zemianski and further developed by Griffiths.

A.1 Governing equations and the iterative solution procedure

The definition of Ertel PV is

$$q = \frac{1}{\rho}\vec{\eta}\cdot\nabla\theta \tag{1}$$

where ρ = density, η =absolute vorticity, θ =potential temperature. Note that (1) assumes that the vertical coordinate is height; if the vertical coordinate is pressure, the $1/\rho$ factor does not appear.

Equation (1) may be expressed approximately in terms of geopotential Φ and stream function Ψ,

$$q = \frac{g\gamma\pi}{p}\left[\left(f+\nabla^2\Psi\right)\Phi_{\pi\pi} - \frac{1}{a^2\cos^2\phi}\Psi_{\lambda\pi}\Phi_{\lambda\pi} - \frac{1}{a^2}\Psi_{\phi\pi}\Phi_{\phi\pi}\right] \tag{2}$$

where λ,ϕ = longitude, latitude; π =Exner pressure (the vertical coordinate); a=Earth radius, g=acceleration due to gravity, $\gamma = R_d / c_p$, p=pressure, f=Coriolis parameter.

The approximations made in converting (1) to (2) are (a) the hydrostatic approximation, i.e. vertical velocity derivatives are neglected; (b) horizontal velocity is expressed in terms of the stream function, which implies that it has zero divergence:

$$\vec{v} = \vec{k}\times\nabla\vec{\psi} \tag{3}$$

where x,y are local horizontal coordinates in the eastward, northward directions. Equation (2) is a Poisson-like elliptic equation. Given a set of PV fields q on pressure levels, we wish to solve this equation for the Ψ,Φ fields. To form a complete system we need another equation relating Ψ and Φ, and this is provided by a balance condition. Various balance conditions may be used in principle; the one used in this algorithm, following Davis and Emanuel (1991), is the Charney non-linear balance condition, which may be expressed in terms of Ψ,Φ as follows:

$$\nabla^2\Phi = \nabla\cdot\left(f\nabla\Psi\right) + \frac{2}{a^4\cos^2\phi}\left(\Psi_{\lambda\lambda}\Psi_{\phi\phi} - \Psi^2{}_{\lambda\phi}\right) \qquad (+\text{ missing terms}) \tag{4}$$

This is essentially a generalisation of gradient wind balance, in that it includes forces arising from the curvature of parcel trajectories.

Equations (2) and (4) form a complete system which can in principle be solved for Ψ,Φ. The balance equation (4) is 2-dimensional, whereas the PV equation (2) is 3-dimensional. Equation (4) is rearranged somewhat:

$$\nabla^2\Psi = \frac{1}{f}\left[\nabla^2\Phi - \frac{1}{a}\beta\Psi_\phi - \frac{2}{a^4\cos^2\phi}\left(\Psi_{\lambda\lambda}\Psi_{\phi\phi} - \Psi^2_{\lambda\phi}\right)\right] \tag{5}$$

where $\beta = df/dy$.

In the PV inversion algorithm employed by this project, equation (2) is replaced by a linear combination of (2) and (4) (Zemianski 1994, Griffiths 1998). Since these two equations have different units, equation (2) is multiplied by a scaling factor c,

$$c = \left(H^2 / fL^2\right)\left(g/\theta_0\right)^2$$

where H,L are characteristic horizontal and vertical length scales, and $\theta_0 = 300K$ is a reference temperature. The resulting equation is

$$\nabla^2\Phi + c\left(f + \nabla^2\Psi\right)\Phi_{\pi\pi} = \frac{p}{g\gamma\pi}cq + c\left[\frac{1}{a^4\cos^2\phi}\Psi_{\lambda\pi}\Phi_{\lambda\pi} + \frac{1}{a^2}\Psi_{\phi\pi}\Phi_{\phi\pi}\right]$$

$$+\nabla\cdot\left(f\nabla\Psi\right) + \frac{2}{a^4\cos^2\phi}\left(\Psi_{\lambda\lambda}\Psi_{\phi\phi} - \Psi_{\phi\lambda}^2\right) \qquad (6)$$

The values of H,L are adjusted for the best convergence rate – 10km and 2000km are generally suitable. In the PV inverter algorithm, the 2-d balance equation (5) and the 3-d PV equation (6) are solved for Ψ, Φ in a system of iterative loops. The balance equation (5) is solved iteratively for the Ψ fields, given a set of Φ fields; and the PV equation (6) is solved iteratively for the Φ fields, given a set of Ψ fields. Both of these iterative procedures employ successive under-relaxation to assist convergence. As the solution approaches convergence, the PV fields recalculated from Ψ, Φ on each iteration should approximate more and more closely to the input PV fields. The convergence criteria may be based on the fractional change in Φ or Ψ from one iteration to the next, or on the difference between the input PV fields and the recalculated PV fields. In practice, any two of these three criteria are used, and the convergence threshold is set according to how accurate the solution is required to be. In general, a compromise is made between accuracy and computation time.

A.2 The divergent component of the wind field

A consequence of approximation (b) above, i.e. the assumption of a non-divergent wind field, is that the wind field computed from the PV inverter's output Ψ, Φ fields is also non-divergent – the divergent part of the wind field is not recovered by the PV inverter. In the case study methodology, this deficiency is largely compensated for by carrying out two PV inversions, one on the adjusted PV fields and one on the unadjusted PV fields, and then computing wind and temperature increments which are then added into the model's initial fields. The divergent part of the wind in the model's initial state is thus preserved.

A.3 PV inversion domain and input fields

The PV fields input to the PV inverter are derived from a set of UM analysis fields or background fields. The PV fields are diagnosed by the UM and then input to the inverter. Alternatively, the PV inverter itself can compute the initial PV fields from the input UM geopotential, wind velocity, and potential temperature fields, but usually the UM-diagnosed PV fields are used. The PV fields computed by the inverter (which are used for convergence testing within the inverter) differ slightly from those diagnosed by the UM, but this difference is virtually insignificant in practice.

The horizontal PV inversion domain is a subset of the UM global domain. The vertical levels are pressure levels, since the inverter is formulated on (exner) pressure levels. The range of levels used is generally 850-100hPa, with an interval of 20 or 25hPa (a total of 38 levels, usually). The horizontal domain is limited by the need to avoid orography, since PV is undefined below the ground; in the N Atlantic this implies that the domain cannot extend further north than the southern tip of Greenland,

unless the lower boundary is raised to 600hPa. A lower boundary of 850hPa does allow the domain to encroach to some extent over western Canada without encountering orography.

A.4 Boundary conditions

The boundary condition used for the 2-d balance equation (5) is to specify Ψ on the boundary. It must be specified in such a way that (a) the tangential derivative $\partial\Psi/\partial s$ matches the normal wind component, to be consistent with equation (3); and (b) the divergence of the velocity through the boundary is zero, i.e. the integral of $\partial\Psi/\partial s$ around the boundary is zero. (In other words, Ψ satisfies the planar version of Green's theorem). This can be achieved if the value of Ψ on the boundary is specified by (Davis and Emanuel 1991),

$$\frac{\partial\Psi}{\partial s} = -\vec{v}\cdot\vec{n} + \frac{\oint \vec{v}\cdot\vec{n}\,dl}{\oint dl}$$

If Ψ is specified at one point on the boundary, then it is determined at all boundary points by this condition.

The boundary conditions for solving the 3-d PV equation (6) are also as in Davis and Emanuel (1991). On the lateral edges, the value of Φ is taken from the input UM fields. On the upper and lower horizontal boundaries, the hydrostatic balance condition is used, in the form $\Phi_\pi = -\theta$, where potential temperature θ is taken from the input UM fields. Alternatively, we could specify the value of Φ rather than its vertical derivative; according to Davis and Emanuel (1991) the solutions are fairly insensitive to the choice of horizontal boundary condition.

A.5 Vertical interpolation to model levels

The wind and temperature fields generated by the PV inverter are defined on pressure levels, as has already been pointed out. Before they can be used for the adjustment of UM model fields, they have to be vertically interpolated onto model levels. This is a straightforward procedure, but it does introduce another stage of approximation.

A.6 Convergence difficulties

The PV inverter sometimes fails to converge for a particular set of PV fields. In some cases the failure is sudden, i.e. the magnitudes of the error parameters become very large on a particular iteration after having been steadily decreasing over a number of previous iterations. In other cases the failure is very gradual and the error parameters may simply maintain more or less constant large values over many iterations without showing any tendency to reduce.

Such failures often appear to be associated with particular troublesome localities in one or more of the PV fields (although there have been cases when it has not been possible to identify such localised sources of instability). Such localities may be sites of negative PV, or regions where the solution becomes either non-elliptic or non-unique. If the solution domain is reduced so that the troublesome locality is excluded, then convergence may well be achieved, although the excluded part of the field may of course encompass a PV anomaly which is relevant to the particular case study.

In cases where the convergence failure is gradual, it may be acceptable to relax the convergence limits and still achieve a sufficiently accurate converged solution.

References

Apenzeller, C. and Davies, H.C. (1992), Structure of Stratospheric Intrusions into the Troposphere, *Nature*,**358**,570-572

Browning, K.A. and Roberts, N.M., Mesoscale Analysis of Arc Rainbands in a Dry Slot *JCMM Internal Report 100, University of Reading*

Carroll, E.B. (1996), The Formulation and Testing of Schemes to Allow Three-Dimensional Consistent Manual Alteration of NWP Fields, *FS Tech. Note 3, UK Met. Office*

Demirtas, M. (1996), Sensitivity of Short-Range Forecasts to Local Potential Vorticity Modifications, *Ph.D. Thesis, University of Reading*

Demirtas, M. and Thorpe, A.J. (1997), Sensitivity of Short-Range Forecasts to Local Potential Vorticity Modifications, *JCMM Internal Report 71, University of Reading*

Davies, C.A. and Emanuel, K.A. (1991), Potential Vorticity Diagnostics of Cyclogenesis, *Mon. Wea. Rev.*, **119**, 1929-1953

Fehlmann, R. and Davies, H.C. (1997), Misforecasts of Synoptic Systems: Diagnosis via PV Retrodiction, *Mon. Wea. Rev.*, **125**, 2247-2264

Fehlmann, R (1997), Dynamics of Seminal PV Elements, *Doctoral Thesis, ETH Zurich*

Fehlmann, R. and Davies, H.C. (1999), Role of Salient PV Elements in an Event of Frontal-Wave Cyclogenesis, *Q.J.R. Metl. Soc.*, **125**, 1801-1824

Georgiev, C.G. (1996), Correlation of Meteosat WV Data to Middle Troposphere PV Anomalies, *Proc. EUMETSAT Met. Satellite Data Users Conference, Vienna,* **EUM P 19**, 129-136

Georgiev, C.G. (1999), Quantitative Relationship between Meteosat WV Data and Positive PV Anomalies: a Mediterranean Case Study, *Meteorol. Appl.*, **6**, 97-109

Griffiths, M., Thorpe, A., and Browning, K. (1998), Convective Destabilisation by a Tropopause Fold Diagnosed Using PV Inversion, *JCMM Internal Report 96, University of Reading*

Hoffman, R.N. et al., (1995), Distortion Representation of Forecast Errors, *Mon. Wea. Rev.*,**123**, 2758-2770

Holton, J.R. (1992), Introduction to Dynamic Meteorology 3rd Edition, Academic Press

Hoskins, B.J., McIntyre, M.E., and Robertson, A.W. (1985), On the Use and Significance of Isentropic PV Maps, *Q.J.R. Met. Soc.*, **111**, 877-946

Li, Y. et al. (1998), A Study on Assimilating Potential Vorticity Data, *Tellus,* **50A**, 490-506

Mansfield, D.A. (1996), The Use of PV as an Operational Forecast Tool, *Met. Appl.* **3**, 195-210

Mansfield, D.A. (1997), The Use of PV and WV Imagery to Validate NWP, *Met. Appl.* **4**, 305-309

Morgan, M.C., and Nielsen-Gammon, J.W. (1998), Using Tropopause Maps to Diagnose Mid-Latitude Weather Systems, *Mon. Wea. Rev.*, **126**, 2555-2579

Pankiewicz, G.S. (1997), Satellite Imagery Pattern Recognition Products for NWP, *FR Tech Rep 206, UK Met Office*

Pankiewicz, G.S., et al. (1999), Potential Vorticity from Meteosat Water Vapour Imagery, *FR Tech Rep 281, UK Met. Office*

Pankiewicz G.S., et al. (1999), Automatic estimation of Potential Vorticity from Meteosat water vapour imagery to adjust initial fields in NWP,
Proc. EUMETSAT Met. Satellite Data Users' Conference, Denmark, Sept. 1999

Rosting, B. et al. (1996), Monitoring of NWP Models by Use of Satellite Data, *Met. Appl.,*. **3**, 331-340

Schmetz, J. and van de Berg, L. (1994), Upper Tropospheric Humidity Observations from Meteosat Compared with Short-Term Forecast Fields, *Geophys. Res. Lett.*, **21**, 573-576

Semple, A.T. (1998), Conceptual Models of Cyclogenesis, *JCMM Internal Rep. 92, Univ. of Reading*

Swarbrick, S.J. (1999), Use of PV Inversion and WV Imagery to Adjust Initial Conditions in NWP, *JCMM Internal Rep. 102, University of Reading*

Ziemianski, M. (1994), Potential Vorticity Inversion, *JCMM Internal Report 39, University of Reading*

CURRENT JCMM INTERNAL REPORTS

This series of JCMM Internal Reports, initiated in 1993, contains unpublished reports and also versions of articles submitted for publication. The complete set of Internal Reports is available from the National Meteorological Library on loan, if required.

1. **Research strategy and programme**
   K A Browning et al
   January 1993

2. **The GEWEX Cloud System Study (GCSS)**
   GEWEX Cloud System Science Team
   January 1993

3. **Evolution of a mesoscale upper tropospheric vorticity maximum and comma cloud from a cloud-free two dimensional potential vorticity anomaly**
   K A Browning
   January 1993

4. **The global energy and water cycle**
   K A Browning
   July 1993

5. **Structure of a midlatitude cyclone before occlusion**
   K A Browning and N Roberts
   July 1993

6. **Developments in systems and tools for weather forecasting**
   K A Browning and G Szejwach
   July 1993

7. **Diagnostic study of a narrow cold frontal rainband and severe winds associated with a stratospheric intrusion**
   K A Browning and R Reynolds
   August 1993

8. **Survey of perceived priority issues in the parametrizations of cloud-related processes in GCMs**
   K A Browning
   September 1993

9. **The effect of rain on longwave radiation**
   I Dharssi
   September 1993

10. **Cloud microphysical processes - a description of the parametrization used in the large eddy model**
    H Swann
    October 1993

11. **An appreciation of the meteorological research of Ernst Kleinschmidt**
    A J Thorpe
    May 1992

12. **Potential vorticity of flow along the Alps**
    A J Thorpe, H Volkert and Dietrich Heimann
    August 1992

13. **The representation of fronts**
    A J Thorpe
    January 1993

14. **A parametrization scheme for symmetric instability: test for an idealised flow**
C S Chan and A J Thorpe
February 1993

15. **The Fronts 92 Experiment: a Quicklook Atlas**
Edited by T D Hewson
November 1993

16. **Frontal wave stability during moist deformation frontogenesis**
Part 1: Linear wave dynamics
C H Bishop and A J Thorpe
May 1993

17. **Frontal wave stability during moist deformation frontogenesis**
Part 2. The suppression of non-linear wave development
C H Bishop and A J Thorpe
May 1993

18. **Gravity waves in sheared ducts**
S Monserrat and A J Thorpe
October 1993

19. **Potential vorticity and the electrostatics analogy: quasi-geostrophic theory**
C Bishop and A J Thorpe
November 1993

20. **Recent advances in the measurement of precipitation by radar**
A J Illingworth
April 1993

21. **Micro-physique et givrage: cloud microphysics and aircraft icing**
A J Illingworth
May 1993

22. **Differential phase measurements of precipitation**
M Blackman and A J Illingworth
May 1993

23. **Estimation of effective radius of cloud particles from the radar reflectivity**
N I Fox and A J Illingworth
May 1993

24. **A simple method of Dopplerising a pulsed magnetron radar**
A Hua, A J Illingworth and J Eastment
November 1993

25. **Radiation and polar lows**
George C Craig
February 1994

26. **Collected preprints submitted to the International Symposium on the Life Cycles of Extratropical Cyclones; Bergen, Norway, 27 June - 1 July 1994**
April 1994

27. **Convective frontogenesis**
Douglas J Parker and Alan J Thorpe
April 1994

28. **Improved measurement of the ice water content in cirrus using a total water evaporator**
Philip R A Brown and Peter N Francis
April 1994

29. **Mesoscale effects of a dry intrusion within a vigorous cyclone**
K A Browning and B W Golding
April 1994

30. **GEWEX Cloud System Study, Science Plan**
May 1994

31. **Parametrization of momentum transport by convectively generated gravity waves**
R Kershaw
May 1994

32. **Mesoscale Modelling Newsletter No 5**
May 1994

33. **Observations of the mesoscale sub-structure in the cold air of a developing frontal cyclone**
K A Browning, S A Clough, C S A Davitt, N M Roberts and T D Hewson
May 1994

34. **Longwave radiative forcing of a simulated tropical squall line**
Imtiaz Dharssi
July 1994

35. **On the nature of the convective circulation at a kata-cold front**
K A Browning
September 1994

36. **Collective preprints of papers submitted to the COST-75 International Seminar on Advanced Weather Radar Systems, Brussels, 20-23 September 1994**
November 1994

37. **Use of satellite imagery to diagnose events leading to frontal thunderstorms: Parts I and II of a case study**
K A Browning and N M Roberts
November 1994

38. **The role of spaceborne millimetre-wave radar in the global monitoring of ice cloud**
P R A Brown, A J Illingworth, A J Heymsfield, G M McFarquhar, K A Browning and M Gosset
December 1994

39. **Potential vorticity inversion**
Michal Ziemianski
October 1994

40. **Theory of mature tropical cyclones; a comparison between Kleinschmidt (1951) and Emanuel (1986)**
Suzanne L Gray
December 1994

41. **Dispersion and removal of pollutants during the passage of an atmospheric frontal system**
N R Gimson
December 1994

42. **The role of snow sublimation in frontogenesis**
D J Parker and A J Thorpe
December 1994

43. **Potential vorticity and the electrostatics Analogy: Ertel-Rossby formulation**
A J Thorpe and C H Bishop
December 1994

44. **Mesoscale aspect of extratropical cyclones: an observational perspective**
K A Browning
January 1995

45. **A polar low outbreak: evolution and mesoscale structures**
T D Hewson, G C Craig and C Claud
February 1995

46. **Generation of near-surface gusts of deep convection**
K Nakamura and R Kershaw
April 1995

47. **Attribution concepts applied to the Omega Equation**
S A Clough, C S A Davitt and A J Thorpe
June 1995

48. **Parametrization of mixed-phase cloud and precipitation**
Susan P Ballard and M Gerard Hutchinson
June 1995

49. **Short-range forecasting of stratocumulus: initialization prediction**
Susan P Ballard, Simon D Jackson and B Macpherson
June 1995

50. **Contributions of the JCMM/Dept of Meteorology Radar Group to the 27th AMS Radar Meteorology Conference, Vail October 1995**
June 1995

51. **Cold pools in shear**
Douglas J Parker
September 1995

52. **High-resolution analysis of frontal fracture**
K A Browning, S P Ballard and C S A Davitt
September 1995

53. **The albedo of broken cloud fields: calculations using a modified two stream radiation code**
Imtiaz Dharssi and Roy Kershaw
October 1995

54. **Parametrization of momentum transport by convection. I: theory and cloud modelling results**
R Kershaw and D Gregory
November 1995

55. **Variation of frontal structure along a cold front**
K A Browning and N M Roberts
November 1995

56. **Secondary frontal waves**
Douglas Parker
December 1995

57. **Objective fronts**
T D Hewson
March 1996

58. **Mesoscale analysis of the activation of a cold front during cyclogenesis**
K A Browning, N M Roberts and A J Illingworth
June 1996

59. **Investigation of different representations of rain in a 1-d evaporation model**
H Swann
May 1996

60. **Parametrization of diabatic processes in the inversion of the omega-equation**
M Athanassiadou and A J Thorpe
June 1996

61. **The role of the environmental flow in the development of secondary frontal cyclones**
I A Renfrew, A J Thorpe and A Joly
June 1996

62. **Consequences of the geostrophic momentum approximation on barotropic instability**
S Malardel, A J Thorpe and A Joly
June 1996

63. **Contributions to the AMS/RMS Conference on Mesoscale Processes**
Reading, 9-13 September 1996

64. **Vorticity and potential vorticity in stratified flows interacting with an isolated obstacle**
Jorge A Gutiérrez and A J Thorpe
September 1996

65. **Triple point development: two case studies**
Douglas Parker
September 1996

66. **Radar observations of wind-shear splitting within evolving atmospheric Kelvin-Helmholtz billows**
D Chapman and K A Browning
April 1997

67. **Cold frontal structure derived from radar wind profilers**
K A Browning, D Jerrett, J Nash, T Oakley and N M Roberts
May 1997

68. **The dry intrusion and its effect on the frontal, cloud and precipitation structure of extratropical cyclones**
K A Browning - Text of invited special lecture at the Spring Conference
of the Meteorological Society of Japan, University of Tsukuba, 22 May 1997

69. **Met. Office Unified Model data, diagnostics, graphics programs, and other observational data available from the JCMM through the aegis of the Universities Weather Research Network (UWERN).** (Plus supplement)
Peter Panagi and Ed Dicks
June 1997

70. **Contributions of the JCMM/Dept of Meteorology Radar Group to the 28th AMS Radar Meteorology Conference.** Austin, Texas
September 1997

71. **Sensitivity of short-range weather forecasts to local potential vorticity modifications**
Meral Demirtas and Alan Thorpe
July 1997

72. **Objective identification of frontal wave cyclones**
T D Hewson
August 1997

73. **Attribution and its application to mesoscale structure associated with tropopause folds**
A J Thorpe
September 1997

74. **The role of the environmental flow in the development of secondary frontal cyclones**
Ian A Renfrew, Alan J Thorpe and Craig H Bishop
September 1997

75. **Potential vorticity: a short history of its definitions and uses**
Alan J Thorpe and Hans Volkert
September 1997

76. **Superposing semi-geostrophic potential vorticity anomalies**
H R Birkett and A J Thorpe
September 1997

77. **Short period forecasting of catchment-scale precipitation.**
Part 1: the role of Numerical Weather Prediction
M A Pedder, M Haile and A J Thorpe
September 1997

78. **Verification of the tracking technique used in an experimental cloud motion wind inferring system**
Z Wang, K A Browning and G A Kelly
October 1997

79. **A preliminary study of Fourier series analysis for cloud tracking with GOES high temporal resolution images**
Z Wang
October 1997

80. **Analysis of an ex-tropical cyclone after reintensifying as a warm-core extratropical cyclone**
K A Browning, G Vaughan and P Panagi
November 1997

81. **A JCMM overview of FASTEX IOPs**
S A Clough, H W Lean, N M Roberts, H Birkett, J-P Chaboureau, R Dixon, M Griffiths, T D Hewson and A Montani
January 1998

82. **Programs for PV inversion and modification**
Meral Demirtas
December 1997

83. **Release of potential shearing instability in warm frontal zones**
D Chapman and K A Browning
February 1998

84. **The European Cloud-Resolving Modelling Programme (EUCREM)**
Summary Report from the coordinator
P W White
April 1998

85. **A frontal wave database**
T D Hewson
April 1998

86. **Layering observed in dropsoundings from IOP 1 of Fronts 92**
S A Clough
May 1998

87. **Use of wind-shear displays for Doppler radar data**
D Chapman and K A Browning
May 1998

88. **Radar estimates of rainfall rates at the ground in bright band and non-bright band events**
T J Smyth and A J Illingworth
June 1998

89. **Correction for attenuation of radar reflectivity using polarisation data**
T J Smyth and A J Illingworth
June 1998

90. **The effects of convection on chemical reactions and precipitation scavenging**
Neil R Gimson
July 1998

91. **How to use the display program DISP**
Nigel Roberts
August 1998

92. **Conceptual models of cyclogenesis**
Adrian T Semple
August 1998

93. **Observations of oblate hail using dual polarisation radar and implications for hail detection schemes**
T J Smyth, T M Blackman and A J Illingworth
September 1998

94. **The semigeostrophic diagnosis of vertical motion. Part I: Formulation and co-ordinate transformations**
Mike A Pedder and Alan J Thorpe
September 1998

95. **The semigeostrophic diagnosis of vertical motion. Part II: Results for an idealised baroclinic wave life cycle**
Alan J Thorpe and Mike A Pedder
September 1998

96. **Convective destabilisation by a tropopause fold diagnosed using potential vorticity inversion**
Morwenna Griffiths, Alan Thorpe and Keith Browning
October 1998

97. **Forecast skill of the ECMWF model using targeted observations during FASTEX**
A Montani, A J Thorpe, R Buizza and P Unden
October 1998

98. **Observations and model simulations of the FASTEX IOP 16 frontal wave - effects of sublimation**
Sid A Clough, Humphrey W Lean, Nigel M Roberts and Richard M Forbes
December 1998

99. **The application of conceptual models in NWP**
Adrian T Semple
January 1999

100. **Mesoscale analysis of arc rainbands in a dry slot**
K A Browning and N M Roberts
January 1999

101. **Interaction of mesoscale tropopause depressions with a warm-core cyclone: observational and model analyses, and sensitivity to analysis errors**
K A Browning, A J Thorpe, A Montani, D Parsons, M Griffiths, P Panagi and E M Dicks
February 1999

102. **The use of water vapour imagery and PV inversion to adjust initial conditions in NWP**
Sean J Swarbrick
February 1999
This report is no longer available; see Internal Report No.108

103. **Summary notes for a lecture course on Waves in the Atmosphere and Ocean**
A A White
March 1999

104. **Results of a questionnaire on the operational value of conceptual models (CMs) of fronts and cyclones**
N M Roberts & M V Young
July 1999

105. **Contributions to the Poster Session at the 1998 UWERN Annual Science Meeting**
assembled by A A White
August 1999

106. **The objective analysis of dropsonde data from FASTEX**
Richard Forbes, Sid Clough, Mark Dixon, Andy Macallan & Nigel Roberts
January 2000

107. *NWP Technical Report No.302*
Implications for Mesoscale Modelling from a Study of the FASTEX IOP 16 Mid-latitude Cyclone
Richard M Forbes, Humphrey W Lean, Nigel M Roberts and Peter A Clark
March 2000

108. *NWP Technical Report No.291*
The use of water vapour imagery and PV inversion to adjust initial conditions in NWP
Final Project Report
Sean J Swarbrick
September 1999

Met Office Joint Centre for Mesoscale Meteorology Department of Meteorology
University of Reading PO Box 243 Reading RG6 6BB United Kingdom
Tel: +44 (0)118 931 8425 Fax: +44 (0)118 931 8791
www.metoffice.com